Etude expérimentale des flux et des caractéristiques physiques des poussières sahariennes dans les régions proches du golfe de guinée

Albert Sunnu

THESE DE DOCTORAT

Présentée à
L'UNIVERSITE DU SUD TOULON-VAR

En vue de l'obtention du:

DOCTORAT DE L'UNIVERSITE DU SUD TOULON-VAR

Spécialité: Science de l'univers

Auteur

Albert Kojo SUNNU

An experimental study of the Saharan dust physical characteristics and fluxes near the Gulf of Guinea

Soutenue le 24 Novembre 2006

Jury :

M. George AFETI	Examinateur
M. Guy CAUTENET	Rapporteur
M. Serge DESPIAU	Examinateur
M. Michel LEGRAND	Rapporteur
M. Jacques PIAZZOLA	Examinateur
M. François RESCH	Directeur de thèse

ACKNOWLEDGEMENTS

I wish to express my sincere gratitude to my first supervisor, Professor François Resch, Director of the Institut des Sciences de l'Ingénieur de Toulon et du Var (ISITV) of the Université du Sud Toulon-Var (USTV) and my second supervisor, Dr George Afeti, Principal of the Ho Polytechnic, Ghana for accepting me to work with them as a team to undertake this research project. As a result, I am a co-author of the published journal and conference papers that this study has produced. I am indebted to them for their valuable suggestions, painstaking approach to research, kindness to share their knowledge and expertise, cooperation and encouragement, which have enabled me to prepare this thesis. I also benefited from their wisdom and rich experience in experimental work and aerosol technology. Their interest in the project, participation and meticulous supervision has led to the success of the thesis.

I would also like to thank the scientists at the LEPI-ISITV of the USTV especially Prof. Yves Lucas, Dr. Jacques Piazzola and Dr. Serge Despiau for their encouragement and help during my stay in the Laboratoire des Echanges Particulaires aux Interfaces (LEPI). I should also mention Mr. Tathy Missamou for his support anytime the sampling equipment was sent to the laboratory for servicing and recalibration as well as his advice on the use of the instruments.

Also, I wish to thank the Head of the Department of Mechanical Engineering of the College of Engineering of the Kwame Nkrumah University of Science and Technology (KNUST), for his encouragement, often reducing my teaching load in order to give me ample time to pursue the research study while working as a lecturer. Therefore, I thank my colleague lecturers in the department who supported this arrangement and continuously encouraged me throughout the study. I should mention Prof. J. P. A. Brew Hammond, Prof F. O. Akuffo, Dr. D. M. Obeng, Dr. J. Antonio, Mr E. E. K. Agbeko, Mr. M. N. Sackey, Dr. F. K. Forson, Mr. I. A. Edwin, Ms. Araba Ntsiful, Dr. L. E. Ansong, Dr. Abroba-Cudjo, Mr. T.Opoku-Agyeman and the students as well as the technicians who helped me to install the experimental equipment at the sampling site at the Faculty of Environmental Developmental Studies (FEDS) of the KNUST, Kumasi.

I wish to thank the French Government through the French Embassy in Ghana for the tremendous support for this study. The French Government gave me a scholarship to register for the PhD degree at the USTV while I carried out the experiment in Ghana. The scholarship package included a monthly stipend in Ghana, study visits to the University of Toulon in France and provision of research material and equipment. I therefore thank His Excellency, the Ambassador, the Cultural and Scientific Counsellor and the staff of the French Embassy in Accra for the warm reception at the Embassy anytime I went there, either to claim the grants or to facilitate my trips to France. I should mention Mr. Neveu, Mr. Goldstein, Madame Zwang-Graillot, Mr. Olivier Robinet, Mr. Cor and Madame Jacqueline Kpodonu for their special assistance for this project at the Embassy. I also extend my gratitude to the Commandant and Staff of the Air Force base in Tamale and the Staff of the Ghana Civil Aviation Authority in Tamale for permitting me to install the sampling equipment at the Air Traffic Control Tower of the Tamale Airport. I thank the Staff of the Ghana Meteorological Services Department in Tamale, Kumasi and Accra for the various meteorological data they readily provided for this work, mostly free of charge.

I would like to express my deepest gratitude to Prof. Guy Cautenet of the Université Blaise Pascal (Clermont-Ferrand) and Prof. Michel Legrand of the Université des Sciences and Techniques de Lille for kindly accepting to be the Rapporteurs for the thesis. Their critical review of the draft thesis has greatly contributed to the quality of presentation of the final version.
Finally, I thank my family for accommodating my irregular presence at home, the numerous journeys I have had to make for days to visit the sampling site in Tamale and other places in search of valuable data. I sincerely thank them for their patience and understanding.

TABLE OF CONTENTS

ABSTRACT

AN EXPERIMENTAL STUDY OF THE SAHARAN DUST PHYSICAL CHARACTERISTICS AND FLUXES NEAR THE GULF OF GUINEA

The physical parameters which characterize the Saharan dust in West Africa during the months from November to March of each year have been determined over a long period of 7 years between 1997 and 2005. These physical parameters include the particle size, number and mass concentrations, transport and deposition flux of the desert aerosols.
Each year large quantities of Saharan aerosols are transported from the Chad basin towards the Gulf of Guinea by the northeast trade winds. This is the Harmattan phenomenon which has serious effects on the population, the environment, engineering systems and equipment as well as on the quality of life: reduction of solar radiation and visibility, variation of temperatures, agriculture, livestock, refrigeration systems, engines filters and cooling systems, respiratory systems, epidemics, etc. The measurements were conducted in Ghana which is located between latitudes 4^{o}N (Gulf of Guinea) and 12^{o}N, at two experimental stations: the first in the centre of the country at Kumasi (6°40''N), the second in the north at Tamale (9°34''N).
The Saharan particle size concentration and distributions have been determined with the help of an optical particle counter in the interval of 0.5 µm to 25 µm. The average values in the Harmattan seasons show particle number concentrations between 24 and 63 particles per cm^3 and the mass concentrations range between 168 and 1331 µg m^{-3} respectively. For the non-Harmattan period, the concentrations are less than 10 particles per cm^3. The average size in diameter over the 7 years is in the order of 1.5 µm.
The size distributions correspond to the typical distribution of atmospheric aerosols with the coarse particle mode around 3.5 µm. The influence of the Inter-Tropical Convergence Zone (ITCZ) and the North Atlantic Oscillation (NAO) on the Harmattan phenomenon has been studied in detail.
The mean transit time of the particles between Tamale and Kumasi (320 km) was estimated to be one day.
The particle deposition flux has been estimated for the two years 2002 and 2005 by measuring the particle concentrations simultaneously at the two sampling stations of Kumasi and Tamale. The results show the deposition rates of 12.7 tonnes/km^2/yr in 2002 (being a thickness of 4.8 µm of ground deposition) and of 31.4 tonnes/km^2/yr in 2005 (being a thickness of 11.8 µm of ground deposition).
The results obtained could be considered as representative for the regions near the Gulf of Guinea.

Key words: Atmospheric aerosol; Saharan dust; particle size distributions; flux deposition; Harmattan; ITCZ; NAO.

Short Abstract

The physical parameters that characterise the Saharan dust aerosol usually present in the environment near the Gulf of Guinea during the months of November to March, known locally as the Harmattan season, have been determined over a 7-year period, using Ghana as a reference geographical location. The dust particle size distributions are obtained and discussed. The dust flux and deposition rate are also estimated. Within the dust particle size range measured (0.5 μm – 25 μm), the yearly average number and mass concentrations are found to vary from 24 to 63 particles per cm^3 and 168 to 1331 μg m^{-3} respectively. The mean particle diameter is 1.47 μm. The annual dust deposition rate varies from 12.7 t/km^2/yr to 31.4 t/km^2/yr, corresponding to a ground dust layer thickness of 4.8 μm and 11.8 μm respectively.

Key words: atmospheric aerosol; Saharan dust; particle size distributions; flux deposition; Harmattan; ITCZ; NAO.

Résumé

ETUDE EXPERIMENTALE DES FLUX ET DES CARACTERISTIQUES PHYSIQUES DES POUSSIERES SAHARIENNES DANS LES REGIONS PROCHES DU GOLFE DE GUINEE

Les paramètres physiques qui caractérisent les poussières sahariennes en Afrique de l'ouest pendant les mois compris entre novembre et mars de chaque année ont été déterminés sur une longue période de 7 années entre de la période 1997 et 2005. Ces paramètres physiques concernent les tailles de particule, les concentrations en nombre et en masse, le transport et les flux de dépôt des aérosols désertiques.
Chaque année de grandes quantités d'aérosols sahariens sont transportées depuis le bassin du Tchad vers le golfe de Guinée par les alizés de Nord-Est. C'est le phénomène de l'Harmattan qui a des répercussions importantes sur les populations, l'environnement, les équipements techniques ainsi que sur la qualité de vie : réduction des radiations solaires et de la visibilité, variations de températures, agriculture, élevage, systèmes de réfrigération, filtres des moteurs et des refroidisseurs, systèmes respiratoires, épidémies, etc. Les mesures ont été effectuées au Ghana, qui se situe entre les latitudes 4°N (golfe de Guinée) et 12°N, dans deux stations expérimentales: la première au centre du pays à Kumasi (6°40''N), la seconde au nord à Tamale (9°34''N).
Les concentrations et distributions en taille des particules sahariennes ont été déterminées à l'aide d'un compteur de particules optique dans un intervalle de 0,5µm à 25µm. Les valeurs moyennées sur toute la saison d'Harmattan montrent des concentrations en nombre comprises entre 24 et 63 particules cm^{-3} et des concentrations en masse comprises entre 168 et 1331 µg m^{-3}. Pour les périodes hors Harmattan on trouve des concentrations en nombre inférieures à 10 particules/cm^3. La taille (diamètre) moyenne (sur l'ensemble des 7 années) est de l'ordre de 1,5 µm.
Les distributions en taille correspondent aux distributions typiques des aérosols atmosphériques avec un mode de particules grossières autour de 3,5µm.
La forte influence exercée sur le phénomène de l'Harmattan par la Zone de Convergence Intertropicale (ITCZ) et l'Oscillation de l'Atlantique Nord (NAO) est étudiée en détail.
Les temps de transit entre Tamale et Kumasi (320 km) ont été estimés à une journée.
Les flux de dépôt sont estimés pour les deux années 2002 et 2005 en mesurant les concentrations simultanément dans les deux stations de Kumasi et de Tamale. Les résultats montrent des taux de dépôt de 12,7 tonnes/km²/an en 2002 (soit une épaisseur de 4,8 µm de dépôt au sol) et de 31,4 tonnes/km²/an (soit une épaisseur de 11,8 µm).
Les résultats obtenus peuvent être considérés comme représentatifs pour les régions proches du Golfe de Guinée.

Mots clés: aérosols atmosphériques ; poussières sahariennes ; granulométrie des particules ; flux de dépôt ; Harmattan ; ITCZ ; NAO

Laboratoire : LSEET-LEPI
Adresse : Institut des Sciences de l'Ingénieur de Toulon et du Var, Avenue Georges Pompidou, BP 56-83162 LA VALETTE Cedex.

1. INTRODUCTION AND PRESENTATION OF THE STUDY

The atmosphere contains many kinds of airborne particles called aerosols. They occur in different forms, such as dust, fume, smoke or insecticide spray. These particles affect visibility, climate, our health and quality of life. This study covers the dust aerosol in Ghana, near the Gulf of Guinea during the dry season. It deals with the quantitative description of the physical properties of the dust aerosol measured in two cities in Ghana, namely Kumasi (6^o 40'N, 1^o 34'W) and Tamale (9^o 34'N, 0^o 52'W), over a period of nine years. This study also examines the influence of two global circulation systems (the ITCZ and NAO) on the evolution of the Saharan dust in West Africa. An attempt is also made to estimate the dust flux and deposition rate in the country.
The presentation of this work is organised as follows. In the second chapter, bibliographic study of related literature is presented. Chapter three is centred on the theoretical supports while chapter four focuses on the experimental study. Chapter five is devoted to the discussions of the results. The conclusion is presented in chapter six.

1.1. What is the Harmattan?

The atmospheric environment in most parts of West Africa, during the dry season months from November to March, is characterized by massive suspension and deposition of Saharan soil dust particles. The presence of the dust aerosol in the West African region creates an opalescent atmosphere during this period. The dust invasions are sustained by the northeast trade winds, which blow across the Sahara Desert towards the Gulf of Guinea and beyond in a south-westerly direction during this period. Most countries near the Gulf of Guinea in West Africa are affected by this dusty wind phenomenon, which is locally called the Harmattan. The Harmattan therefore can be defined as the weather condition in West Africa during the northern winter season, where the atmospheric environment becomes ubiquitously dusty and hazy as a result of the suspension of Saharan dust floating in the northeast winds. In fact, Harmattan is the name of the dusty northeast winds in West Africa. It is only by extension that we use this name for the 'season' such as the 'Harmattan season', the 'weather condition' for instance the 'Harmattan weather condition', the 'period' to mean the 'Harmattan period' or the 'climate' such as the 'Harmattan climate'. We may also use the 'Harmattan phenomenon' to describe this intense Saharan dust production period in West Africa.
Local winds enhanced by periodic incursions of cold polar air into the Saharan region results in prominent subtropical anticyclones on the surface with an associated upper-level trough (Samways, 1975). This mechanism generates convergence of air aloft and divergence below. Meanwhile, intense solar heating of the bare desert surface during the day, gives rise to strong dry convective activities and turbulent fluctuations, which raises up the desert soil dust particles lifted by wind drag. These processes create dense dust clouds several kilometres thick into the atmosphere (Schutz, 1980), mainly over the Bilma and Faya-Largeau areas of the Chad basin, also known in current literature as the Bodele depression, in the Sahara Desert (Hamilton and Archbold, 1945; Kalu, 1979; McTainsh, 1980; Cox et al., 1982; McTainsh and Walker, 1982). There are other regions where this phenomenon is observed (e.g. the region of northwest Mali, south Algeria and eastern Mauritania). The northeast trade winds, which prevail during the period entrains the raised dust particles, then travel in a

southwest direction, and deposit the particles over the areas the winds traverse. With the absence of hydrometeors, the dust particles mainly settle under gravity and aerodynamic forces. Thus, sedimentation of the dust particles begins immediately after entrainment, with the largest particles dropping out first and quickly. Therefore, there is a systematic reduction in the dust aerosol concentration and particle sizes with distance from the source areas (or along the flow downstream). Hence, the characteristics of these Saharan dust particles, including the size and number distributions vary from place to place as a function of distance from the source. Preferential deposition of coarser particles leaves the dust plume reaching farther away places from the source to be composed mainly of smaller particles which can remain in suspension for longer periods. Consequently, deposition is typically uniform at a location and time. The Harmattan winds are not gusty but gentle with low, near surface velocities normally less than 6 m/s (Samways, 1975) and extend up to an altitude of the highest wind speed, approximately between 850 mbar and 900 mbar levels, corresponding to about 1500 m above sea level (McTainsh et al., 1980; Tiessen et al., 1991).

Meteorologically, the Harmattan affects those areas with latitudes north of the latitudinal position of the Inter-Tropical Convergence Zone (ITCZ), which separates the Saharan dust-laden northeast winds from the southwest monsoon winds. The Saharan dust aerosol hardly extends southwards beyond the Gulf of Guinea because of the presence of the ITCZ barrier which is located around latitude 5° N most of the time during the Harmattan season (Adeyafa et al., 1995). Therefore, the dry northeast trade winds, which carry the Saharan dust, meet the wet southwest monsoon winds along the Gulf of Guinea, where most of the dust particles are scavenged and deposited on the countries along the West African coast. The Harmattan phenomenon is important to governments and scientists because of its effect on the economy and quality of life. There is therefore the need to establish the particle size distribution along the course of the dust aerosol plumes both over land and water surfaces. This will give an in-depth understanding of these Saharan dust physical behaviour (including the dust deposition flux on land), impact on materials, effect on human health and technical equipment. Actually, very little is known about the concentration and size distribution of the dust particles in Ghana.

The Saharan dust is not limited to the West Africa region alone. The dust particles are also transported at distances of thousands of kilometres from the sources in the Sahara Desert, across the tropical Atlantic to the Caribbean and northeast coast of South America as well as across the Mediterranean to Europe and the Near East (Kalu, 1979; Schutz, 1980; Swap et al., 1992, 1996; Romero et al., 1999). From the dust sources in the Sahara Desert, different wind patterns deflate the Saharan dust particles to the areas adjacent to the dust sources at different times of the year. For example, in summer, the dust storms travel from the central and western Sahara as well as the Sahel area westwards over the Atlantic and are reported to reach the North America continent and the Caribbean region (Carlson and Prospero, 1972; Prospero, 1979, 1999; Karyampudi et al., 1992; Chiapello et al., 1995; Moulin et al., 1997; Chiapello and Moulin, 2002; Chiapello et al., 2005; Kaufman et al., 2005, Petit et al., 2005). This research work is a contribution to the advancement of our knowledge of the Harmattan phenomenon in West Africa.

1.2 Importance and practical implications of the study

The suspension and deposition of the Saharan dust in the West African region induces marked changes in the weather, the environment and ecosystem of the sub-region. Therefore, the Harmattan phenomenon has attracted a lot of interest from scientists in various fields, including engineering, meteorology, geography, oceanography, pedology (i.e. formation, composition and distribution of soils and their classification) and related social science. The importance and numerous effects of the Harmattan season have prompted scientists to investigate the origin of the Saharan soil dust, its composition, distribution, production, transport, deposition and effect on the environment. Also, scientists are interested in the nature of the desert soil, in terms of mineralogy and chemical composition, particle size distribution and potential to be entrained. A thorough knowledge of the Saharan meteorology, the convective activities that raise the soil dust particles, the pattern and dynamics of the wind flows responsible for initiating the particulate movement and lifting as well as the trade wind system over the desert and its trajectory are important in understanding the transport processes out of the desert and beyond its margins. Generally, scientific interest on the impact of Saharan dust in the atmosphere relates to two broad areas. The first area of attention concerns climate-oriented effects, which focus on the properties of the dust aerosols that affect radiative forcing through the attenuation of solar radiation and cloud formation. The second broad area of interest relates to air quality and health implications. The following sections explain the consequences and the scientific interests.

General characteristics
The Harmattan period is characterized by cold nights, hot afternoons, highest daily temperature range in the year, very low relative humidity, dry and dying vegetation, reduced visibility, massive deposition of the grey or yellow Saharan dust particles on surfaces and soiling of materials in the atmosphere by the dust particles.

Solar radiation balance
Dust particle sizes comparable to the wavelength of light (0.3-0.7 μm) effectively attenuate solar radiation. Therefore, there is the need to know the sizes and effect of the dust aerosol on the solar radiation balance, which can change the temperatures of the troposphere, the surface below and the aerosol plume itself. Reduction of ground temperature during Harmattan spells and increase of tropospheric temperature due to absorption of solar radiation are interesting to scientists since most of the Saharan dust particles contained in the Harmattan fall in this range of particle diameter, $D < 1$ μm. For example Sunnu, 1997 obtained 80% to be composed of particles in the diameter range of 0.5-1.0 μm out of the sample size range of 0.5 – 25 μm. The heating up of the dust aerosol is limited to the daytime. In the night, radiative cooling of the dust aerosol is enhanced due to absence of solar radiation resulting in relatively cold night ambient temperatures (Adedokun et al., 1980).

The ambient air
The suspended Saharan soil dust particles reaching Ghana, for example, are mostly microscopic, and less than 10 μm diameter. Sunnu (1997) obtained 95% of particles to be

within 0.5-10.0 μm diameter. These particles can be found all over the place including rooms as the particles can penetrate through woven materials, textiles as well as door and window curtains. Thus, an aerodynamic enclosure in space contains the Saharan dust particles in addition to the normal constituents of the air in such a mixture that both dust particles and the normal air molecules are indistinguishable by unaided vision but the settling particles can be seen on surfaces. Observations during the period show that the Harmattan leads to a quasi-stable concentration and homogenous aerosol suspension of Saharan mineral particles in space and time, and only changing slowly enough to enable hourly measurements.

Forest canopy

Tree canopy and structure also serve as an important sink for the aerosol particles by collecting them through impaction, interception, diffusion and gravitational settling. They serve as effective pathway for the particles to get into the forest ecosystem. Designers of town architecture would therefore be interested in the effectiveness of trees in protecting residential and office areas from the onslaught of the Saharan dust aerosol.

The atmosphere and Visibility reduction

The presence of the Saharan dust aerosol in the atmosphere gives rise to many optical processes, characteristic of colloidal solutions; apart from visibility reduction, we have colouration of the sky. Moreover, apart from the effect on the visible wavelengths, the solar radiation absorption and scattering are dependent on the quality of the aerosols.

One of the single and conspicuous consequences of the presence of the Harmattan is the opalescent atmosphere and reduction in visibility. During the Harmattan period, casual observation points to a strong relationship between visibility and dust concentrations in the atmosphere. It would be interesting to know the particle concentration in the various size-ranges especially the Saharan dust particle size range of 0.5-2 μm, which can affect visibility reduction most. It is known (Hinds, 1999) that visibility reduction due to atmospheric aerosols is governed by the concentration of particles in the size range 0.1 – 2 μm. For areas near the ITCZ, there is occasional heavy fog, which poses serious visibility threats as a result of moisture incursion from the moist southwest winds over high grounds and forest areas during the period.

Global circulations

The Saharan dust episode is a natural phenomenon, related to various other natural occurrences, including large-scale atmospheric circulations, like the movement of the Inter-Tropical Convergence Zone (ITCZ) (Resch et al., 2002) and the North Atlantic Oscillation (NAO) (Ginoux et al., 2005). Scientists are interested in the influence of these large-scale circulations on the Saharan dust phenomenon. This is because for example, on meeting the relatively wet southwest monsoon winds, the dust-laden northeast winds loose most of the dust particles through wash-out and rain-out at the ITCZ. Another large-scale weather feature that affects the northern hemisphere is the North Atlantic Oscillation (NAO). Large variations in the NAO index affect regional temperature and precipitation variability, agricultural yields, water management activities and fish inventories (Hurrel, 1995). The NAO index also appears to have a correlation with the Harmattan phenomenon. The full knowledge of these is attractive to scientists and is also approached in this study.

Industry
In industry, controlled and cleaner environments are essential in many areas of modern precision manufacturing technology where the presence of particulates can affect the reliability and performance of the product. This is especially true in aerospace equipment, electrical components and integrated circuits. And in high technology production processes where, for example, a single sub micrometer sized particle can lead to contamination of the circuits of semiconductor circuit boards. In the pharmaceutical and food processing industries, dust levels have to be controlled in order to reduce contamination and have uniform quality and products. Another area of importance is the need for air-quality monitoring to ensure that the industrial work force is not exposed to hazardous aerosols (for example, asbestos dust aerosol) at undesirable concentration levels. Thus a lot of effort and knowledge are needed on dust particle prevention in many industries.

Homes and offices
The Harmattan condition in Ghana lasts for about two months and during the period, cleaning and dusting costs increase for offices and home systems such as clothing, household gadgets, as well as national monuments, buildings and statutes. The dust deposits could be found on any available solid surface creating a nuisance. Apart from the dirt, there is extensive warping of wooden doors, windows and other wooden structures due to the low humidity associated with the Harmattan period. Understanding the characteristics of the Saharan dust will be important in resolving some of these problems.

Equipment design and performance
In the design of ventilation and air-conditioning systems, engineers would need to have a clear understanding and detailed knowledge of the physical and chemical properties of the particulates, including the size distribution and load as well as adhesive properties in order to select appropriate filters for a given system. Very dusty air may affect heat transfer equipment performance by, for example, blocking air passages and as a result reducing the cooling effect and increasing the running cost. Also, the impact of the Saharan dust on surfaces can produce large electrostatic charges that can affect the operation of electronic equipment. Therefore, prevention or reduction in the dust collection on equipment needs attention. The Saharan dust causes drastic reduction in direct solar radiation intensity. Therefore, in solar engineering, the amount of solar radiation received is affected and needs to be known precisely for the design of solar systems. On the other hand, for operating photovoltaic solar cells and pannels, the dust cover can cause serious reduction in the amount of solar electricity generation. Thus knowledge on the Saharan dust characteristics is crucial in solar technology too.

Signal transmission
In telecommunication and remote sensing, signal transmission through the atmosphere may be affected by the presence of Saharan dust particles, which increase the optical depth. Indeed, a change in the dielectric constants of the Saharan dust particles can lead to different transmission phenomena and a shift in reception of radio waves (Gibbins, 1988; Eyo et al., 2003).

Transportation and horizontal visibility

The dust episodes reduce horizontal visibility. In transportation, this often poses serious hazards in mainly air (for airplanes) and ground (rail and road) transport. Meanwhile, air safety is sometimes threatened too. Frequent cancellation of flights as a result of poor visibility causes a heavy loss of revenue annually to the countries affected by the Harmattan episodes. Poor visibility, often caused by thick Saharan dust haze, frequently results in disruption of aviation schedules and sometimes aviation accidents over West Africa sub-region, which can also lead to heavy loss of revenue annually. For example, because of the Saharan dust, visibility was only 300 m at Kano Airport, Nigeria, in the morning of 22 January 1973, when 183 people lost their lives in the crash of a Jordanian airliner (Adedokun et al., 1989). Another airliner, a Kenya Airways Airbus A310 jet carrying 169 passengers and 10 crew members crashed into the sea on the night of Sunday, 30th January 2000, shortly after takeoff from Abidjan. The flight originated in Nairobi and was meant to stop over in Lagos but flew directly to Abidjan because of a heavy dust haze that reduced visibility over Lagos and the airport stopped incoming flights. After a three-hour layover, the Kenya Airways Flight 431 took off at 9:08 p.m. and crashed into the Atlantic Ocean, off the Ivory Coast, one minute later. Immediate speculations among reporters and newspapers on whether the plane's engines could have been affected by the Saharan dust and sand were good assumptions. This was because the plane might have flown through the Saharan aerosol on course from Kenya to Abidjan as shown on the satellite data on the day of the accident. The satellite data show the streaks of dust being generated near Lake Chad and then transported in a southwest direction towards the Gulf of Guinea. The Navy Operational Global Atmospheric Prediction System (NOGAPS) weather model showed high winds in the Lake Chad region. The sun photometer data showed extremely high aerosol optical depths at Ilorin (near Lagos). The Navy Aerosol Analysis and Prediction System (NAAPS) aerosol model showed the dust being mobilized and then transported to Nigeria and the Gulf of Guinea. Most of the dust was below 4 km above ground level. (Extracted from Internet: Naval Research Laboratory, Marine Meteorology at www.nrlmry.navy.mil/ aerosol/case_studies/ 20000130_ivorycoast /-11k).

Crops and plants

The dust particles can harm plants and food crops and also coat the surfaces of leaves, reducing the amount of sunlight available for photosynthesis. The tiny pores (stomates) on the surfaces of leaves that allow carbon dioxide to enter for photosynthesis and water vapour to escape for transpiration also provide access for tiny dust particles. These particles can block the stomata and damage the chlorophyll leading to chlorosis or yellowing of leaves due to chlorophyll loss. Scientific knowledge on these processes is also important to understanding the Harmattan consequences. During the Harmattan period, farmlands become dry, as a result of the dry atmosphere, and hardened, forcing farmers to fallow the lands, thus prolonged Harmattan can cause drought and famine. However, on the positive note, the mineral sediments on farmlands may improve the nutrients of the marginal soil (Hayward and Oguntoyinbo, 1987; Swap et al., 1992; Tiessen et al., 1991).

Water surfaces

The mineral elements of the Saharan dust aerosols are transported into water bodies and the oceans resulting in significant concentrations of such elements. The Harmattan quartz and clay sediments would affect the chemical composition of the ocean-bed micro layer thus sustaining marine phytoplankton population (McTainsh 1999). However, the dehydrating effect on the weather during the Harmattan can make water-logged lands and ponds disappear, and their alluvial surfaces crack. The cracks may trap and absorb the settling dust particles, which may later affect the variation of the mineral elements in the water bodies.

Saharan dust sediments on solid surfaces

The mechanisms of deterioration of material exposed to the Saharan dust aerosol can occur as abrasion, deposition, removal, direct and indirect chemical attack or electrochemical corrosion. The particle settlement on exposed surfaces cause aesthetic deterioration to monuments, buildings and any exposed material. For most surfaces, it is the cleaning processes that cause the damage. For example, frequent washing of clothes weakens their fibres while frequent washing of painted surfaces dulls their finish. The Saharan dust collects in crevices, between materials and can cause oxidation and reduction reactions. Oxidation and or reduction reactions cause local physical and chemical differences on metal surfaces. These differences, in turn result in the formation of microscopic anodes and cathodes. Electrochemical corrosion results from the potential that develops in the microscopic batteries. Corrosion of materials is prevalent in the region and so scientists would be interested in the role of the Saharan dust aerosol on corrosion processes.

The human body

Aerosol surface properties such as adhesion, sorption (i.e. adsorption and absorption), and condensation are involved in a large number of chemical reactions including surfaces for micro-organism transport and the spread of air-borne diseases. It will therefore be interesting to know the influence of the Saharan dust on children and diseases like irritation in the throat, cold symptoms, catarrh and cerebrospinal meningitis (CSM), whose outbreak occurs in the Harmattan period (Hayward and Oguntoyinbo, 1987). The Saharan dust aerosol fills the surrounding air within which all atmospheric processes occur. The particles can directly affect the eye and skin, physically causing irritation to them. The Saharan dust also dehydrates the body causing injury to the parts sensitive to dryness such as the sides of the feet and lips of the mouth. The major effect is on the respiratory system of man and animals since dust particles smaller than 2.5 μm diameter can penetrate through the non-ciliated airways and then induce specific effects on the lungs (Wilson and Spengler, 1996). Scientists will therefore be interested in the Saharan dust particle size distribution, particularly in Ghana and West Africa.

Inhalation of particles

The Saharan dust aerosol particles reaching Ghana are mostly less than 20 μm in diameter. Sunnu (1997) observed that 95 % of the number of particles of the Saharan dust is composed of particle numbers with sizes less than 10 μm in diameter and the number of particles in the range 0.5-1.0 μm constitute 80% of the sample size range of 0.5-25 μm while Oduro-Afriyie & Anderson, (1996) found 98.7 % of the number of particles of the Saharan dust particle numbers in Accra to be composed of less than or equal to 5 μm diameter particles. Hence, the

Saharan dust particle size range reaching Ghana is very significant for breathing, which involves particles less than 2.5 μm diameter. Therefore, through respiration, Harmattan aerosol particles can reach the lungs, with possible health consequences on the respiratory system of mammals. The inhalation of large quantities of dust can result in a variety of lung damage, the degree of damage depending on the composition of the dust.
Although particle size is important, the shape e.g. asbestos, density and reactivity of the particles together determine how the particles are transported and react in the human respiratory tract. Target sites within the respiratory tract vary with aerodynamic size of particles as well as other factors. This can be seen by examining the variation of respiratory penetration and retention with particle size shown in the Table 1.1 below (Wilson and Spengler, 1996). Most of the particles greater than 10 μm in diameter and about 60-80% of particles between 5 μm and 10 μm are trapped in the nasopharyngeal region of the respiratory system. Larger particles are subject to inertial and centrifugal deposition before reaching the deeper respiratory system.
Very small particles (<0.1 μm diameter) penetrate and deposit deeper in the lungs by diffusion forces. Here, the air movement is slow and distances between surfaces are short. The lungs are least efficient at retaining the particle sizes that accumulate in the atmosphere. These particles circumvent many of the respiratory system's defence mechanisms, such as cilia, and are capable of delivering relatively high concentrations of potentially harmful substances, often causing severe damage at the cellular level. Thus it is observed that the effect on health due to aerosol particles inhalation is associated with fine particles rather than coarse particles.

Table 1.1. Respiratory penetration versus particle size. After Wilson and Spengler (1996)

Particle size (μm)	Respiratory penetration
11 ≤	Particles do not penetrate
7-11	Particles penetrate nasal passage
4.7-7	Particles penetrate pharynx
3.3-4.7	Particles penetrate the trachea and primary bronchi
2.1-3.3	Particles penetrate secondary bronchi
1.1-2.1	Particles penetrate terminal bronchi
0.65-1.1	Particles penetrate bronchioli
0.43-0.65	Particles penetrate alveoli

The following are some mechanisms underlying association between atmospheric particulate dust pollution and mortality: increased airways permeability and airways inflammation leading to impaired gas exchange and hypoxia (or acute oxygen deficiency), increased susceptibility to infection from impaired host defences, increased lung permeability leading to pulmonary oedema, provocation of alveolar inflammation by ultra fine (<0.02 μm) particles with release of mediators that exacerbate underlying lung disease and increase blood coagulability and specific toxicities, among others. Generally, ultra-fine particles cause greater inflammation than larger (coarse) particles of the same substance (Wilson and Spengler, 1996). Therefore, increased dust level in the tidal (respiratory / respirable) air can

also put a lot of stress on the respiratory system of mammals, resulting in chest and respiratory disease and sickness thus capable of increasing morbidity and mortality.

In all, the Harmattan phenomenon has major environmental and engineering implications as well as indirect economic importance. The interference of the dust particles with human health, climate, quality of life and general behaviour of the ecosystem calls for a better scientific understanding of this important weather phenomenon. This study is in that direction. It reflects the sub regional concern about the Harmattan by exploring the physical characteristics of the dust particles within the size range, 0.5-25 μm. This study is an attempt to give a comprehensive description of the Harmattan phenomenon, which will help in the development of solutions associated with the dust particle exposure in engineering, communication, signal transmission, tourism, environment and resulting health effects.

2. RELATED BIBLIOGRAPHY ON THE SAHARAN DUST HAZE

The Saharan dust episode in West Africa occurs as a result of the mobilization of dust particles deflated from the Sahara Desert and transported by the northeast trade winds. These dust particles have significant effect on the atmospheric environment and quality of life through the suspension and deposition of large amounts of the aeolian material. This chapter deals with the current knowledge of the Saharan dust phenomenon. Although this study focuses primarily on the presence of the Saharan dust in West Africa, it may be of interest, in our opinion, to present a more extensive literature review that covers the origin, physical and chemical characteristics as well as the propagation of the dust particles into other geographical regions of the world.

2.1. Atmospheric aerosol particles

Atmospheric aerosols are a collection of microscopic solid or liquid particles of various compositions suspended in the atmosphere with the exception of rain and snow, water droplets and ice crystals in clouds. These aerosols are generated by natural processes such as volcanoes, ground and sea surface sources, and by anthropogenic or human activities. The latter consists primarily of fossil fuel combustion and metal smelting, which produce gases containing sulphur, carbon, and nitrogen. Chemical reactions in the atmosphere convert these gases to suspended particulate matter mainly sulphate (SO_4^{2-}) compounds and elemental carbon. Aerosol particle sizes range from about 0.0001 to about 100 μm (Junge, 1963; Whitby, 1978) and include a wide range of phenomena such dry haze and smoke. Aerosol particles are microscopic in size, for example, by comparison, the diameter of human hair is between 50 -100 μm and is at the upper limit of the aerosol size range (Willeke and Baron, 1993).
Some interesting everyday experiences of aerosols include: smoke from fire (burning), which is a visible aerosol comprising particles of incomplete combustion and the hot air; liquid-particle aerosols formed by condensation or atomization, such as in nebulization or spraying; dust is a solid-particle aerosol formed by mechanical disintegration of a parent material, such as by crushing or grinding from mining activities, demolition, street sweeping and agricultural land ploughing, etc. Others are vehicle exhaust smoke and industrial stack fumes. The types of particles found in the atmosphere are classified as in Table 2.1 (After Junge, 1963; Brimblecombe, 1986; Piazzola, 1996) and their distributions are shown in Figure 2.1. Initial nuclei are formed by condensation of vapours or chemical reactions. This covers Aitken nuclei particles, viruses and positive or negative ions. These are always in suspension. They coagulate to form Aitken large particles comprising condensation nuclei most of which are sulphates, nitrates, chlorides, etc. The giant particles comprise particles from dust, pollen and spores, sea salt, forest fires, etc. These particles continuously diffuse into the atmosphere and are subject to various removal mechanisms including rain-out, wash-out and sedimentation. Thus, there is always a creation of small particles that grow larger and larger until they sediment out of the atmosphere by gravity or scavenged by hydrometeors or precipitation. Therefore, the lifetime and importance of an aerosol particle is very much dependent on its size. Their measurement is also strongly dependent on their size as shown in Table 2.2. Dust particles derived from soil are classified as clay when the size of the particles is less than 2 μm in diameter. Soil particles with sizes between 2 μm and 20 μm in diameter

are called silt and above 20 μm soil particles are termed sand (Eyre, 1963). Bagnold (1971) classified soil particles as dust when the diameter of the particles is between 1.0 and 10 μm and between 0.1 and 1.0 μm, it is named dust haze.

Table 2.1. Nomenclature for atmospheric particles (Junge, 1963; Brimblecombe, 1986; Piazzola, 1996).

Diameter (μm)	Particles	Nuclei	Samples
10^{2}			Snow, rain
	Giant particles		Pollen, sea spray,
10^{1}		Dispersion nuclei	cloud, fog, dust
		Coagulation nuclei	Sea salts,
10^{0}			products of combustion, mist,
	Large particles		industrial fumes
10^{-1}		Initial nuclei	
10^{-2}	Aitken particles		Viruses
10^{-3}			
10^{-4}			Gas molecules, ions

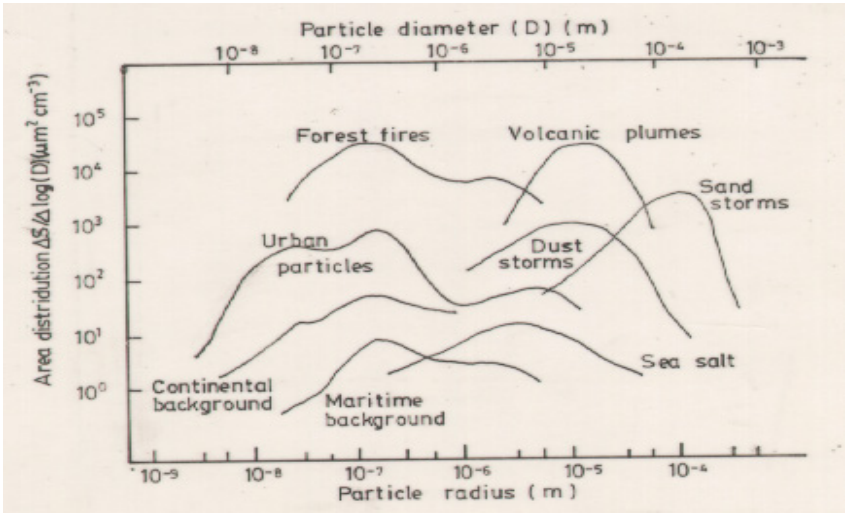

Figure 2.1. Distributions of different types of atmospheric particles (after Slinn, 1983).

Table 2.2. Particle types and their method of measurement (Stern et al., 1984).

Particle diameter (μm)	Type of particle	Method of measurement
10^{-3} - 10^{-1}	Aitken and large nuclei	Electron charge carried by particles, measured by electron microscopy method.
10^{-1} - 10^{-0}	Condensation nuclei	Electron microscope, optical counters.
10^{0} - 10^{1}	Dust, fumes	Optical microscope, optical counters, high-volume samplers (PM-10, PM-2.5)
10^{1} - 10^{2}	Dust, fumes, pollen, etc.	Filtration (followed by gravimetric, microscopic, chemical analysis, etc.); Inertial (impactors and cyclones), gravitational, centrifugal, thermal precipitation techniques and optical counters.

Natural background aerosols

As pointed out above, atmospheric aerosol sizes range from about 10^{-4} to 10^{2} μm. The behaviour of the aerosol particles follows physical laws, which are strong functions of the particles size. As a result, the particles have been observed to have definite behaviour in various size classes. According to Renoux and Boulaud (1998), the atmospheric aerosols distribution can be found in three modes namely: the nuclei mode, which comprise particles less than 0.08 μm and involves particles formed from mainly gas-to-particle conversion; the accumulation mode, which include particles from 0.08 to 2 μm; and coarse particle mode, which involve particles larger than 2 μm and are mainly created from soil dust, sea spray, botanical debris, volcanic dust and forest fires. The average natural background aerosol number concentrations for the three modes are 6400 cm^{-3}, 2300 cm^{-3}, and 3 cm^{-3} respectively according to Hinds (1999). Each size distribution can also be represented as a lognormal distribution. The count median diameter sizes for the various distributions are (Hinds 1999): around 0.015 μm for the nuclei mode, 0.076 μm for the accumulation mode and 1.02 μm for the coarse-particle mode. Figure 2.2, after Whitby (1978), summarises the background–level aerosol size distributions (Renoux and Boulaud, 1998).

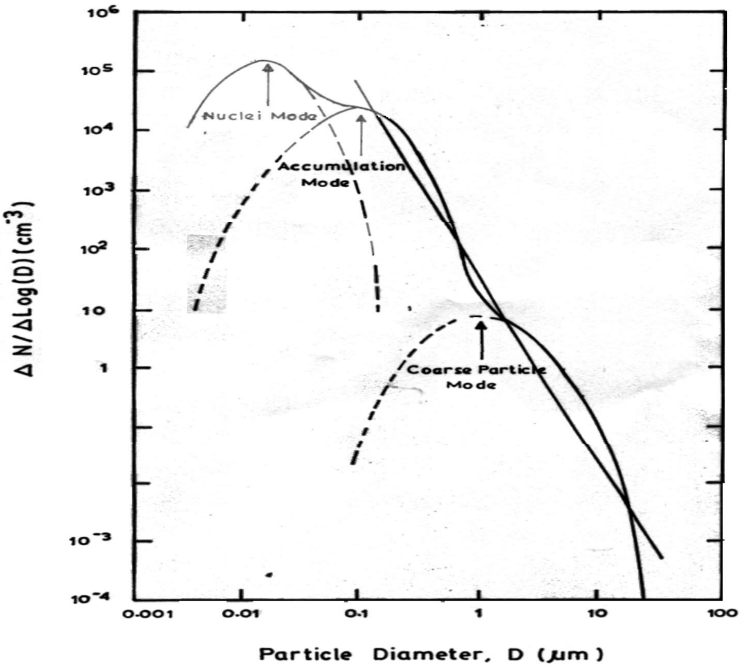

Figure 2.2. The distribution of the three atmospheric natural background aerosol modes: nuclei mode, accumulation mode and coarse particles mode, after Whitby (1978).

2.2. The Saharan dust haze

The Saharan dust haze is one of the many aerosols in the atmosphere and it is important to show the relationship between the various aerosols. The current understanding of the transport of the Saharan dust has been achieved through various studies (Schutz and Jaenicke, 1974; D'Almeida and Schutz, 1983; Hamonou et al., 1999; Prospero, 1999; etc.), which focused on the climatology, frequency of occurrence, areal extent of impact, vertical distribution, total mass loadings, and origin of the dust particle characteristics and others. These were derived from a limited number of discrete measurements, a limited number of ship haze observations, atmospheric optical thickness measurements, visibility studies and remote sensing research. Measurements of the Saharan aeolian aerosols have been conducted in West Africa, over the Atlantic Ocean and the islands in it as well as the lands near the Gulf of Mexico, south-eastern North America, North Africa and Europe (Hamilton and Archbold, 1945; Carlson and Prospero, 1972; Griffiths et al., 1972; Bertrand et al., 1974; Samways, 1975; Glaccum, 1978; Dubief, 1979; Kalu, 1979; Morales, 1979, 1981; McTainsh, 1980; Schutz, 1980; Cox et al., 1982; McTainsh et al., 1982; McTainsh and Walker, 1982; Adedokun et al., 1989; Tiessen et al., 1991; Swap et al., 1992, 1996; Adeyafa et al., 1995; Arimoto et al., 1992, 1995; Gatz and Prospero, 1996; Herwitz et al., 1996; Perry et al., 1997; Romero et al., 1999; Prospero, 1979, 1999; Karyampudi et al., 1992; Chiapello et al., 1995; Moulin et al., 1997; Chiapello and Moulin, 2002; Chiapello et al., 2005; Kaufman et al., 2005). Further, data acquisition of the Saharan dust and studies are still in progress such as the Aerosol Robotic Network (AERONET) at the website, http://aeronet.gsfc.nasa.gov/ (Holben et al., 1998) and this research is in that direction, that is, to provide a long-term measurement and analysis of the Saharan aeolian dust during the dry season, sufficient to yield a representative and accurate description of the Harmattan phenomenon in West Africa.

However, very little is known about the size and number distributions of the dust particles especially at low latitudes near the Gulf of Guinea (5°N), such as in southern Ghana.
The climate of Ghana is characterised by two main seasons: the dry season and the wet (or rainy) season. The advent of these two seasons is dependent on the migratory position of the Inter-Tropical Convergence Zone (ITCZ) or the Inter-Tropical Discontinuity (ITD) between the dry northeast trade winds carrying dust from the Sahara Desert and the wet southwest monsoon winds, which blow inland from the Gulf of Guinea. During the Harmattan season, the ITCZ and the dust-loaded northeast winds can descend to latitudes as low as 5°N (Griffiths et al., 1972; Adeyefa et al., 1995) while during the rainy season, the dry northeast winds are restricted to latitudes above 20°N and the dust-free, humid south-westerly winds from the Gulf of Guinea predominate (Schutz, 1980) with the rains.
In order to understand the phenomenon of the Saharan dust in the atmosphere, there is the need for an adequate knowledge of the source areas, their location and strength as well as the seasonal and long-term variations. Such information, which is abundant in print literature and the Internet, will enable more reliable estimates to be made of the fluxes leaving the Sahara, their fate in the atmosphere and their composition elsewhere (Karyampudi et al., 1992; Chiapello et al., 1995; Swap et al., 1996; Moulin et al., 1997; Marticorena et al., 1997; Prospero, 1999; Hamonou et al., 1999; Chiapello and Moulin, 2002; Chiapello et al., 2005; Kaufman et al., 2005). However, changes in the source strength over long periods may also be significant. There have been suggestions (Prospero and Nees, 1977) that there was a three-fold increase in the dust concentration in Barbados between 1965 and 1976 and this might be due to an increase in the source strength in the Sahel, possibly associated with the drought in this region.
The production of dust in the desert has been related to variables of surface soil texture, wind speed, vegetation, vegetative residue, surface roughness, soil aggregate size distribution and soil moisture and rainfall. Soil texture or aggregates which may be in the form of a surface crust, large clods, small pellets of soil, largely determine the threshold velocity and intensity of deflation (Chepil, 1945; Gillette, 1980; Bagnold, 1971; Marticorena and Bergametti, 1995). The packing and inter-particle cohesive forces of very small particles may make them difficult to entrain whereas larger particles will be too heavy to be lifted by the erosive forces. Vegetation exerts an influence in various ways: by the stabilisation of soil by roots, by absorption of some momentum flux to the soil surface, by alteration of the moisture, and by decay which adds organic material to the soil. Vegetative material protects the surface by covering the soil. Vegetation, rocks and boulders, which are non erodible absorb the wind stress and reduce particle mobilisation. Roughness of the soil traps sand grains and inhibits saltation. Soil moisture and rainfall help to stabilise the soil and prevent erosion. Dubief (1979) and Kalu (1977) compiled the occurrence of dust storms of different areas in the Sahara Desert. They established that there were different kinds of disturbances affecting different parts of the Sahara during different seasons. In winter, dust storms are connected with the Mediterranean polar front with upper tropospheric troughs. In summer, they are related to easterly winds associated with the Inter-Tropical Convergence Zone (ITCZ) and the North Atlantic Oscillation (NAO).
The areas in the Sahara Desert from which most of the air-borne particulate matter originate are referred to as the source regions (D'Almeida, 1986; Prospero, 1999; Brooks and Legrand, 2000; Prospero et al., 2002). Identification of these areas has been made by different techniques including satellite observations, comparison of aerosol element composition,

comparison of aerosol and soil sample colour, monitoring of air mass trajectory and visibility distribution analysis (Bertrand et al., 1974; Morales, 1979, 1981; Kaufman et al., 2005). Thus some authors including McTainsh et al., (1982), in Kano, Nigeria; Adedokun et al., (1989) in Ile Ife, Nigeria, inferred from element composition analysis of the settling Saharan dust particles to establish that the Chad basin is the major source area of dust over most parts of West Africa.

D'Almeida (1986) and Brooks and Legrand (2000) have provided estimates of the annual and monthly dust emissions from the Sahel and Sahara Desert of the northern Africa. Figure 2.3 is taken from Brooks and Legrand (2000). It shows the annual average dust production over northern Africa as indicated by time-average Infra-red Difference Dust Indices (IDDI) values for 1984-1993.

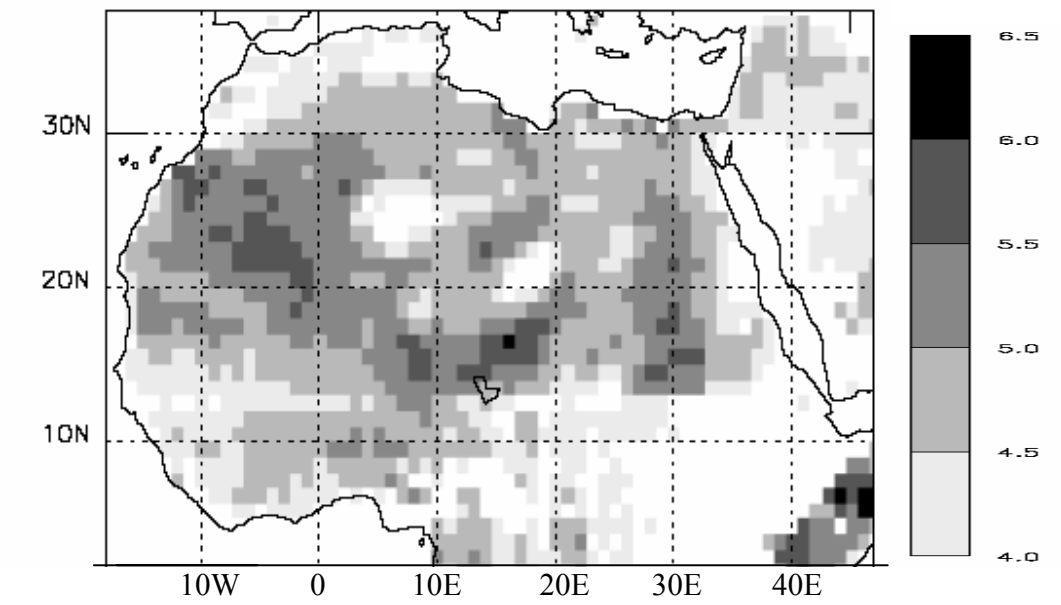

Figure 2.3. Location of the major source areas for airborne dust after Brooks and Legrand (2000). The shades are the IDDI. On the colour bar, on right, darker shades indicate higher dust loadings. The scale is in Kelvin.

The dust reserves in the Sahara Desert are composed of rocky deserts, principally igneous rocks and calcareous crusts, clay plains, sand dunes, gravely soils, loamy soils, salt deserts, and sandy deserts. The fluvial transports of sand from the overflowing water bodies including the Chad, which overflowed its banks about nine occasions in a past hundred and fifty years, (Touchebeuf de Lussigny, 1969) supply additional deposits of clay, silt and fine sand particles in the source regions.

The Sahara soils have been analysed by D'Almeida and Schutz (1983), and Schutz and Jaenicke (1974). They showed that soils from central Sahara Desert (from Libya) show a distribution in the size ranges of 0.01 μm to 1000 μm in radius with a mode of 0.1 μm in radius for mineral soil samples. For mineral aerosol samples, they obtained a range from 0.01 μm up to over 100 μm radius with a nuclei mode from 0.06 to 0.08 μm radius. These fine

soils might be loosely packed to enable mobilisation as dust storms and to be transported by wind over long distances.

The dominant mineral compositions of the Saharan dust observed are clay minerals and quartz as well as other primary minerals including feldspars, kaolinite and mica (Adedokun et al., 1989; Oduro-Afriyie and Anderson 1996; Tiessen et al., 1991). Meanwhile, the composition of the soils on Bermuda are found to be consistent with Saharan dust sources and shows little evidence of inputs from North America (Herwitz et al., 1996; Glaccum and Prospero, 1980). The elemental composition of the dust sources have also been compared with the elemental composition of the soils of the West Atlantic and found to be consistent (Glaccum, 1978; Arimoto et al., 1992, 1995; Gatz and Prospero, 1996; Herwitz et al., 1996; Perry et al., 1997) while Herman et al., (1997) and Husar et al., (1997) used various satellite products to arrive at the same conclusion.

So far, there is no doubt about the origin of the Saharan dust from the Sahara Desert and Sahel. And that it is the same dust that constitutes a major component of the atmospheric aerosol during the Harmattan season. Also, in connection with the dominant wind direction, the Saharan dust haze over West Africa is found to originate from several dust sources but a dominant source has been reported to come from the Faya Largeau area in the Chad basin (Hamilton et al., l945; Kalu, 1977; McTainsh, 1980; McTainsh & Walker, 1982). This is because the main transporting agent, the Northeast trade winds, blow from the Sahara Desert in a Southwest direction across the West Africa region. In particular, it is noted that dust sources around the Chad basin especially in the Bodele depression affect the countries around the Gulf of Guinea. Additional supplies of dust from fluvial and wind activity in Tibesti mountains, which are not dust sources but can provide dust material to be transported by water along wadis or temporary water courses to the Bodele depression, have been recorded by Kalu, (l977); Balogun, (l974); Adedokun, et al., (l989) and Tiessen et al., (l991). The fluvio-lacustrine (river-lake) transport systems within the desert are believed to be efficient to supply and replenish the clay and silt components of the lake deposits in this source area.

D'Almeida and Schutz, (1983) reported a direct method to determine the mineral size distribution of aerosols and topsoils of the desert dust sources. The desert aerosol was sampled using a high volume sampler of flow rate, 100 m^3/h. This was followed by wet sieving and transfer of particles onto membrane and nuclepore filters for sizing and counting using a scanning electron microscope and an optical microscope. They found all mineral aerosol size distribution to indicate a maximum between 0.06 and 0.08 μm radius while the volume distributions showed modes at 3 μm and 30 μm radius. The soil size distribution showed a maximum at 0.1 μm radius while the soil volume distribution revealed two modes, one less than 5 μm radius and one in the larger particles. Schutz and Jaenicke (1974) conducted similar analysis on the soil and aerosol particles of the Libyan desert in central Sahara Desert covering particles larger than 1μm in radius and observed similar distributions. D'Almeida (1985) measured the source strength and deposition rate of the dust emerging from the Sahara Desert using turbidity results from sun photometers, which were installed at 11 stations in the Sahara Desert and surrounding areas. A dust mass concentration measurement was also done at one of the stations for correlation with the turbidity and hence estimated the mass production of the Saharan dust to be between 630 x 10^6 and 710 x 10^6 tonnes per year for all suspended particulate matter and between 80 x 10^6 and 90 x 10^6 tonnes per year for aerosol particles smaller than 5 μm radius. Peterson and Junge (1971) had earlier

estimated the global contribution of wind-blown dust derived from soil erosion to be approximately 500 x 10^6 tonnes per year. Their rough calculation was based on average concentrations and residence time. D'Almeida (1985) further assessed the dust moving southwards to the Gulf of Guinea to be 60 %, 28 % westwards towards the equatorial North Atlantic Ocean and 12 % northwards towards Europe. He finally presumed that a considerable part of the dust is deposited in the Atlantic Ocean and the Mediterranean Sea forming deep-sea sediments. D'Almeida (1985) also obtained from his model, an amount of between 350 x 10^6 and 410 x 10^6 tonnes per year of all suspended dust particles towards the Gulf of Guinea and for dust particles involved in long-range transport (particles of size less than 20 μm) he obtained between 45 x 10^6 and 35 x 10^6 tonnes per year. His work also points out that the dust mobilisation takes place throughout the year but is particularly strengthened between March and June. The transport direction is determined by the general wind circulation pattern over the desert and areas affected by the dust particles. The dust plume travelling towards the Gulf of Guinea is strengthened during wintertime being promoted by the prevailing northeast trade winds. He further traced the source region of the Saharan dust towards the Gulf of Guinea to the lowlands around Dirku in Niger and the Faya Largeau area. The dust production and transport in the rainy season (summer) is scavenged by the wet southwest monsoon winds, which prevails then up to the desert. Thus he also confirmed that the region south of the ITCZ is shielded during this season from the dust-loaded winds, coming from the Sahara. He further pointed out that there is a dust transport to the west towards the equatorial North Atlantic and the Antilles throughout the year as observed by Schutz (1977), and Carlson and Prospero (1972). He noted that the amount of dust towards Europe is less pronounced, sporadic and occurring in summer but not negligible as observed by Schwiskowski et al., 1995 and Bergametti et al., 1989. The general circulation over the Sahara prevents the eastwards transport that only occurs occasionally.

2.3 Saharan dust transport

Saltating sand-sized particles on the surface break larger aggregates into smaller particles which can go into suspension in a process called sandblasting, which is the main mechanism responsible for the deflation and transport of the Saharan dust. The prevailing north-east trade winds show the direction of the dust plumes. It is known that the Saharan dust is not transported everywhere all year round but it is transported in discrete, concentrated, latitudinal and longitudinal (towards Europe) corridors that vary in all directions throughout the year. The nature of the deflation, transport, and deposition of the aeolian dust material from the Sahara is episodic and has aslo been linked to seasonal and annual rainfall as well as large-scale weather features such as the Inter-Tropical Convergence Zone and the North Atlantic Oscillation. The latest technique of tracking the Saharan plume is remote sensing of the dust air parcel trajectories using satellite imagery and atmospheric transport models, which makes it possible to predict large areas that will be impacted by specific dust events (Swap et al., 1996; Moulin et al., 1997; Karyampudi V. M. et al., 1999; Hamonou et al., 1999; Brooks and Legrand, 2000; Chiapello et al., 2005).

2.3.1 Influence of winds

The north-east trade winds which blow across the Sahara Desert towards the Gulf of Guinea during northern winter is the most important parameter responsible for the propagation of the dust particles. Thus, as a result of the wind activities (Adedokun, l989), a continuous vertical flux of dust particles builds up a dust reservoir several kilometres thick within the atmosphere of the Sahara Desert (Schutz, l980). The dust generated is fed into the major trade winds system and consequently transported across the desert's margins. In central Ghana (6.5^{o}N), the Sahara dust haze is suspended by a stable low velocity wind of about 2 m/s (Sunnu, 1997).

Most of the particles carried by the N-E trade winds are scavenged, washed-out or rained-out on meeting the S-W monsoon winds, which have high moisture content. The transport of Saharan dust over West Africa is thus a seasonal phenomenon with the migration of the ITCZ as an important parameter. During summer (May-October), the regime of the N-E winds with the dry dust load are restricted to above 20°N (Barry et al., 1992). Adeyefa et al., l995 recorded that during the Harmattan season, the ITCZ is observed at longitude 3° E between 5 °N and 10 °N. The N-E winds carrying dust can then reach the Gulf of Guinea (McTainsh,1980). About 87% of these winds blow from between east and north (McTainsh and Walker, 1982), thus indicating the principal direction of the dust transport (Figure 2.4).

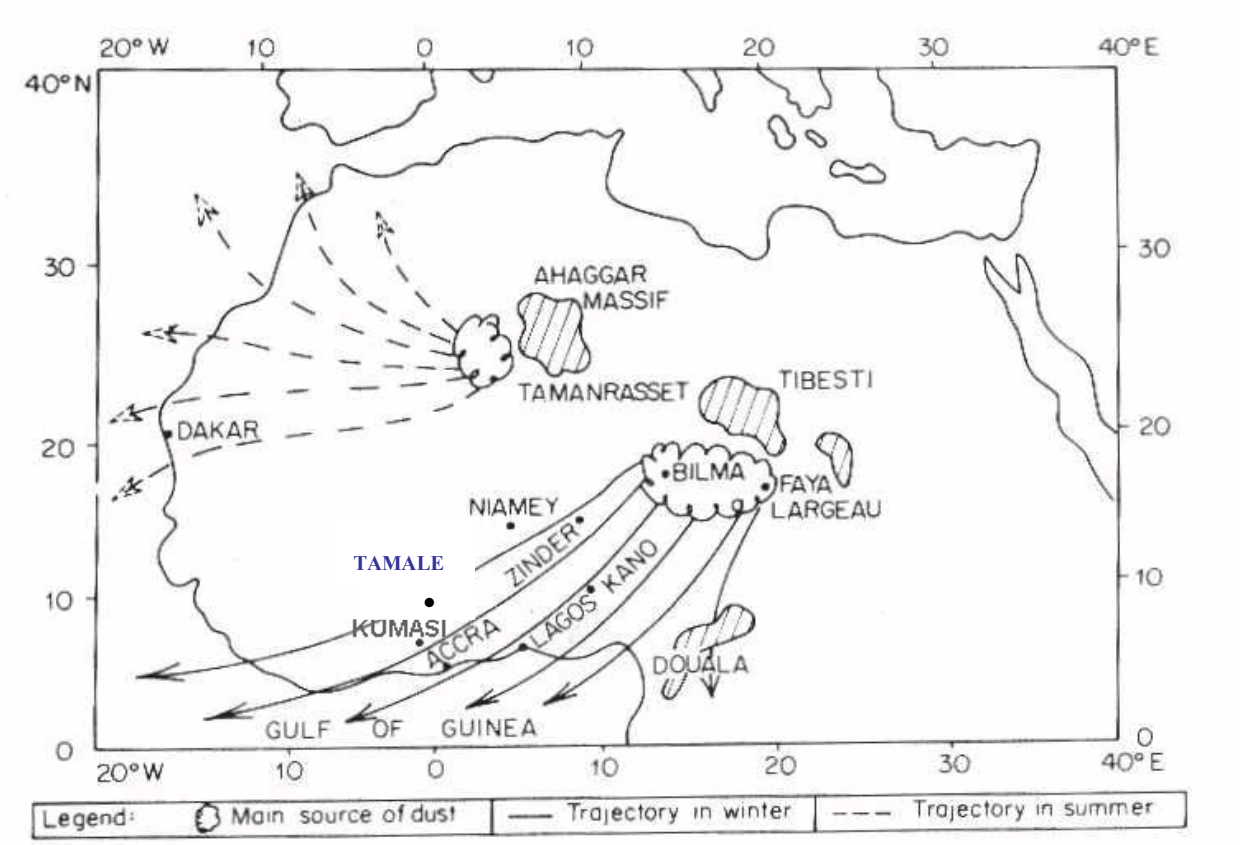

Figure 2.4 Saharan dust trajectories in West Africa, reference: Kalu (1977).
(Also indicated are the cities of Kumasi and Tamale)

2.3.2 Influence of temperature and convective activities on dust mobilisation

Intense heating of the bare desert gives rise to high surface temperatures. For example, Cloudsey-Thompson (l964) obtained about 80°C on an extreme sand surface temperature at Wadi Halfa, Sudan, and near-surface temperature of 58°C at El Azizia, Libya. The high surface temperatures promote a steep lapse rate at lower layers enabling a strong convective activity and turbulent fluctuations, during the day. As warmer air rises, a low pressure area is created. Air from higher pressure areas rushes in giving rise to surface winds which can strongly enhance the dust mobilisation during the daytime. These processes create the lift force required to initiate particle entrainment and mobilisation from the source region. At night, the absence of clouds enables rapid loss of long wave radiation that can cause an inversion, which prevents mobilisation. This results in large scale atmospheric cooling and subsequent decrease of temperatures between midnight and early morning hours. The inversion also produces stability in the atmosphere thereby suppressing the vertical motion that causes the vertical spreading of dust.

2.3.3 Dust transport models

A number of authors (Gillette and Goodwin, 1974; Gillette, 1974, 1981; Fairchild and Tillery, 1982; Babiker et al., 1987; Borma and Jaenicke, 1987; Tsoar and Pye, 1987; Gillette and Passi, 1988; Cautenet et al., 2000; Marticorena et al., 1997) have adopted the technique of modelling involving mathematical expressions to estimate the dust deflation, dispersion and deposition. The models are based on main surface features including the erosion threshold wind friction velocity, which is dependent on effects of vegetative residue, roughness of the soil, live standing plants, soil texture and nature as well as effects of atmospheric precipitation. The model outputs are the total quantity of soil particles mobilized by wind (horizontal flux) and the flux of dust particles emitted into the atmosphere (vertical flux). Gillette and Goodwin (1974) developed a mathematical model that expresses the dependence of the concentration of dust particles at a given height on vertical diffusion and sedimentation. The approach treats sand as a diffusion agent rather than as projectiles that are affected by the wind only on the horizontal direction. Thus the vertical profiles of the horizontal flux of sand-sized particles observed during soil wind erosion incidents may be simulated by the model. Good agreement was found for horizontal fluxes larger than $5x10^{-4}$ g/cm.s. Babiker et al., (1987) have shown the mass flux of erodible soil transported by a statistically distributed wind flow has a statistical distribution. Gillette and Passi (1988) also devised a model for estimation of total dust production caused by wind erosion. Marticorena et al., (1997) developed a model to estimate the quantity of the Saharan dust flux emitted during significant dust events.

2.4 The Saharan dust particle measurements

Literature on the Saharan dust shows that measurements have been conducted in the principal regions affected by the dust transport including West Africa, the North Atlantic and the Caribbean as well as the Mediterranean Basin and Europe.

2.4.1 Characteristics over West Africa

McTainsh (1980), studied the Saharan dust deposition measurement at Kano in Nigeria. He confirmed that the dust originates from the Faya Largeau area in the Chad basin. The sampling technique employed involved a dust trap constructed from a basin of distilled water and placed at 9 m above ground level on the roof of a building on the campus of Bayero University in Nigeria. This height ensured that the trap was isolated from local soil dust movement. The dust laden distilled water was evaporated in the laboratory oven and the residue weighed and analysed. He obtained 99.1 g/m^2 being the total Saharan dust deposition at Kano in 1978-79 Harmattan period. By this technique, he could not determine the size distribution of the particles.

McTainsh and Walker (1982) extended the study started by McTainsh (1980) by adding dry deposition measurement (empty basin covered with mosquito netting wire mesh) and sampling at five cities. The main measuring site was at Bayero University in Kano and the other occasional sites were Zaria which is 180 km southwest of Kano, Maiduguri, Jos and Sokoto. The dust deposition rate measured at Kano range from 137 to 181 $t/km^2/yr$. They noted that the Harmattan winds at Kano were gentle at ground level with a mean daily maximum speed of about 8 m/s and that they blew from a constant direction. They observed that the Harmattan at Kano sometimes reduced visibility to about 500 m. The dust samples collected in dry traps were washed out with distilled water, oven-dried and weighed, followed by particle size analysis with sieves, Coulter counter, ultrasonic probes and for the mineralogy, X-ray diffraction and fluorescence analysis were used. Measurements of the rate of deposition was made with one exceptionally severe event, during 3-14 March 1977, recording 54 $tonnes/km^2$ being about 39 % of the total for the season. The spatial deposition rates decreased downwind and also in the direction transverse to the direction of movement of the dust plume (e.g. Kano, Zaria and Jos). Clearly, while one single intense event, over thirty years ago, would provide useful information on dust transport and dust loading of the atmosphere, without more detailed measurements or models, such studies may not contribute significantly to the body of knowledge of the dust processes.

Adedokun et al., (1989) reported the physical, mineralogical and chemical properties of the Saharan dust at Ile-Ife in Nigeria. They collected the dust in clean petri dishes exposed on tall buildings and used X-ray diffractometry for the analysis. The chemical composition was done using a Perkin-Elmer atomic absorption spectrophotometer. The mineral composition shows mostly quartz at over 70 % followed by microcline, kaolinite and traces of mica and halloysite. They recorded predominance of SiO_2, which is over 60 % followed by Al_2O_3 (17.4 %), Na_2O (10.1 %), Fe_2O_3 (5.6 %), TiO_2 (3.33 %), K_2O (1.88 %), MgO (0.56 %), and CaO (0.37 %). The following trace elements were also identified: Zn (931 ppm), Mn (83 ppm), Ni (113 ppm), Cr (103 ppm), Cu (106 ppm), Co (77 ppm), V (65 ppm) and Li (25 ppm). In addition, they measured the size distribution of the Saharan dust particles using techniques of dry deposition on glass slides exposed at the top of 20-30 meter high buildings followed by microscopy. They obtained a mode of 2.5 μm, a mean diameter of 3.12 μm with a standard deviation of 1.59 μm. They further alluded to the origin of the Saharan dust affecting the region to come from the Chad basin indicating that their fine nature makes them easy to be deflated and transported.

Tiessen et al., (1991) reported the deposition of the Saharan dust and its influence on base saturation of soils in northern Ghana. They collected the dust during the Harmattan period on

plastic sheeting placed in sheltered positions in Nyankpala (9^o 23' N, 0^o 59'W), near Tamale during two Harmattan seasons and Bolgatanga (10^o 47'N, 0^o 51'W) during several Harmattan seasons. They observed that the Saharan dust samples in northern Ghana contained base-rich primary minerals including Mg, Ca, K, Na, Mn, Ti, Al, Fe, as shown by X-ray microscopy and chemical analysis. Further findings include: the base saturation of top soils are generally above 80 % and composed of high iron and aluminium oxides contents and mineralogy dominated by quartz and low activity clays and generally deficient in basic cations. They therefore reported that the long-distant travelling Saharan dust had a clearly finer particle size distribution than dust collected during local storms within the Harmattan period. However, they were not able to quantify the sizes of the particles. They also noted that the angularity and evidence of weathering on the dust particles did not distinguish dust from different sources. The Bolgatanga soils contained unweathered minerals derived from local parent materials and both local storm and Saharan dust contain large amount of bases. Significant amount of micas and feldsparths and potassium (K) contents up to 3 % in the dust collected at Nyankpala showed the Saharan dust to be the source of K and other bases found on the Volta shale soils. Short distance drifting dust particles in Nyankpala was mostly quartz. Saharan dust deposition in one Harmattan season in Nyankpala amounted to about 15 g/m^2 and carried a total of 140, 400, 300, and 60 mg $/m^2$ of Mg, Ca, K, and Na respectively. These amounts could account for the high base saturation of the soils in the Volta shale soils. Their work did not explain the physical characteristics of the Harmattan as well as the influence of large-scale circulations such as the NAO and the ITCZ.

Adeyefa et al., (1995) studied the spectral solar irradiance under Harmattan conditions at Ile Ife in Nigeria. Their studies show that Angstrom atmospheric turbidity coefficients β, which is related to the amount of aerosol particles present and $\beta_{0.5}$ (0.5 referring to 0.5 μm) measured high values of 1.06 and 1.38 respectively. The average value of the wavelength exponent which relates the particle size and frequency of distribution, α for the wavelength interval 0.35-1.038 μm was about 0.5. They derived a classification of the Harmattan as periods with moderate characteristics (background Harmattan) and periods with intense spells. The mean background conditions had β values ranging from 0.99 (at 0.35 μm) to 0.53 (at 0.862 μm) while Harmattan spell conditions, which have higher turbidities vary from 1.95 at 0.35 μm to 1.51 at 0.862 μm. They observed that there were severe reductions in direct solar irradiance at Ile Ife during this period due to the strong attenuating effect of the Harmattan in accordance with general behaviour of dust particles with sizes comparable to the wavelength of visible solar radiation. They also studied the dependence of the movement of the ITCZ on the dust concentration, noting that the coefficient α, increased with the northward movement of the ITCZ and decreased when it moved southwards. The parameters β, and $\beta_{0.5}$ decreased when the ITCZ moved north of a station and increased when the ITCZ moved south of the station during the Harmattan period. This observation complements this study by examining the relationship between the ITCZ and the Saharan dust concentration in the region.

Oduro Afriyie and Anderson (1996) reported on the analysis of the Saharan dust over Accra in Ghana during the 1993/94 Harmattan periods. They used glass slides placed on top of tall buildings to collect the dust samples for size determination followed by gravimetric analysis. They obtained a mass of about 4.8 g/m^2 during the 1993/94 Harmattan period. The particle size analysis indicated that majority of the particles have a diameter of more than 1 μm with mean, mode and median diameters of 2.11, 2.00 and 1.73 μm, respectively. The X-ray

fluorescence analysis showed the following elements with the order of abundance on mass basis as Fe>Ca>Cu>Ti>Zr>Pb>Sr>Rb>Y>Nb. The neutron activation analysis showed the presence of Na, K, Mn and Mg. Clearly, this work gives a rough estimate of the settling particles and rather focuses on the chemical composition analysis of the Saharan dust.

2.4.2 Characteristics over North Atlantic and the Caribbean

The transport of Saharan dust over the North Atlantic was studied by Prospero and Carlson, 1972; Prospero, 1979; Schutz, 1980; Schutz et al., 1980; Cox et al., 1982; Chiapello et al., 1995; Swap et al., 1996; Moulin et al., 1997; Karyampudi et al., 1999; Prospero, 1999; Kaufman et al., 2005. Prospero and Carlson (1972) estimated the dust deposition rates over the Atlantic ocean to be between 2 and 10 mm/kyr. Delaney et al., (1967), reported 0.6 mm/ kyr for the same area. These deposition rates are far lower than the amount expected in West Africa. Prospero (1979) showed that the highest concentration of soil dust deflated by the trade winds from the Sahara Desert to Bermuda and the tropical North Atlantic Ocean amounted to a geometric mean of 14.2 $\mu g/m^3$ and that most of the dust is deposited in the ocean by washout and rainout. Schutz (1980) observed that the vertical extent of the dust particle cloud on the Sahara could reach 6 km. Variations in the diurnal deposition rates with day values higher than the night values observed, were attributed to night temperature inversion at low altitudes. The spatial spread of the WSW moving dust plume passing over West Africa has been identified from satellite imagery and from visibility records (Samways, 1975; Prospero and Carlson, 1972; Schutz et al., 1981; McTainsh and Walker, 1982; D'Almeida, 1985; Adedokun et al., 1989; Adeyafa et al., 1995; Swap et al., 1996; Oduro-Afriyie and Anderson, 1996; Prospero, 1999; Chiapello et al., 2005). The particle size range, the mineralogical and geochemical characteristics of the deposited particles were linked to the Chad basin soil dust source. They also proposed a Harmattan aeolian system as a result of fluvial and wind activity that recycles dust from the source in the Chad basin (Prospero and Carlson, 1972). The annual mineral mass budget of the Sahara dust plume was estimated using the transport model devised by Schutz (1980). He proposed that the main transport across the north Atlantic takes place within a transport channel of about 1000 km wide (15^o-25^o N) and 3.5 km high (1.5 km – 5 km altitude). He estimated that approximately 260 x 10^6 tonnes per year of mineral dust leave the desert towards the west. This Figure compares well with an estimate by Lepple (1975) on the order of 290 x 10^6 tonnes per year for the same latitudinal band. About 50 x 10^6 tonnes per year reach the Caribbean area. The Figure also agrees reasonably well with the half annual flux of about 37 x 10^6 tonnes per year reported by Prospero et al., (1972).

Cox et al., (1982) monitored terrestrial lipid detritus in the dusts collected off the West African coast associated with the Saharan aeolian transport and related it to some pelagic (oceanic) sediments in the North Atlantic while Swap et al., (1996) reported the temporal and spatial characteristics of the Saharan dust outbreaks over the northern Atlantic Ocean using NOAA's Advanced Very High Resolution Radiometer (AVHRR) aerosol optical thickness (AOT) data. They found an annual westward mass fluxes of the Saharan dust on the Atlantic Ocean, bounded by the Equator to 40^oN latitude and 20^oE to 80^oW longitude which corresponds to ocean surface area of about 2.6 x 10^6 km^2, to range from a minimum of 130 Megatonnes for 1990 to a maximum of 460 Megatonnes for 1991.

Moulin et al., (1997) reported the seasonal migration of the dust concentration to be associated with the latitudinal movement of the large-scale circulations, NAO and the ITCZ during winter. This is one of the first attempts to study the relationship between the Saharan dust and the NAO. The present study will examine in more detail the relationship between the Sahan dust in West Africa and the NAO. Prospero (1999) reports the long-term measurement of the transport of the Saharan dust to the southeastern United States. He reported daily concentrations in the range of about 10 $\mu g\ m^{-3}$ to 100 $\mu g\ m^{-3}$. He observed that the maximum dust concentration occurred in July (monthly mean, 16.3 $\mu g/m^3$), but relatively high concentrations are also observed in June (8.4 $\mu g/m^3$) and August (9.8 $\mu g/m^3$).

2.4.3 Characteristics over the Mediterranean Basin and Europe

The transport of the Saharan dust to the Mediterranean Basin and Europe is less pronounced but quite significant. Schwikowski et al., (1995) observed the deposition of the Saharan dust episode in the period, 20-23 March 1990. They studied the physical and chemical composition of the Saharan dust particles collected. They observed an increase in the coarse particle number concentration accompanied by depletion in the ultrafine particle concentration due to coagulation and growth of particle sizes at the level of cloud formation.
Yaalon (1997) reported the transport of Saharan dust particles to Europe. He used the back tracking and chemical composition of samples to estimate the source of the Sahara dust that affects the Mediterranean Sea and the southern Europe. He estimated that about 700 million tonnes of dust per year was transported over short, medium and long distances from the mineral dust deposits in North Africa, to the Atlantic, Mediterranean Sea, southern Europe and the Levant (countries in the Eastern Mediterrenean).
Hamonou et al., (1999) reported the movement and characterisation of the vertical structure of the Saharan dust export to the Mediterranean Basin. The interaction of the Saharan dust particles with the environment is important because it concerns key phenomenon such as the earth's radiative budget (Legrand et al., 1992). Hamonou et al., (1999) used two-backscatter lidar systems operated at two different sites in western and eastern parts of the Mediterranean. They observed an aerosol optical thickness of 0.3-0.4 in the planetary boundary layer using simultaneous lidar and sun photometer measurements. This work is important because it determines the optical depth of the Saharan dust over the Mediterranean basin, which is quite relevant in determining the global atmospheric dust load.
Jaenicke et al., (http://www.uni-mainz.de/FB/PhysikIPA/sahara.html), also studied the size distribution of the Sahara Desert aerosols over north-east Morocco using mass concentration determination, atmospheric turbidity and optical depth techniques. They noted that the Saharan dust is almost permanently present in the atmosphere which impacts on the ecology and economy of Morocco in the following areas: use of solar systems, soil quality and air quality. They have observed that Morocco receives particulate matter originating from Western European pollution sources, marine sources of the Atlantic Ocean and the Mediterranean Sea as well as from the continental sources of Africa itself including Saharan dust.

3. THEORETICAL CONSIDERATIONS

This chapter is devoted to the general principles of the dust generation, transport and settling as well as its measurement. The basic laws of deflation of soil materials from the ground surface and the equations that govern the transport and deposition of the aerosol are presented. The transporting wind and the meteorological conditions of the atmosphere that affect the aerosol particle propagation are also explained. The theories of some optical effects of the aerosols are also discussed. It is not necessary to demonstrate and explain all the important theories and equations that we will constantly refer to in this study. However, we have tried to recall the principal results that are directly relevant to this study and are necessary for a better understanding of the dust suspension and deposition. We have, however, developed in greater detail the section dealing with the flux deposition rate.

3.1 Aerosols and fluid motion

Aerosols are two-phase systems namely the particulate phase and the fluid (normally air) phase in which the particles are suspended. The behaviour of the particles within the fluid depends, to a large extent, on the motion and the intrinsic properties of the suspending fluid. Sub-micrometer particles (diameter < 1.0 μm) or normally aerosol particles with sizes approaching the mean free path of the suspending fluid are affected by the motion of the individual fluid molecules and are therefore analysed by the kinetic theory of gases under the free molecular regime. The mean free path of air molecules that defines the limit between Brownian and Newtonian motion is about 0.1 μm while larger particles (diameter > 3 μm) are examined under fluid dynamics or the continuum regime. Intermediate-sized particles are treated under the fluid transition or slip regime.
The general equation that governs the motion of particles in air (or a gas) depends upon the relative velocity between the particle and the air. The effect of the interaction between the fluid and the flowing particle produces a resisting force of the fluid on the particle in the direction of the upstream velocity. This force is termed the drag, F_D. The flow field is a function of the shape of the particle and the parameters such as particle size, orientation, speed and fluid properties. The drag force on small spherical suspended particles in a flow of low Reynolds numbers, Re <<1, is given by the Stokes law (Hinds, 1999, pp 42-74; Massey 1994, pp 172):

$$F_D = 3\pi\mu DV \qquad (3.1)$$

where μ is the absolute viscosity of the fluid, D is the diameter of the particle and V is the velocity of the particle relative to the prevailing undisturbed wind speed. The Stokes law applies to flow situations where:
i) the fluid is incompressible: there are no walls or other particles nearby, the motion of the particle is constant, the particle is a rigid sphere, and the fluid velocity at the particle's surface is zero,
(ii) the diameter of the particle is the characteristic length and;
(iii) the settling velocity of the particle relative to the prevailing wind velocity is the characteristic velocity.

In order to predict if a falling particle is governed by Stokes law, the particle Reynolds number, Re must be less than unity (Re <1) see Hinds (1999 pp 45). Re is defined as

$$\mathrm{Re} = \frac{\rho V D}{\mu} \tag{3.2}$$

where ρ is the density. If the drag force given by Stokes' law and that given by Newton's law are compared we obtain the coefficient of drag, C_D that relates the drag force to the velocity pressure, and as a function of Re. This relationship between particle Reynolds number, Re, and drag coefficient C_D is therefore divided into 3 regimes for laminar flow or Stokes regime, transition flow regime (an intermediate regime) and Newton or turbulent flow regime. The relationships according to Allen (l981) are given as:

$$C_D = 24 / \mathrm{Re} \qquad \text{if } \mathrm{Re} < 0.2$$

$$C_D = 24 / \mathrm{Re}\,(1 + 0.3\,\mathrm{Re}), \qquad 0.2 < \mathrm{Re} < 2.0$$

$$C_D = \frac{24\,(1 + 0.15\,\mathrm{Re}^{0.687})}{\mathrm{Re}} \qquad 2 \le \mathrm{Re} < 700 \tag{3. 3}$$

Stokes equation may therefore be used for low Reynolds numbers, (Re < 0.2) to determine the settling velocity of particles flowing in the atmosphere. When the characteristics of the settling particles diverge farther from the stated assumptions, corrections may be applied to determine the actual settling behaviour such as for non-spherical particles and very small particles (D < 1 μm), which cause non-zero velocity at the particle surface. The equation for drag and settling velocity are based on spherical particles. However, most solid particles are non-spherical such as cubic (for sea salt particle), cylindrical (bacteria and fibres), single crystals, clusters of spheres, agglomerated particles or crushed materials, which have irregular shapes. The shape of a particle affects its drag force and settling velocity. A usual form of the settling velocity of a suspending particle of density ρ_p is given as (Hinds, 1999 pp 49):

$$V_s = \frac{1}{18}\frac{D^2 \rho_p g C_c}{\mu} \tag{3.4}$$

where C_c is the Cunningham slip correction factor, which for small particles whose size approaches the mean free path, (λ) of the suspending gas is given as (Hinds, 1999 pp 49)

$$C_c = 1 + \frac{2.52\lambda}{D} \tag{3.5}$$

where C_c is significant for particles less than 1 μm in diameter.

3.2. Dust transport

Wind deflation has been observed as an effective factor that controls the mobilisation of loose dust particles from the dust source areas. The wind forces responsible for the entrainment, advection and dispersion as well as settlement of the dust particles are discussed in the following section.

Entrainment of sand particles from the ground occurs where soils are loosely consolidated, bare or poorly protected by vegetation. Soil moisture is critically important since water binds the soil particles together and supports the growth of plants. The Harmattan aerosol originates from the Sahara Desert, which presents suitable dust reserves for entrainment. Three basic

mechanisms have been identified to be responsible for wind entrainment of sand sized particles from one place to another. For large sized particles, that is, particles of diameter in excess of 0.5 mm, motion takes place as creep, i.e. rolling or sliding along the surface. For moderate size, i.e. diameters in the range 0.1 mm-0.5 mm, the particles travel by saltation or bouncing along the surface. For particles smaller than 100 μm in diameter, the particles are ejected into the air where they travel as a suspension (Pye, 1987; Skidmore, 1986). Figure 3.1 illustrates the generation of dust particles and their transport. The bouncing removes the aggregates or breaks them into both, large particles which continue the saltation process, and small particles which can go into suspension. This process of soil particle deflation is known as sandblasting. The entrainment force is derived from the shear stress exerted by the wind, the frictional drag, aerodynamic lift, and especially by ballistic impact.

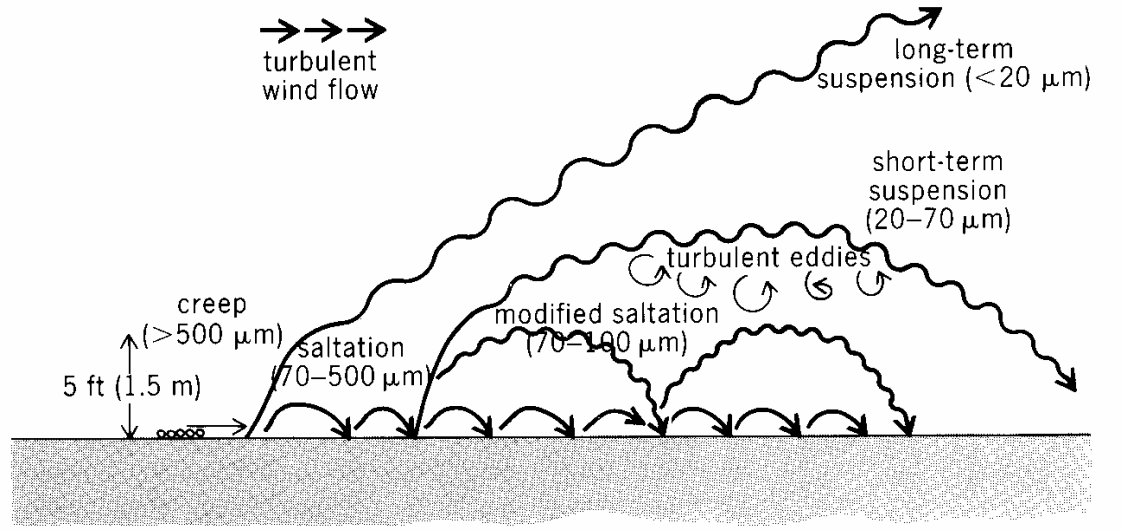

Figure 3.1 Dust generation and transport near the soil surface. (After K. Pye. Aeolian Dust and Dust Deposits, Academic Press, 1987)

Gillette and Passi (l988) developed a semi-empirical model to compute the expectation of dust emission using a dust emission function that extremely depends on the threshold wind velocity. The threshold velocity is also dependent on effects of vegetative residue, roughness of the soil, live standing plants, soil texture and moisture as well previous mechanical disturbance. Values of threshold velocity for various barren landforms are given as in Table 3.1.

Table 3.1. Threshold velocity assigned to barren land forms (After Gillette and Passi, 1988).

Land form	Threshold friction velocity (cm/s)
Dry salt	100
Bare rock exposure	999
Strip mines, quarries, gravel and barrow pits	30
Beaches	30
Sand dunes	25
Mixed barren lands	65
Mud flats and river wash	70
Sand barren land	45

The entrained dust particles are dispersed into the atmosphere or settled to ground, by gravity. The speed and turbulence level of the wind affect the aerosol characteristics such that the number concentration, size distribution and composition vary with time and space in response to different meteorological conditions of the atmosphere. The particles are distributed throughout the atmosphere by advection with the winds and they sediment under gravity and other atmospheric effects such as subsidence of air masses. The length of time and the distance travelled depend on the settling velocity (V_s) of the particles, the wind velocity (V) and the turbulence level of the flow.
Furthermore, dispersion of aerosol particles emitted into the atmosphere can be accomplished by diffusion. In laminar flow, diffusion occurs by molecular transport and in turbulent flow, by eddy transport. Dispersion occurs by turbulent transport in neutral and unstable atmospheres and approaches laminar diffusion under highly stable conditions. The diffusion equation describing the transport of aerosol particles through a fluid is given as (Hinds, 1999):

$$\frac{dC}{dt} = \vec{\nabla} \cdot (k\vec{\nabla}C) \qquad (3.6)$$

where C is the particle concentration, t is the time and k is the diffusion coefficient. Solutions to this equation can be obtained for many types of initial and boundary-layer conditions.

3.3. Dust deposition

The deposition of an aerosol particle is the result of two kinds of forces namely a constant external force such as gravity and the resistance of the air to particle motion. Analyses of these forces are important in determining the deposition flux of the aerosols in the following section.

3.3.1. Sedimentation of an aerosol particle

One important application of the Stoke's law is the determination of the velocity of an aerosol particle undergoing gravitational settling in still air. The Harmattan period is marked by suspension and deposition of fine dust carried by the trade winds. It has been noted that Harmattan wind speeds near the surface become sufficiently low to facilitate sedimentation once the particles fall below 800 mb level (about 1800 m), (Tiessen et al., l991). Thus, the principle of deposition of the dust particles is generally by dry gravitational settling. Therefore the Stokes law, which applies to the settling of small particles, can be used for the deposition of the dust particles.
When a particle is released in air it quickly reaches its terminal settling velocity, a condition of constant velocity where the drag force is equal and opposite to the force of gravity and buoyancy. The air-particle system is a dilute one. Another assumption is that the presence of the aerosol particles does not change the structure of the carrier fluid, and then Stokes law is applicable to the settling of the particles. The force balance on a falling particle is obtained in the analysis that follows:

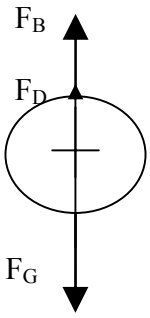

Figure 3.2. Free body sketch of a dust particle.

The particle assumes settling velocity when the forces balance i.e.

$$F_B + F_D = F_G \quad (3.7)$$

where F_B is the buoyancy of the surrounding air given as

$$F_B = \frac{\pi}{6}\rho_a g D^3 \quad (3.8)$$

F_D is the aerodynamic drag on the particle given by Stokes law as

$$F_D = 3\,\pi\mu V_s D \quad (3.9)$$

(for particles settling in Stokes regime, $C_D = 24/Re$)

F_G is the gravity force or weight of the particle, given as

$$F_G = \frac{\pi}{6}\rho_p g D^3 \quad (3.10)$$

V_s is the settling velocity of particles relative to the wind velocity. All other forces including electrostatic forces are neglected, hence V_s is equal to the gravitational settling velocity, V_g. Substituting (3.8), (3.9) and (3.10) into (3.7) and solving gives

$$V_g = \frac{(\rho_{p-}\rho_a)gD^2}{18\mu} \quad (3.11)$$

If we neglect the air density relative to the particle density, the settling velocity is given as:

$$V_g = \frac{\rho_p g D^2}{18\mu} \quad (3.12)$$

The settling velocity of particles in a fluid of infinite extent is widely used to:

i) determine the size of the particle, which is proportional to the square root of the settling velocity;

ii) separate polydisperse aerosol particles ;

iii) Determine the rate of collection of the particles.

From equation (3.12), it can be seen that the settling velocity increases rapidly with particle size, being proportional to the square of the particle diameter.

3.3.2. Dust deposition flux

Dust concentration measurements have been performed at two locations in Ghana, Tamale (9^o 34’ N; 0^o 52’ W) and Kumasi (6^o 40’N; 1^o 34’W) with the view to estimate the dust deposition flux during the Harmattan period. We are aware of the fact that we can only use a

simplified model derived from the equation of conservation of mass. However, it is well known that for low temperature, a single box model based on the mass conservation represents quite a good description of the aerosol deposition (see Carruthers and Choularton, 1986).
This classical approach is presented as follows:
Let us start with the equation of mass conservation:

$$\frac{\partial M}{\partial t} + \vec{\nabla} \bullet (M\vec{V}) = 0 \qquad (3.13)$$

where M is the average particle mass concentration, t the time and $\vec{V}$ the velocity vector.
Let us consider the control volume of Figure 3.3 oriented in the Tamale-Kumasi direction and slightly east-west. Then in order to proceed, a series of strong simplifying assumptions should be stated and discussed as follows:
-The flow is steady which means that the wind velocity is constant during the period of measurement,
- no dust particle is supposed to enter or leave through the lateral walls of the box, assumed parallel to the direction Tamale–Kumasi, also taken here as the OX direction, and is slightly oriented towards west as the wind direction.
-no particle is supposed to enter through the bottom wall of the box: this is probably the weakest assumption as it is impossible to check if dust was emitted for any reason (such as due to fires, road works, etc.) during those periods. Let us assume that that production is negligible compared to the one induced by the Harmattan. The wind is probably too weak to entrain particles into the atmosphere and particles from anthropogenic sources (fires, vehicle exhaust, etc.) are too small compared to the ones measured.
-no particle is supposed to enter or leave through the top wall: it could pass some particle in and out but we believe that those fluxes should be relatively weak compared to the fluxes present in the boundary layer.
-the particle concentrations measured at 15 m, either in Tamale or Kumasi are considered constant throughout the vertical boundary layer leading therefore to a presence of a well mixed layer. Let us simply mention again that during those highest concentration periods, the ITCZ is much more south and most probably not interfering with the control volume therefore leading to a rather uniform profile.
The mass flow through the entrance of the region looses some of its larger particles due to sedimentation in the control volume. The mass at the exit is less than the mass at the entrance by the amount of particles deposited in the region. Let us try to estimate the deposition flux.
The particle mass concentration is M_1 at the entrance of the control volume and is M_2 at the exit. The length of the control volume is L, of unit width (1 m) and of height h which is taken as the height of the atmospheric boundary layer and taken here as h = 1000 m (Fairall and Davidson,1986). Obviously, this height is not strictly constant because it may vary due to both diurnal variation and wind velocity. However, the error on the deposition velocity using h as a constant value can be neglected for the present study (Slinn, 1983).

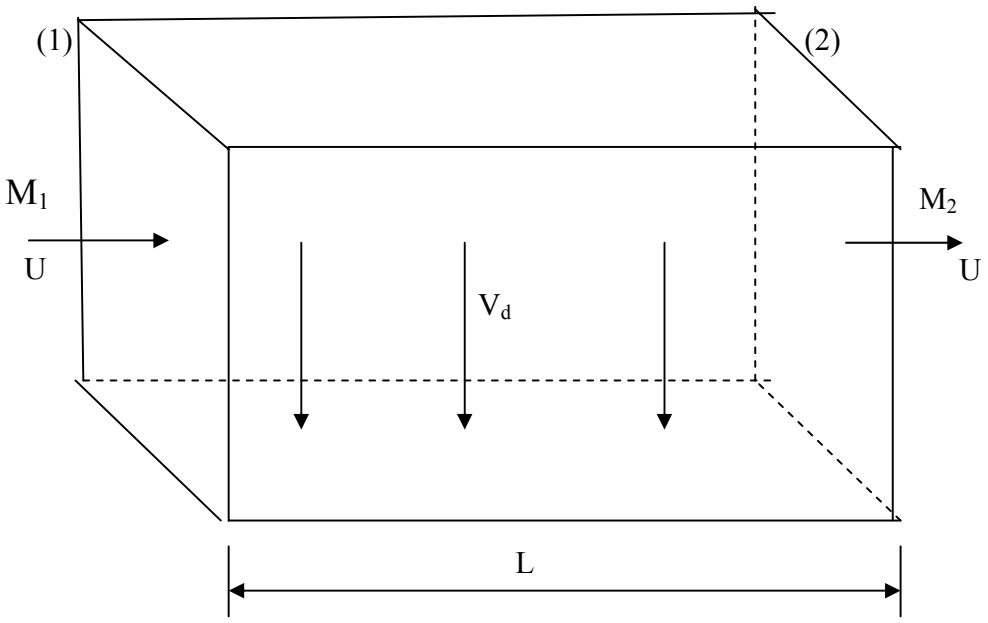

Figure 3.3. Control volume representation for the dust transport.

The deposition flux per unit surface area is given by:

$$F_d = V_d M \qquad (3.14)$$

where V_d is the unknown deposition velocity, which is different from the gravitational settling velocity, V_g of equation 3.12 [$V_g = \rho g D^2/(18\mu)$]. The deposition velocity, V_d takes into account the effects of turbulence as well. We know, however, that M is not constant, but varies from M_1 at the entrance section (1) of the control volume to M_2 at the exit section (2). It is this variation that allows us to determine the deposition velocity V_d.
Let us consider then a volume element in two dimensions, see Figure 3.4, for which the concentration varies from M(x) at a horizontal distance x to M(x+dx) at a horizontal distance (x + dx) and under a mainstream wind speed U.

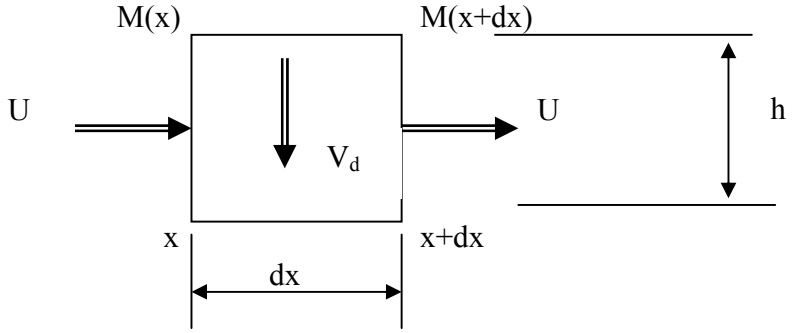

Figure 3.4. Control volume analysis of dust flux.

The mass flux of particles entering the volume element (dx, h, 1) per unit time is:
M(x) U h
The mass flux of particles leaving the control volume per unit time is:
M(x+dx)Uh
The mass flux of particles settling within the control volume per unit time is:
V_d M(x) dx

Applying the principle of conservation of mass, net outflow of mass of particles through the surface surrounding the control volume must be equal to the decrease of mass of particles within the control volume, we have
Flux entering = flux leaving + deposition flux
or
Rate at which mass of particles leaves the control volume – rate at which mass of particles enters the control volume = - rate of decrease of mass of particles in the control volume

$$M(x+dx)\ U\ h - M(x)\ U\ h = -V_d\ M(x)\ dx \qquad (3.15)$$

$$\frac{U[M(x+dx)-M(x)]}{dx} = -\frac{M(x)V_d}{h}$$

But as dx $\rightarrow$0,

$$\frac{M\ (x\ +\ dx\ )\ -\ M\ (x\ )}{dx} = \frac{dM\ (x\ )}{dx}$$

Therefore,

$$U\frac{dM(x)}{dx} = -M(x)\frac{V_d}{h} \qquad (3.16)$$

Since $\frac{dx}{dt} = U$, we have

$$\frac{dx}{dt}\frac{dM(x)}{dx} = -M(x)\frac{V_d}{h}$$

or $$\frac{dM(x)}{dt} = -M(x)\frac{V_d}{h}$$

Finally,

$$\frac{dM(x)}{M(x)} = -\frac{V_d}{h}dt \qquad (3.17)$$

Integrating over the entire volume, from section (1) to section (2) and from 0 to T ($=\frac{L}{U}$), the time necessary to go from (1) to (2), we obtain

$$\int_{M_1}^{M_2} \frac{dM(x)}{M(x)} = -\int_0^T \frac{V_d}{h} dt \qquad (3.18)$$

$$\Leftrightarrow \ln M_2 - \ln M_1 = -\frac{V_d}{h} T$$

$$\Leftrightarrow \ln \frac{M_2}{M_1} = -\frac{V_d}{h} T$$

or $$V_d = \frac{h}{T} \ln \frac{M_1}{M_2} \qquad (3.19)$$

Knowing M_1, M_2, h and T, the deposition velocity V_d can be determined and hence the deposition flux per unit area

$$F_d = V_d M_1 \qquad (3.20)$$

In the present study, samples were taken at two locations, namely Tamale (9^o 34' N; 0^o 52' W) and Kumasi (6^o 40'N; 1^o 34'W) situated about 320 km apart in a north-south direction, and are found in the flow field of the Harmattan aerosol. In order to estimate the deposition flux, concurrent sampling of the dust at the two locations was required.
The mainstream wind velocity U was assumed constant between the two locations and taken as $U = V_{15}/0.8$ (V_{15} is the wind velocity at a height of 15 metres measured at location (1). This estimation comes simply from the fact that over 50 meters above ground level, the velocity is supposed to have reached the value U. (see Hasager and Jansen, 1999). It can be seen from equation (3.19) that V_d is related to the variation of the mass concentration between the two measurement sites and therefore embodies all sedimentation effects including gravity and turbulence.

3.4. Influence of large-scale atmospheric systems

The Inter-Tropical Convergence Zone (ITCZ) and the North Atlantic Oscillation (NAO) are the two large scale atmospheric factors which influence the transport of the Saharan dust. These are large scale atmospheric features that are known to affect the weather in the northern hemisphere. Although there are some non-quantitative reports on the influence of the ITCZ on the dust transport from the Saharan desert over most of West Africa, the study on the links between the NAO and the dust transport is still very recent (Chiapello et al., 2005).

3.4.1 The Inter-Tropical Convergence Zone (ITCZ)

The Inter-Tropical Convergence Zone is an area of low pressure that forms where the northeast trade winds meet the southwest monsoon winds near the Earth's equator in West Africa. It is important to realise that the ITCZ, as the name implies, is indeed a zone rather than a line of demarcation. However, a line is defined as the Inter-Tropical Front (ITF), which is the same as the northernmost limit of the ITCZ. The ITF stays always at 3^{o}-5^{o}N of the ITCZ (http://ams.conflex.com/ams/pdfpapers/85268.pdf). Since the ITF is a line limit of the ITCZ, we shall use the ITCZ which is generally used to represent the boundary between the dry north winds and the warm humid winds to the south (www.wrc.org.za/archive). The ITCZ band moves seasonally. It moves towards the southern Hemisphere from September through February and reverses direction during the northern Hemisphere summer that occurs in the middle of the calendar year. Thus the ITCZ is an average feature and it is highly variable giving rise to greater variability in daily temperatures than normal. As the ITCZ moves in association with the zone of maximum seasonal temperature (or the thermal equator), it reaches the farthest northward position at about latitude 25^{o} N in summer and moves to the most southward position at about latitude 4^{o} N in winter. The average positions of the ITCZ on Africa in January and July are shown in Figure 3.5. The seasonal extremes of the ITCZ have a definite effect on the climate of the areas over which it moves. Areas north of the ITCZ are normally under the northeast trade winds system and are dry. Areas south of the ITCZ are under the Southwest monsoon winds and are wet. Normally, within the region affected by the Harmattan, the farther north a location is from the ITCZ, the more severe will be the Harmattan condition and the more pronounced will be the Saharan dust concentration. Therefore, the ITCZ position has a strong influence over the Saharan dust transport. The relative position of the ITCZ is a major determinant of the steadiness of the Saharan dust transport toward the Gulf of Guinea. The latitudinal position of the ITCZ is the strongest factor that determines the severity and level of concentration of the Saharan dust at a particular location near the Gulf of Guinea.

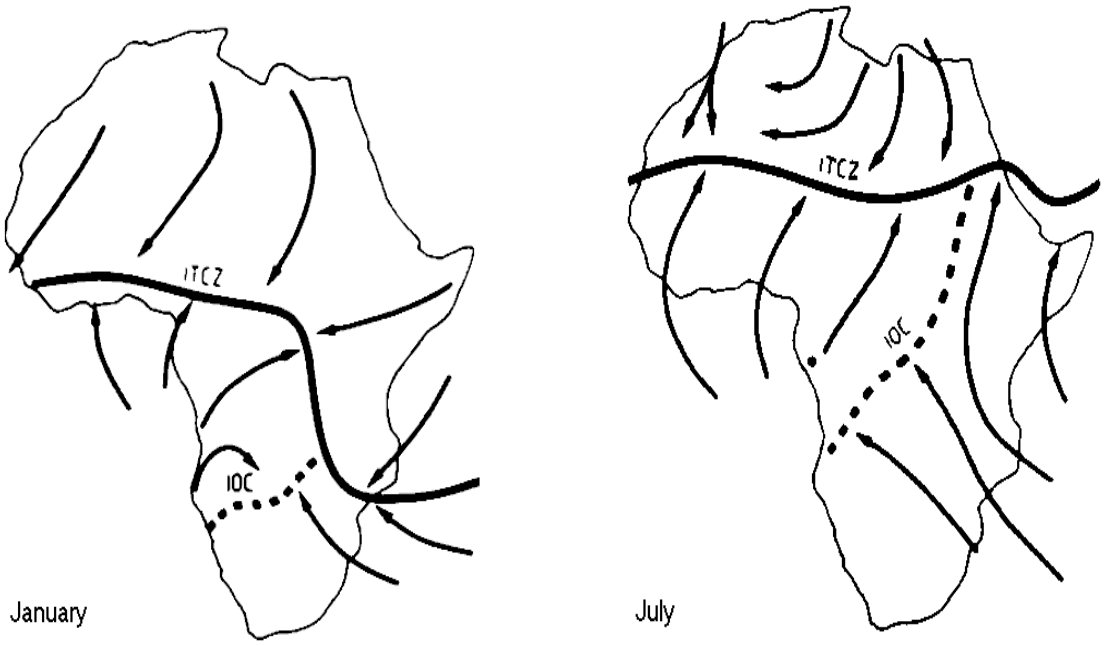

Figure 3.5. The ITCZ over Africa in January and July (IOC refers to the Inter-Tropical Oceanic Confluence, which separates winds coming from the southern Atlantic and those from the Indian Ocean).

3.4.2 The North Atlantic Oscillation (NAO)

The climate variability over the North Atlantic Ocean basin is associated to a large extent with the NAO, which is a dominant pattern of atmospheric circulation variability. Over this North Atlantic Ocean basin, the atmospheric circulation normally displays a strong meridional (north-south) contrast, with low sea-level pressure in the northern edge of the basin, centered close to Iceland, and high pressure in the subtropics, centered near the Azores. This pressure contrast drives the mean surface winds and the winter-time mid-latitude storms from west to east across the north Atlantic, bringing warm moist air to the European continent. It has long been observed that the monthly and seasonal (particularly winter time) average sea level pressure in stations in Iceland and the Azores display an out-of-phase relationship with one another. More precisely, there is a tendency for sea level pressure to be lower than normal in the Icelandic low pressure centre when it is higher than normal near the Azores and vice versa. This fluctuation is referred to as the NAO (http://www.iabm.org_atlantic _oscilation.htm).

The North Atlantic Oscillation index (NAO index)
One of the most famous NAO features is the NAO index. The NAO index can be obtained for a year, a month or a day. The procedure involves calculating the expression for the respective time as follows:

$$\text{NAO index} = \frac{x-\bar{x}}{\sigma_x} - \frac{y-\bar{y}}{\sigma_y} \qquad (3.21)$$

where x is the Azores sea-level pressure, in hectopascals (or millibars), for the respective year, month or day. Similarly, $\bar{x}$ and σ_x are the average and standard deviation (SD) of these values over the period (1950-1990), respectively. The symbol y represents the Iceland low average sea-level pressure for the respective day, month or year, and $\bar{y}$ and σ_y are the long-term average and SD of these values over the period (1950-1990), respectively (Hameed et al., 1995; Shi, 1999). The North Atlantic Oscillation (NAO) index data was taken from the Internet at the following website. http://www.cru.uea.ac.uk/cru/data/vinther/nao1821.txt

Positive NAO index
The positive NAO index phase (calculated NAO index > 0) shows a stronger than usual subtropical high-pressure centre and a deeper than normal Icelandic low. The increased pressure difference results in stronger winter storms crossing the Atlantic Ocean, on a more northerly track. This results in warm and wet winters in Europe and in cold and dry winters in northern Canada and Greenland. The eastern United States of America experiences mild and wet winter conditions. In West Africa, the weather will be drier in winter, due to enhanced Saharan dust transport and severe Harmattan condition.

Negative NAO index
The negative NAO index phase (NAO index < 0) shows a weak subtropical high and a weak Icelandic low. The reduced pressure gradient results in fewer and weaker winter storms crossing on a more west-east pathway. They bring moist air into the Mediterranean and cold air to northern Europe. The east coast of the United States of America experiences more cold air outbreaks and hence snowy weather conditions. Greenland, however, will have milder winter temperatures. West Africa may experience wet winter, decreased Saharan dust transport and mild Harmattan condition.

Influence of North Atlantic Oscillation index on the Harmattan
It is observed that the monthly NAO indices during the Harmattan months of November-March reach a maximum value around February. On the basis of year-by-year comparison, it is found that the higher the NAO index the stronger the Harmattan conditions in Ghana.

Generally, the NAO index is the dominant mode of winter climate variability in the North Atlantic region ranging from central North America to Europe and much into Northern Asia. The corresponding index varies from year to year, but also exhibits a tendency to remain in one phase for intervals lasting several years. A remarkable feature of the NAO that has motivated much recent study is its trend toward a more positive phase over the past 30 years (Hurrel, 1995). The most pronounced anomalies have occurred since the winter of 1989 when positive values of an index of the NAO have been recorded (Hurrel, 1995). Moreover, the trend in the NAO accounts for several remarkable changes recently in the climate and weather over the middle and high latitudes of the Northern Hemisphere, as well as in marine and terrestrial ecosystems. Among these changes are (Hurrell, 1995): milder winters in Europe and Asia, pronounced regional changes in precipitation patterns and changes in sea-ice cover in both the Labrador and Greenland seas as well as over the Arctic.

4. EXPERIMENTAL STUDY

In this chapter, the operating principles of the optical technique employed to measure the particles are explained. First, it is worth noting that aerosol particles behave differently in various size ranges and are therefore governed by different physical laws. Particles just larger than the gas particles are governed by Brownian motion and their light scattering depends on the Rayleigh law. Larger particles are affected by gravitational and inertial forces while their light scattering is dependent on the general Mie theory. Hence, to measure the entire size range of atmospheric particles, different measurement techniques are used for the various size ranges. Some of these techniques were classified in section 2.1. By measuring each range of the particle size spectrum, a graph of the size distribution of the various aerosols can also be obtained as shown in section 2.1.

The method of aerosol measurement also depends on the environment where the measurement is to be made. The quantity to be measured, the particle concentration and size range also affect the decision on how to make the measurement. High particle mass concentrations more than 10 g/m^3 may be encountered in industrial process streams such as smoke chimneys and stacks. In work environments such as factories and quarries, the mass concentration ranges from about 0.1 mg/m^3 to about 10 mg/m^3. The particle concentrations in ambient and indoor air are usually less than 0.1 mg/m^3. In a highly controlled clean-room environment, the particle concentrations are so low that they are recorded as number of particles instead of mass per unit volume of air. When dealing with radioactive aerosols, the concentration range corresponding to maximum allowable activity concentrations extends down to 1 pg/m^3. Thus the range of aerosol mass concentrations extends over 13 decades. Several methods and techniques are required to cover such a wide range of particle concentrations.

The wide range of particle sizes that may have to be covered further increases the diversity of aerosol measurement techniques. Meanwhile, the range of aerosol particle size extends over five decades from about 0.001 μm to about 100 μm. Most aerosol measurement instruments have an operational range of about 1.5 decade of particle size. Usually therefore, various measuring instruments and techniques are utilised to measure the entire size range of atmospheric aerosols and one instrument would measure just a part of this range. Meanwhile, because aerosol particles are microscopic, our knowledge concerning their properties has been gained mainly through experimental means. Thus the use of the appropriate measuring techniques is important in any fieldwork and basic research on airborne particles.

Aerosol measurements can also be classified according to the property to be determined. The most commonly measured aerosol properties are particle number and mass concentrations, particle size and particle shape. Particle mass concentration is defined as the amount of particulate mass in a unit volume of air. Other instruments record the number of particles in a unit volume of air.

There are two basic approaches to the measurement of aerosol particles. The traditional approach is to sample or withdraw the aerosol particles onto a collection surface or substrate, followed by analysis of the collected particles in the laboratory. The other approach is to sample the aerosol directly into a real–time dynamic measuring instrument, which gives results of the measurement in the airborne state. Thus the first step to characterise aerosol particles is their sampling. The key objective here is to obtain a representative sample so that the characteristics of the particles are not altered by the sampling technique.

A frequently used collection method is a porous medium that allows the air to flow through but retains all or a fraction of the particles suspended in the incident aerosol flow. Passage through such a porous medium generally has to be at a rather low flow rate and all of the aerosol flow must pass through this medium for the particle collection. In many applications it is desirable not to pass the flow through such great pressure drops but to extract the particles from the aerosol flow by an externally applied force. That is to allow the particles to sediment out of the flow under the applied force. The external force may be due to gravity or to inertia when the particles are subjected to centrifugal motion in the bend of a duct, the nozzle of an impactor or the helical path of a cyclone. The application of electric, thermal, or magnetic fields may also obtain the extractive forces. Under the influence of these external forces, the particle drift towards the collecting substrate along its trajectory is dependent on the settling velocity and airflow velocity.

The most common methods used to collect samples from an aerosol flow where the particles are removed for subsequent analysis is the filter collection. Typical filters used for aerosol sampling consist of glass, cellulose, or plastic fibres, porous membranes, or polycarbonate pore materials. Other collection methods employ inertial and gravitational techniques. The diffusion motion of aerosol particles is utilised in the measurement of small, sub-micrometer particles.

The inertia of particles is utilised in many aerosol samplers to remove particles from the aerosol flow. In a curved flow field, inertia makes the particle trajectories deviate from the flow streamlines. This inertial impaction technique is utilised in different types of impactors and cyclones in which particles are removed by centrifugal forces. Particles with high inertia are separated out by centrifugal forces while smaller particles continue with the air flow. The interaction of aerosol particles with light forms the basis for another class of instruments used for measuring aerosol particle size and concentration, known as the optical measurement method. Optical techniques, one of which is employed in this study, have the advantage of being quick, very sensitive and not requiring physical contact with the particles.

In this work, the principal parameters monitored include the particle number concentration per unit volume of the atmosphere (in m^{-3}) within the instrument size range of 0.5 μm - 25 μm. Eight contiguous size ranges, the maximum for this equipment, were monitored during the sampling. The key issue of representative atmosphere was achieved by sampling on top of tall buildings. With this key parameter, the particle vertical deposition fluxes as well as the mean diameter and mass distributions were determined. Meteorological parameters including wind speed and direction as well as the ITCZ position values were available at the Ghana Meteorological Services Department (GMSD) and the Internet. The GMSD weather stations were at the Kumasi Airport, the Tamale Airport and Accra. The GMSD station at the Kumasi Airport is located at about 15 km in a north-northwest direction from the sampling station at the University campus, while the sampling station at Tamale was located at the Airport. However, the ITCZ global data were taken from the data base of the National Oceanic and Atmospheric Administration (NOAA) of the United States. Since it was easy to assess the NOAA data on the Internet, the global ITCZ from the NOAA site was used for analysing the results of this work. The input parameters required to assess the chart for a location include, the centre latitude and longitude, the date, time of day, the size of chart, and the spacing between the wind streamlines. A sample chart derived from the NOAA site (http:www.arl.noaa.gov/ready/disclaimer.html) is shown in Figure 4.1 for 19th December

2002 at 12:00 UTC. The estimated ITCZ latitude from this chart is 2.6°N with respect to longitude 0°.

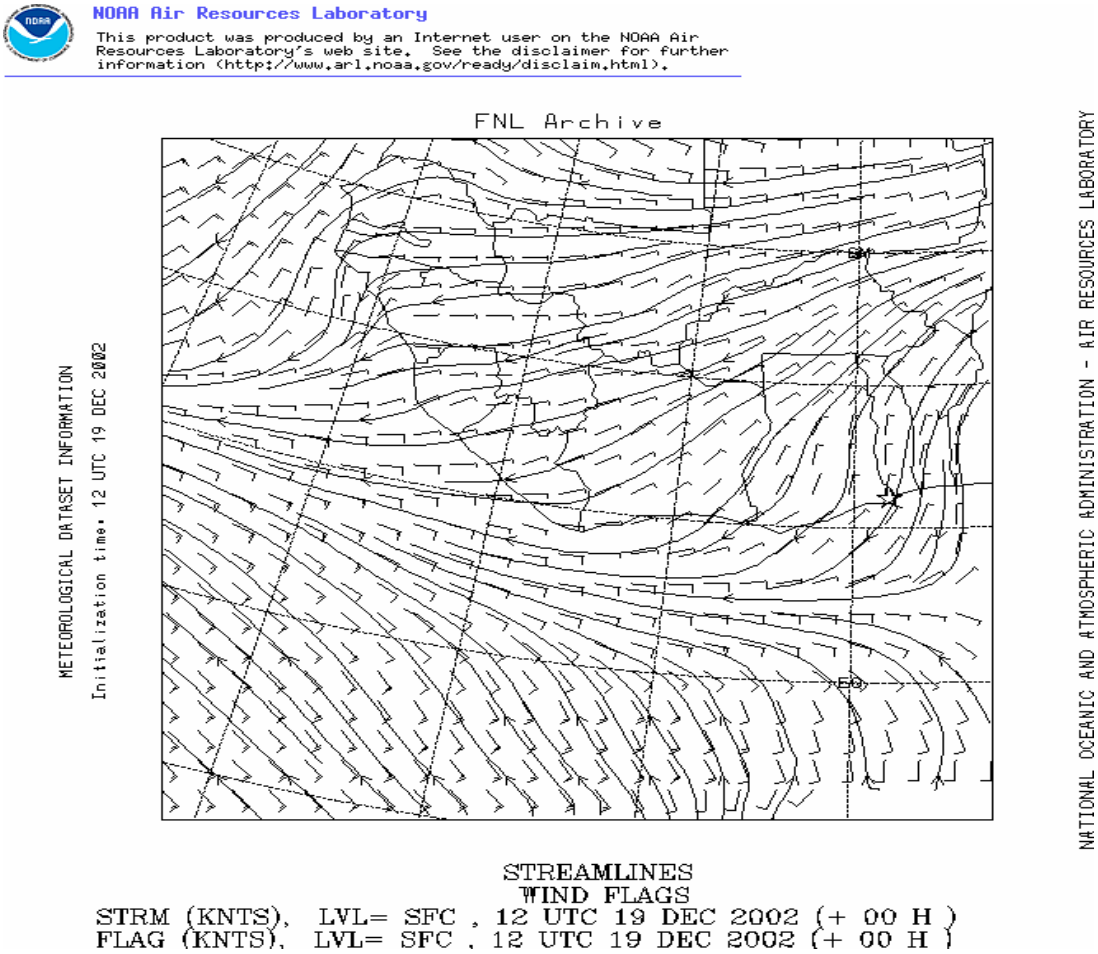

Figure 4.1. Sample chart of winds streamlines on 19th December, 2002, over West Africa, showing the northeast and southwest streamlines meeting around latitude 2.6° N south Ghana.

4.1. Optical technique for sampling aerosol particles

Many optical instruments depend on the scattering (reflection, refraction and diffraction of light) and extinction (attenuation of light due to absorption and scattering) of light by particles suspended in a fluid to determine the size and number of these particles in a unit volume. This is because when a beam of light is interrupted by the presence of a particle, the interaction yields the particle size information, which is derived from the intensity of the scattered light or the light attenuation of the incident beam. The technique used in this study to obtain the size and number concentration of the Saharan dust particles, is based on this principle and it combines in-situ measurements of the airborne particles with a high degree of automation.

Optical techniques can be divided into two classes, namely extractive and in situ techniques. In extractive technique, a particle-laden volume of the aerosol is removed from its environment, by a sampler, and transported to a separate location where the particle measurement is made. The Hiac/Royco 5250A belongs to this classification. It monitors a sample of aerosol particles removed from their natural environment, using sampling tubes, and passed through the counter. The in situ technique involves measurement of the aerosol particles in situ by illumination of a well-defined volume with a high-intensity laser light. Another classification of the optical techniques is based on whether they analyse single-particle events or particles ensemble. Single particle counters generally make a size determination on a particle at a time by analysing its scattering and extinction behaviour while the particle passes through a sampling cell illuminated by high-intensity (usually laser) light; again, Hiac/Royco 5250A falls in this group of instruments. The ensemble techniques (not employed by the Hiac/Royco 5250A) generally operate by illumination of a volume containing a large number of particles and analysing the collective scattering such as in a photographic snapshot or photometers.

Generally, optical direct-reading particle monitoring techniques that give real time measurement with spontaneous results have the advantage of rapid, continuous, non-destructive particle detection. At high concentration, single-particle counting techniques suffer from coincidence error, which occurs when more than one particle occupies the sensing volume at a time, while ensemble techniques are well suited for measurements at high particle concentrations but become ineffective at low concentrations. Generally, ensemble techniques (provide spatial averaging) do not provide as detailed information as single particle counters (temporal averaging) since individual particle information is lost in the averaging.

The scattering of light by very small particles, less than 0.05 μm in diameter, is described by the Rayleigh theory, which is also known as the theory of molecular scattering. Scattering by particles greater than 100 μm in diameter is analysed by the theory of classical optics or geometric optics, which includes diffraction, reflection and refraction. For particles with sizes between these ranges, 0.05 μm to 100 μm including this study (0.5-25μm), scattering of light is analysed by the complex Mie theory. It is practical to analyse refracted and reflected rays from particles larger than 50 μm but it is unrealistic to do the same analysis for particles less than 50 μm, so the interaction of light with particle in this size range is described in terms of the angular distribution of its scattered light. This angular scattering pattern depends on the refractive index of the particle and the particle diameter. Therefore, knowing the refractive index and the size of a mono-disperse aerosol, the scattering pattern of the particles can be assessed. This forms the basis for the calibration of the optical counter.

The important characteristic features of an optical particle counter are its permissible range of number concentration, its sampling flow rate, its sensitivity (lower detection limit) and its classification accuracy. Optical particle counters are nowadays used in basic aerosol research, air pollution studies and clean room monitoring. Since the requirements for an optical particle counter are quite different for these different kinds of application, the specifications of an instrument have to be adjusted to the special measurement problem.

4.2. Calibration of optical counters: theoretical response functions

Although it is advisable to calibrate an optical instrument experimentally by means of test aerosol of known size and refractive index, theoretical response functions give a general survey of an optical system. By means of electromagnetic theory, the response functions of optical systems, which describe the power of light scattered by a spherical aerosol particle through the collecting aperture, can be calculated as a function of the particle diameter. The key parameter of these functions is the refractive index of the particle material. The response characteristics of coherent laser aerosol spectrometers have been calculated by Garvey and Pinnick (1983). The response functions of the light scattering and absorption by small particles produce a dipole or Rayleigh scattering for particles much smaller than the wavelength of light ($D < 0.05$ μm) and Mie scattering for spherical homogenous particles with sizes comparable to the wavelength of light ($D > 0.05$ μm). The spatial distribution of the light scattered by the particle per unit solid angle can then be described by a scattering function that depends on the scattering angle, the polarization angle, the particle diameter, the wavelength λ and the refractive index of the particle material.
The experimental calibration of optical particle counters involves drawing the aerosol through a light beam and light flashes scattered by single particles are received by a photo-detector. From the height of the photoelectric pulses and the count rate, the size of the particles and the number concentrations in the various size intervals are respectively evaluated. However, characteristic features such as permissible range of number concentration, sensitivity (smallest particle diameter detectable with the counter), sampling flow rate, classification accuracy and size resolution are determined on the basis of experimental results. The experimental equipment used for this study, Hiac/Royco 5250A, has been serviced and calibrated whenever the existing calibration expired.

4.3. Calibration of the experimental equipment

Since the experimental equipment response cannot be predicted theoretically, it must be calibrated by comparison with the reference standard sizes. In calibration, a well-characterized aerosol with respect to size, shape and refractive index is presented to the instrument under prescribed conditions of temperature, humidity, and other instrument parameters upon which the measurement values depend. The instrument response is compared with the known results. The current calibration date and the subsequent one are indicated on a sticker pasted on the counters by the manufacturer or its servicing and calibration representative.
During this study, the precautions regarding the use of the counters were strictly observed during the main sampling campaigns. Particularly, the daily automatic (self adjustments) calibration and cleaning of the internal aerosol passages with the filter (0.2 μm cut off) as well as cleaning of the outside surfaces of the instruments were done thoroughly. The counters have an error message feature, which indicates on the screen when there is a major fault on the counter. When this happened, the counters were serviced and recalibrated. The sampling instruments, Hiac/Royco 5250A with serial numbers, E06465 (the second acquired counter) and 95060047 (the first acquired counter) were serviced and recalibrated with mono-disperse latex spheres in the year 2004 before use in the sampling campaign of the 2005 Harmattan.

4.3.1. Instrument performance verification

The optical counter Hiac/Royco 5250A presents an adequate resource for the measurement of aerosol size distribution and concentration in the particle size range 0.5 μm - 25 μm. However, there is the need to ensure that the instrument is used within its proper operating conditions set by the manufacturer. Therefore, a means of verifying the instrument performance is essential in order to characterize the instrument limits and identify any inherent bias and inaccuracies.
Pressing the self-adjustment soft keys, 'auto adjus and quick adjus' enables access to the counter's automatic calibration function features. When these soft keys are employed, the counter automatically accesses its automatic self-adjusting features to perform internal measurement and compensate for any deviations in voltage gains, and offset in the analogue circuitry from their nominal values. The self-calibration enables the channel or bin size settings and thresholds to be set more accurately or fine-tuned. During the study, the self-adjustment calibration was done before any daily sampling, according to the manufacturer's recommendation. When the counter worked well, it did not fail the auto-adjustment calibrations. When an auto-adjustment failure occurred, the counter required servicing.

Verification activities
The manufacturer has recommended that automatic adjustment be done before actual sampling campaign. After passing the automatic adjustments, the counter was run with a filter, of cut off size D = 0.2 μm, provided by the manufacturer to clean the aerosol passages within the counter. The filter was inserted into the inlet nozzle of the counter and run for several sample times while keeping the same settings as for the actual sampling. This operation was to allow all particles, lodged in the aerosol passages, within the counter, to be purged with a clean air, obtained by filtering off all particles larger than 0.2 μm from the air entering the counter. The counter results were observed until they read zero or constant near-zero for a number of runs for all the size intervals. This operation was also conducted daily before a main sampling experiment. Sometimes, sampling in a clean air-conditioned room, which recorded zero or little particle concentration in the various particle size classes also gave indication of confidence and assurance that the counter results were correct and reliable.

4.3.2. Comparison of the optical counters (Inter-calibration)

This experimental work started with one optical counter, Hiac/Royco 5250A with serial number, 95060047 and used to sample alone from 1995 to 2000. The second counter of the same make and performance characteristics, Hiac/Royco 5250A with serial number, E06465 was acquired in 2001 and used to sample simultaneously with the first, at separate sampling stations. The two counters are based on the same measurement principle and the same definition of particle diameter. Therefore, in order to compare data from the counters, it was necessary to ensure that the two counters have the same characteristics in terms of sensitivity, reliability and calibration. The old counter was also recalibrated by a servicing and calibration agent, with the arrival of the new counter and thus offered a good opportunity for performance verification and reliability of the counters. Making the two counters measure the same aerosol was sufficient and enough to inter-calibrate them for data comparison, analyses and statistics. Before the start of each sampling campaign, the two counters were thoroughly

inter-calibrated by running them in the same environment, indoors and outdoors, at the start of the Harmattan period before separating them to their respective sampling stations.
The two counters were set to the same selectable features including same channel number of eight; same particle size intervals (in μm), 0.5-0.7, 0.7-1, 1-2, 2-5, 5-10, 10-15, 15-25, >25; same sampling time of two minutes; and same delay time of one hour between sample runs; as well as the same sampling tube length. First, the counters were purged of internal dirt by running them with the filter of 0.2 μm cut off. Then the two counters were run with the same length of inlet sample tubing of about 15 cm (as used for the actual sampling in 2005) simultaneously while adjusting the airflow rate within the manufacturer's recommended range of 0.9 – 1.1 ft^3/min, excluding the limits. The particle concentrations in the various size classes on the readouts of the counters were observed for equality. When the concentrations were found the same and stable for a number of runs, the calibration was deemed complete. The inter calibration was further checked a number of times every day for about three days before separating the counters for their respective sampling stations. The counter with serial number, 95060047 was stationed at the Kumasi sampling station and the one with the serial number, E06465 was stationed at the Tamale sampling station. Some of the results of the inter-calibration in 2002 and 2004 are shown in Table 4.1. As shown in Table 4.1, the two counters recorded about the same concentration numbers throughout the various size classes. As a result, the two counters can be said to have a similar characteristics for comparison of results from them. This inter-calibration was the basis for comparison of simultaneous data from the two sampling stations in 2002 and 2005.

Table 4.1. Intercalibration of the two optical counters. (The counter with serial number 95060047 is called the 'old' counter and the one with serial number E06465 is the 'new' counter).
(a)

Date:1/11/01	Old counter	New counter	
Size (μm)	particles/m^3	particles/m^3	Ratio of values(old/new)
0.5	5884491	5890016	0.999
0.7	1856475	1849299	1.004
1	2098675	2098609	1.000
2	1100464	1100487	1.000
5	60649	60681	0.999
10	2943	2940	1.001
15	740	742	0.997
>25	101	101	1.000
Total	11004538	11002875	1.000

(b)

Date:30/12/02	Old counter	New counter	
Size (μm)	particles/m^3	particles/m^3	Ratio of values(old/new)
0.5	12357432	12350844	1.001
0.7	3898598	3897775	1.000
1	4407218	4407528	1.000
2	2310974	2310837	1.000
5	127362	127238	1.001
10	6180	6185	0.999
15	1553	1554	0.999
>25	212	213	0.995
Total	23109529	23102173.4	1.000

(c)

Date:4/10/04	Old counter	New counter	
Size (μm)	particles/m^3	particles/m^3	Ratio of values(old/new)
0.5	6045606	6047411	1.000
0.7	1087432	1095937	0.992
1	917297	917856	0.999
2	601019	601747	0.999
5	41382	41694	0.993
10	4100	4098	1.000
15	997	989	1.008
>25	128	128	1.000
Total	8697960	8709859	0.999

(d)

Date:5/10/04	Old counter	New counter	
Size (μm)	particles/m^3	particles/m^3	Ratio of values(old/new)
0.5	1319923	1319963	1.000
0.7	338958	339683	0.998
1	310669	310913	0.999
2	164191	164575	0.998
5	6720	6739	0.997
10	818	825	0.992
15	532	531	1.002
>25	109	109	1.000
Total	2141920	2143338	0.999

4.3.3. Verification of sampling tube length

Aerosol measurement by the Hiac/Royco optical counter is based on the extractive technique. A sample of the flowing aerosol is extracted and conveyed to the measurement unit. This method is accomplished by withdrawing a sample of aerosol from its original environment through transporting tubes. The extractive system therefore consists of (a) a sample inlet, where the aerosol is removed from its environment and (b) the sample transport system consisting of tubes, which may include bends, inclines and constrictions. It is desired that the sample be representative and that the aerosol is not affected in anyway by the sampling process with respect to the number concentration and size distribution (and chemical composition). It is however difficult to prevent losses during the aerosol sampling and transport. Losses can occur at the inlet of the tube as a result of curving streamlines entering the inlet or along the conducting tubing. Losses or depositions in the sample tube are a result of particle inertia, impaction, interception, diffusion and gravitational settling as well as electrostatic attraction. These deposition losses can also depend on the flow rate, the tube diameter and orientation as well as temperature gradient, vapour condensation onto the walls of the tube and particle size. However, for the same equipment, set up and location, making the transport path as short as possible and using the same tube diameter throughout, reduce the effects of these losses. Any changes should be assessed quantitatively in order to correct the measurement. For example, the reduction of the tube length for the Kumasi counter from 2.5 m in the period 1997-2002 to 15 cm in 2005 was to improve the sampling efficiency. It was therefore important to verify the losses in the sampling tube and effect corrections due to the tube length before measurement results were compared with those data taken with the shorter tube lengths. The counter placed at the Tamale station had a tube length of about 15 cm throughout. Since the two counters were inter-calibrated with the same tube length of about 15 cm, it was necessary to assess the losses that might occur in the longer tubing used in the Kumasi sampling station for any accurate data comparison and statistics with the Tamale data. Table 4.2 shows the characteristics of the sampling tube length and particle concentration using the old counter placed at Kumasi. The particle loss in the sampling tube (2.5 m) was negligible for particle sizes less than 2 μm. This result conforms to that of Piazzola (1996). For particle sizes larger than 2 μm, the particle distribution with the 0.15 m tubing was compared with the 2.5 m tubing. The ratio of the particle concentration with 0.15 m tubing to the 2.5 m tubing was about 1.0 for particle size ranges (in μm) 0.5-0.7, 0.7-1 and 1-2; 1.1 for the particle size ranges, 2-5 μm, 5-10 μm, and 15-25 μm; 1.2 for the particle size range 10-15 μm, and 1.3 for particles > 25 μm. Meanwhile, the ratio for the total particle concentration (0.5-25 μm) was about one. Thus the difference in the total particle concentration when using the 0.15 m and the 2.5 m tubing was negligible. However, generally, the results shown in Table 4.2 reveal that the particle distribution in the various size-classes decreases with increasing tube length. The difference is the particle loss in the longer sampling tube. Therefore, corrections to account for the loss in the sampling tube were effected by multiplying the data from Kumasi, for the Harmattan periods 1997-2002, by the correction factor in column four of Table 4.2c.

Table 4.2. Sampling tube length and particle concentration

(a) Tube length = 0.15 m. Date: 14/3/06

	Counter: Old counter (serial number, 95060047)						
Size (μm)	Particle concentration (m^{-3})						Average (m^{-3})
0.5-0.7	10574252	10463224	10153514	10142124	10500640	10740815	10429095
0.7-1	6444203	6386093	6248825	6231768	6305240	6356587	6328786
1-2	9949590	9901632	9696807	9685171	9762968	9797083	9798875
2-5	7457840	7453743	7348100	7341355	7341690	7334820	7379591
5-10	330016	336178	326590	331093	329203	320498	328930
10-15	12890	13119	13278	13349	12413	12448	12916
15-25	2118	1801	1377	2683	1642	1606	1871
>25	141	317	194	317	194	105	211
Total	34771052	34556108	33788684	33747860	34253992	34563964	34280277

(b) Tube length = 2.5 m. Date: 14/3/06

	Counter: Old counter (serial number, 95060047)						
Size (μm)	Particle concentration (m^{-3})						Average (m^{-3})
0.5-0.7	10572019	10457151	10152012	10140055	10495007	10733121	10424894
0.7-1	6443888	6385913	6248678	6229996	6304988	6349975	6327240
1-2	9949399	9900025	9688992	9675391	9750316	9693576	9776283
2-5	6701166	6720089	6800152	6771813	6700246	6740202	6738945
5-10	292271	293333	295019	293882	295290	292447	293707
10-15	10747	10962	10265	10056	11261	11962	10875
15-25	1959	1891	1601	1786	1591	1579	1735
>25	140	162	183	176	169	154	164
Total	33971590	33769526	33196902	33123154	33558868	33823016	33573843

(c) Particle concentration ratios with 0.15 m to 2.5 m tube lengths

14/3/06	Concentration (m^{-3})		Ratio (correction factor)
Size (μm)	(0.15 m tubing)	(2.5 m tubing)	(0.15 to 2.5 m tubing)
0.5-0.7	10429095	10424894	1.00
0.7-1	6328786	6327240	1.00
1-2	9798875	9776283	1.00
2-5	7379591	6738945	1.10
5-10	328930	293707	1.12
10-15	12916	10875	1.19
15-25	1871	1735	1.08
>25	211	164	1.29
Total	34280277	33721846	1.02

4.4. Experimental equipment and set-up

In this study, the monitoring equipment used is an automatic optical particle counter made by Pacific-Scientific marked under the trade name of, Hiac/Royco 5250A. It is an in-situ high-tech single particle counting system. It uses a He-Ne laser light source for particle illumination. It has 8 user-select size channels with particle size range of 0.5-25 μm ± 5 % size sensitivity, specified by the manufacturer. The laser diode aerosol sensor is calibrated with the National Institute of Standards and Technology of the United States of America (NIST) - traceable particle size standards. From the calibration curve the counter interpolates the data points for the selected nominal channel or bin sizes. The system includes a keyboard, a liquid crystal display (LCD), a thermal printer, a flow meter, sockets to connect input and output computers and other processors, and power supply socket. These are all integrated within a single portable unit measuring, 46 cm x 30 cm x 26 cm and weighing 14 kg.
The particle number concentration capacity of 35 particles/cm^3 is expandable to 1800 particles/cm^3 by connecting an isodiluter to the aerosol inlet. An isodiluter is a flow device that dilutes the concentration by means of filtering off some of the sampled particles and diluting the rest of the sample by a factor of say 50 times as in this study, to fall in the concentration capacity of the instrument. The counter's pump draws the aerosol at a flow rate of 28.3 ℓ /min. (1 ft^3/min). The counter has a variable sample time (period of monitoring the aerosol from outside) and delay time (period of idle pump, between monitoring times) that can be selected. The sampling results are first displayed on the LCD screen; they can also be read on the thermal printout, stored on the data buffer or on a connected PC. Two of these identical devices (Hiac/Royco 5250 A) were used for the sampling campaigns at two sampling sites during the Harmattan periods, from 2001 to 2005. They both functioned properly and were within up-to-date calibration during the experimental measurement periods.

4.5. Principle of operation of sampling equipment

Figure 4.2 illustrates the principle of operation of a single particle Hiac/Royco optical counter. The pump provides the transport of aerosol from the inlet through the sensor to exhaust. An electronic flow meter, downstream from the sensor assembly monitors the flow rate through the sensor. The sensor system is composed of a dedicated power supply, a laser diode illumination source, an optic micro-cell (sensing volume), light collection optics, preamplifier printed circuit board and photodiodes. The sensor system detects the presence of particles in the aerosol medium and converts them into electrical pulses whose amplitude is proportional to the particle sizes. These pulses are applied to the eight channel circuits, within the counter and for each pulse amplitude that exceeds the channel threshold setting, a count will be triggered in that channel. Each channel counts pulses within a specified range; the ranges between the channels (channel 1 to 8) are contiguous. During and after the counting run, the channel counts are visually displayed on the LCD either differentially or cumulatively. The results are also printed on a paper by the thermal printer. In this study, a portable memory device, called Datalync, was used sometimes to store data for later recall on the computer.

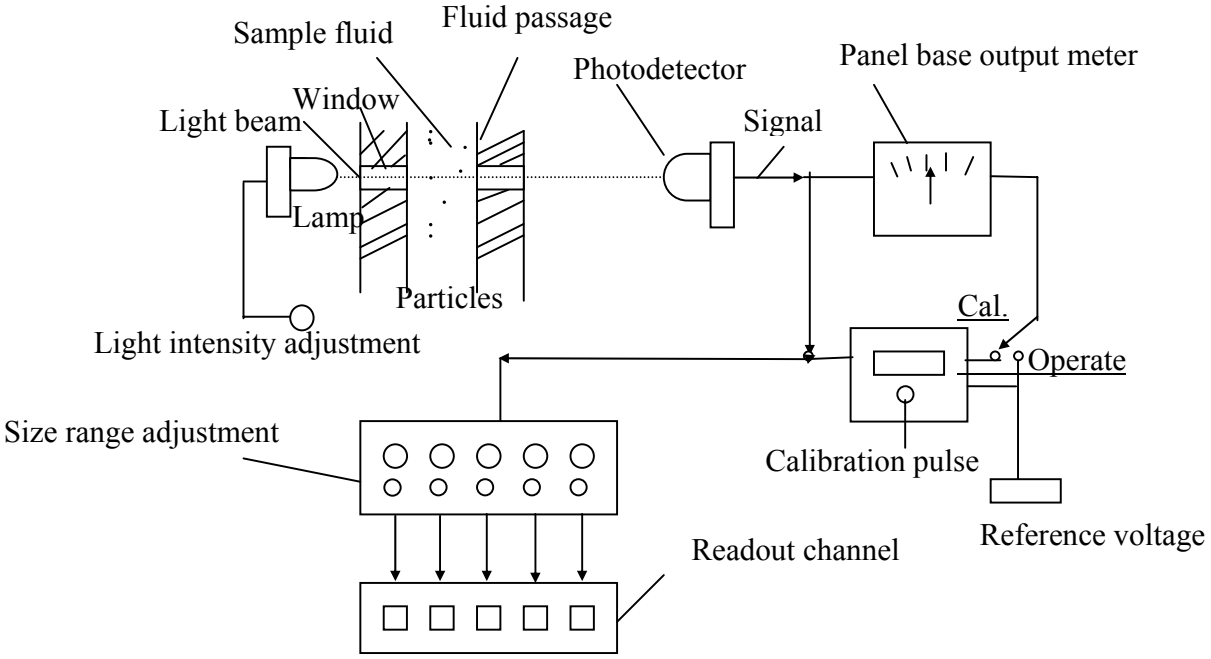

Figure 4.2. Operation of a basic Hiac/Royco optical counter.

4.6. Experimental methods and measurement techniques

The following precautions were observed during the measurements to achieve quality data.

Flow rate control
The airflow rate was maintained strictly within the range 0.9-1.1 ft^3/min (28.3 ℓ/min ±5%), excluding the limits. This is important because the flow rate determines the speed of the particle in the sensor chamber, designed to count a particle at a time. If the flow rate falls outside the operating range, the counter will give spurious results. For example, coincidence error, which occurs when two or more particles occupy the sensing volume at the same time, can occur. This causes an underestimation of the particle number concentration and an overestimation of the particle size. The specified flow rate in the sensor chamber produces the right level of turbulence and thus enhances tumbling of particles. This enables the maximum area of a particle to be focused and recorded. The operating temperature of 52°C prevents any condensation of water vapour, which may cause coagulation of particles and also dew on the optics transmitting the laser beam.

Choice of particle class size
The particle size ranges were carefully selected in order to give a good coverage of particles within the 8-maximum size-ranges of the Hiac/Royco measuring equipment. The smallest measured size is 0.5 μm, which is the sensitivity or the smallest particle size the instrument can detect and measure. The largest particle diameter measurable by our technique is 25 μm.

As shown in the literature, mean diameter of particles reaching Kumasi, which is about 3000 km away from the source regions, may fall below 5 μm. In particlular, Kalu (1977) obtained 8.9 μm mean diameter at Kano in Nigeria, Adedokun (1989) obtained 3.12 μm in Ile Ife also in Nigeria and in Accra, Anderson (1994) obtained a mean of 2.11 μm while Sunnu (1997) obtained a mean of 1.1 μm with particles having diameter less than 10 μm constituting 95% of the dust aerosol. Thus the assumption that the mean size measured at the experimental site of Kumasi (a city farther from the Sahara desert than Kano and Ile Ife) should be less than 5 μm is a reasonable one.
Therefore, based on the above analysis, the following class sizes were chosen. For Kumasi, the classes chosen for sampling during the 1996-97 Harmattan period (in μm) are: 0.5-0.8; 0.8-1.2; 1.2-1.8; 1.8-3; 3-5; 5-10; 10-20; >20. These were later adjusted from 1998 to 2000 to give a better coverage to the particle distributions as follows: 0.5-0.7; 0.7-1; 1-2; 2-4; 4-7; 7-13; 13-25; >25, and from 2001-2005, for both Kumasi and Tamale, they were adjusted to 0.5-0.7; 0.7-1; 1-2; 2-5; 5-10; 10-15; 15-25; >25. A reason for the class size adjustments in 2001-2005 was to match the results to inhalation in human health impacts of suspended particulate matter (SPM) of sizes less than 10 μm, 5 μm or 2.5 μm in diameter (PM10, PM5 and PM2.5, respectively). The particle distribution for the day and night samples did not show any change therefore, only daytime sampling was done for the years 1997-2005. The data were automatically acquired hourly between 6:00 and 18:00UTC.

4.7. Description of experimental sites

Data acquisition took place at two sampling sites namely, Kumasi in central Ghana and Tamale in the north. The sampling site in Kumasi was located at the rooftop of the cooling tower apartment of the classroom block of the Faculty of Environmental and Development Studies (FEDS) of the Kwame Nkrumah University of Science and Technology (KNUST) Kumasi. The geodetic point of this site is: 6°40'N, 1°34'W, as determined by the Geodetic Engineering Department of the KNUST. The height of this location is about 311 m above sea level and about 15 m above ground level. The site is the highest point in the faculty area of the KNUST and is thus higher than all the surrounding trees, (which are below 10 m) and taller than other buildings in the faculty area. It is therefore assured that this site is beyond the reach of any fugitive dust, smoke and other locally generated aerosol particles and is the best that can be selected on the campus. The FEDS is at the south-eastern border of the KNUST. The immediate settlement, near the FEDS site, downstream of the northeast trade winds, is the village of Ayeduase, which stretches from northeast to south of the site. In the immediate north bordering the site are other faculty buildings. The western side of the building had a canopy of trees to a height of about ten metres above ground level. Under the canopy of trees was the Faculty car park, which had a tarmac surface.
The nearest asphalted road is about 70 m away on the northern side running west to east and leading to the car parks of the FEDS. Thus there is no possibility of traffic pollution at the site. Low-lying grass or concrete pavements cover every other surface. Between the faculty area and the main university residential areas, including the Administration and

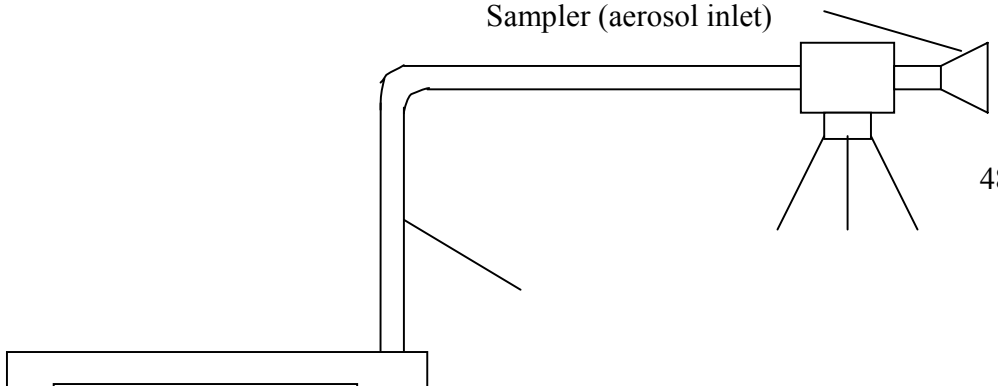

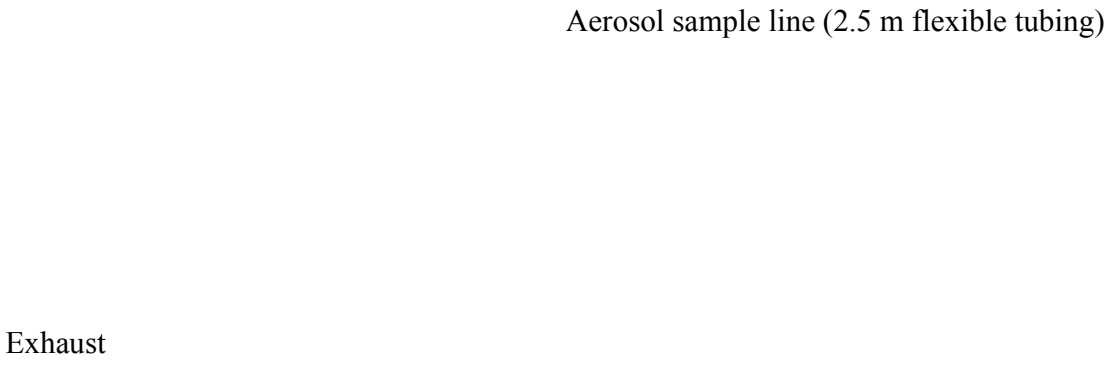

Figure 4.3. Sampling configuration.

student halls of residence, there is a valley, a stream and an evergreen forest belt stretching from west to east on the northern side. The faculty is about one kilometre from the main university campus. No farming activities are allowed in the forest. There are some vegetable farms about a kilometre to the western fringe of the campus, which is about the same latitude as the site and so are not in the mainstream of the northeast winds with respect to the sampling site. About two kilometres away, in a west-northwest direction starts the city of Kumasi. As free as possible from local contamination, the height and surrounding of this location, selected for data acquisition, make it favourable for a representative sampling of the dust aerosol.

Figure 4.3 shows the system configuration of the set-up. The isokinetic diffuser sampler is mounted on a wooden stand about 0.6 m above the rooftop (Figure 4.4). The diffuser faces the north east in the direction of the incoming winds. The flexible sampler hose connecting the sampler to the optical counter is passed through a hatch in the concrete roof down to the floor below where the counter is mounted on a table. The location of the sampling site on the KNUST campus is shown on the topographical map of Kumasi (Figure 4.5). Figure 4.6 is the map of Ghana showing the cities where sampling took place.

The sampling point in Tamale is situated at the air traffic control tower (Figure 4.7) of the Tamale Airport with geodetic point of 9° 34’ N, 0° 52’W. It was about 180 m above sea level and 13 m above ground level. About 150 m away to the north of the tower is the weather station and about 400 m further north is a small hanger beyond which is all grassland with short trees of about 5 m maximum height, sparsely distributed for over 10 km.

Figure 4.4. The aerosol sampler on the rooftop of FEDS Kumasi.

Along the line of the control tower, the weather station and the hanger, is the runway that stretches beyond the hanger for about a kilometre. Air traffic at the airport is very light with only one takeoff and one landing in a day. To the east of the sampling point are the airport arrival and departure halls, car parks, and a road that enters the airport. All the roads are properly surfaced with bitumen. Surrounding the airport is all grassland and about 10 km towards the west starts the city of Tamale.
The sampling period coincides with the non-farming season and grazing by cattle is restricted to the valleys, which are not found in the vicinity of the airport. The counter was placed on a stand of about 0.8 m tall from the top floor of the flight control tower. The isokinetic sampler was placed directly on the counter without any interconnecting hose for direct aspiration.

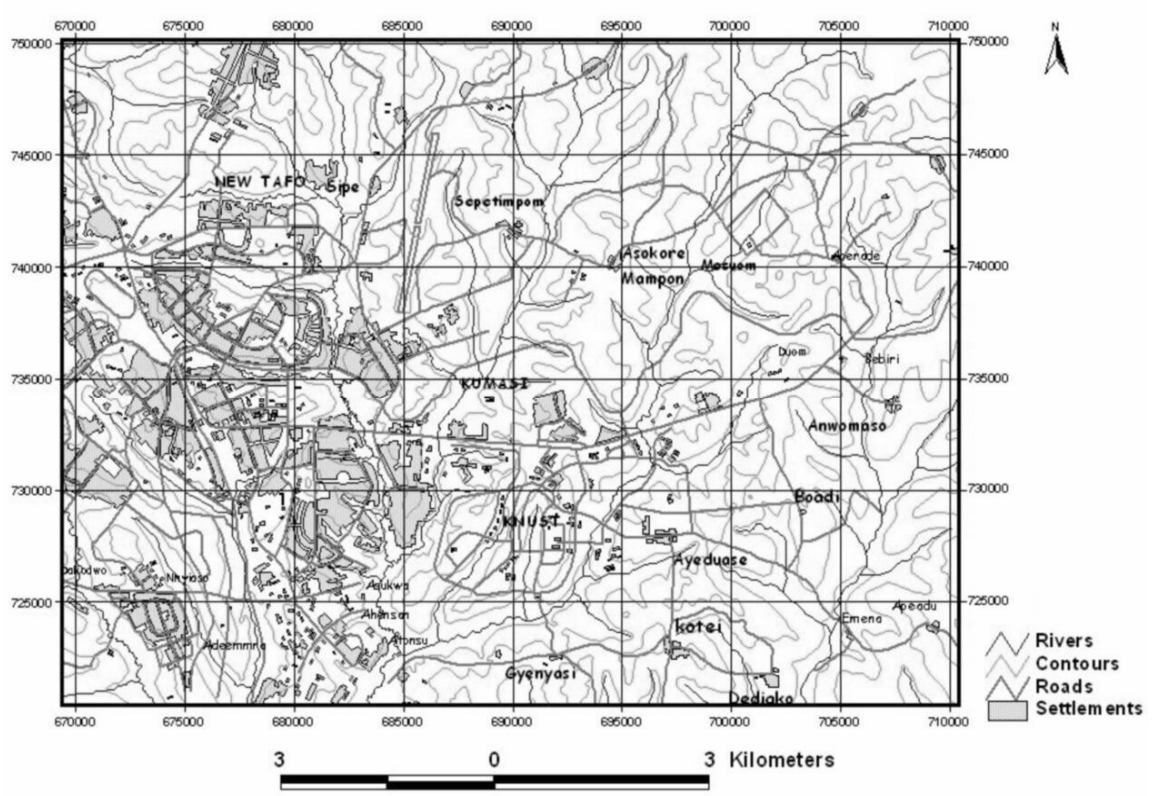

Figure 4.5. Topographical map of Kumasi showing location of sampling site on KNUST campus.

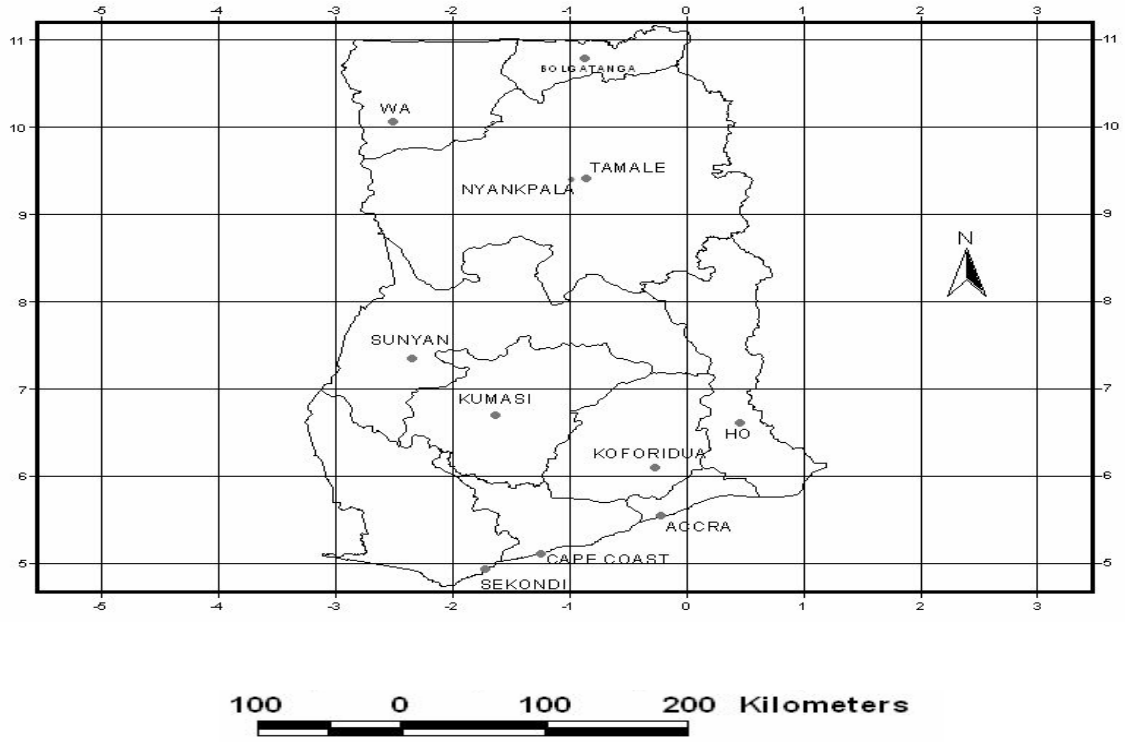

Figure 4.6. A map of Ghana showing location of some towns, including Kumasi and Tamale.

(a)

(b)

Figure 4.7. (a) and (b) Sampling site at the air traffic control tower of the Tamale Airport. Figure (a) is a photograph of the site taken during the wet season on the 10th August 2004. The vegetation surrounding the site is all green grass and short trees. The blue colour of the skies is the result of air-molecule scattering and absence of haze. Figure 4.8 (b) shows a photograph of the same sampling site taken during the dry (Harmattan) season, in December 2000. The dying and dry vegetation surrounding the sampling location as well as the hazy sky are shown, typical of the dry season.

4.8. Data analysis

The evolution of the ITCZ and the NAO during the Harmattan period (November-March) is analysed and graphs of the average ITCZ positions and the NAO are plotted on daily basis. A Julian day numbering system, the day-of-year or ordinal day, has been adopted for the temporal, daily analyses. Thus 1st January is Julian day 1, 1st February is 32 and 31st December is 365 except in a leap year where it will be 366. 31st December and 30th November, in the previous year, will be Julian day -1 and -32 respectively.

The optical counter reports, for each sample run, the number concentration in each diameter class and the cumulative concentration over the entire size range (0.5-25 μm). The daily average concentration is calculated for each size interval as well as the daily average concentration over the entire size range. The size distribution curves are obtained by plotting the number of particles/cm^3 (N) against the mid-point size in micrometer (D) for each class, using a log-log scale. These logarithmic plots enable easy comparison of concentrations with different size distributions. The midpoint size of each class was then used to calculate the average mass of a particle belonging to that size class.

5. RESULTS AND DISCUSSION

The results reported in this chapter concern the measurements of the Saharan dust in Kumasi (1^o 34' W, 6^o 40'N) and Tamale (0^o 52' W, 9^o 34'N) both in Ghana, during the Harmattan period, from 1997 to 2005. The data were acquired for Kumasi throughout the period, from 1997 to 2005 and for Tamale, from 2001 to 2005. Essentially, sampling for the Saharan dust particles started a year before 1997 using a 10 m long sampling tube. However, the data obtained for that Harmattan period were discarded because of a rather too long sampling tube. Subsequent verification of the effect of sampling tube length on sampling efficiency implied that the 10 m long sampling tube, used in the previous year, may have introduced significant errors in the results by under-estimating the particle number concentrations. Similarly, the data obtained during the 2003 Harmattan period at the Tamale station were found to be inconsistent with expected trends probably, due to equipment failure and hence rejected. Thus, there were no data for the 2004 Harmattan period because the sampling equipment used at both stations were down and were under servicing and recalibration although that year (2004), the Harmattan was observed from the visibility reduction, to be one of the most severe in the period. The overall data include the particle number concentration per cubic metre of air for each selected size range, the total concentration over the entire instrument size range (0.5-25 μm) and the daily average concentrations in each size range. The particle size distributions, particle statistics and the dust particle flux will be estimated.

5.1. Evolution of ITCZ and NAO

The Inter-Tropical Convergence Zone (ITCZ) variations with respect to Ghana were also determined and analysed. Furthermore, analyses of the North Atlantic Oscillation (NAO) data have been reported. It is worth noting that the differences between the ITCZ data on local basis obtained by the local meteorological services department and that obtained at the NOAA website on the Internet, based on global scale, were found to be negligible and therefore each of these data could be used for this work. However, for reasons related to ease of access, the data from the NOAA website were preferred.

As noted previously, the Inter-Tropical Convergence Zone (ITCZ) and the North Atlantic Oscillation (NAO) are the two large-scale atmospheric systems that are known to affect weather in the northern hemisphere. Qualitatively, the link between the ITCZ and the transport of dust from the Sahara desert over most of West Africa, during the months of November to March, has been reported (Resch et al., 2002; d'Almeida, 1986; Kalu, 1977). The link with NAO has not been extensively explored. However, just recently, Chiapello et al., (2005) studied the impact of the NAO on the Sahara dust aerosol over southern Mauritania, the tropical Atlantic and the Bodele depression in the central Chad. Before, (Hurrel, 1995) the relationship between the NAO and the Sahara dust transport has been inferred from the influence of the NAO on the Northern Hemisphere in general. The following describes the evolution of the ITCZ and the NAO.

5.1.1. The ITCZ

The presence of the Harmattan is strongly dependent on the ITCZ position with respect to the two sampling locations namely, Tamale and Kumasi. Therefore, the ITCZ position and movement during the Harmattan season, from 1997 to 2005, have been carefully examined. The daily ITCZ positions, derived from the NOAA website, were analysed. Figure 5.1 shows charts of the streamlines of the surface winds system obtained from a standard height of 30 feet above ground level (approximately 9.14 m) according to NOAA Satellite and Information Service on the Internet, http:www.ncdc.noaa.gov/) over Ghana in West Africa during the Harmattan period. The point of convergence of the northeast wind streamlines and the southwest wind streamlines is taken as the average position of the ITCZ over the country on daily basis. Figure 5.1(a)-(d) shows the variation of the ITCZ position with the Julian days. The ITCZ is located around latitude 5^{o}N on 2^{nd} January 2005, latitude 4^{o}N on 3^{rd} January, over the equator on 8^{th} January and below the equator on 11^{th} January. On these days the Harmattan winds have fully overcome the country producing severe Harmattan events. The ending of the Harmattan period is indicated by the ITCZ position, which is found receding to higher latitudes as shown in Figure 5.1(e)-(h) where the ITCZ is located around latitude 2^{o}N on 18^{th} January, 4^{o}N on 1^{st} February, 7^{o}N on 12^{th} February and 10^{o}N on 20^{th} February respectively. These ITCZ positions show a reduced Harmattan wind strength over the country and lessening of the Saharan dust haze conditions.

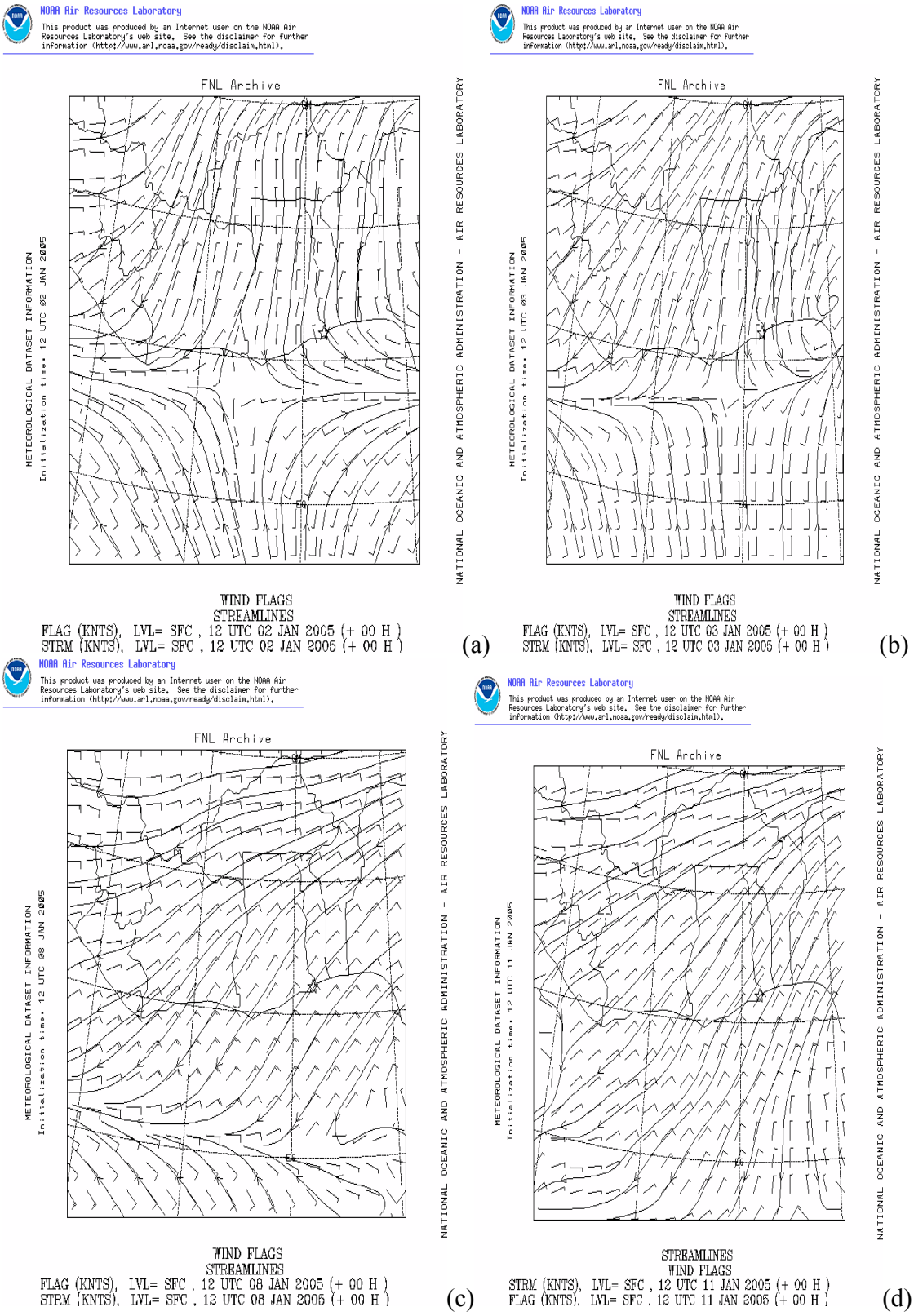

Figure 5.1. (a)-(d) Typical wind streamlines over Ghana during the Harmattan period.

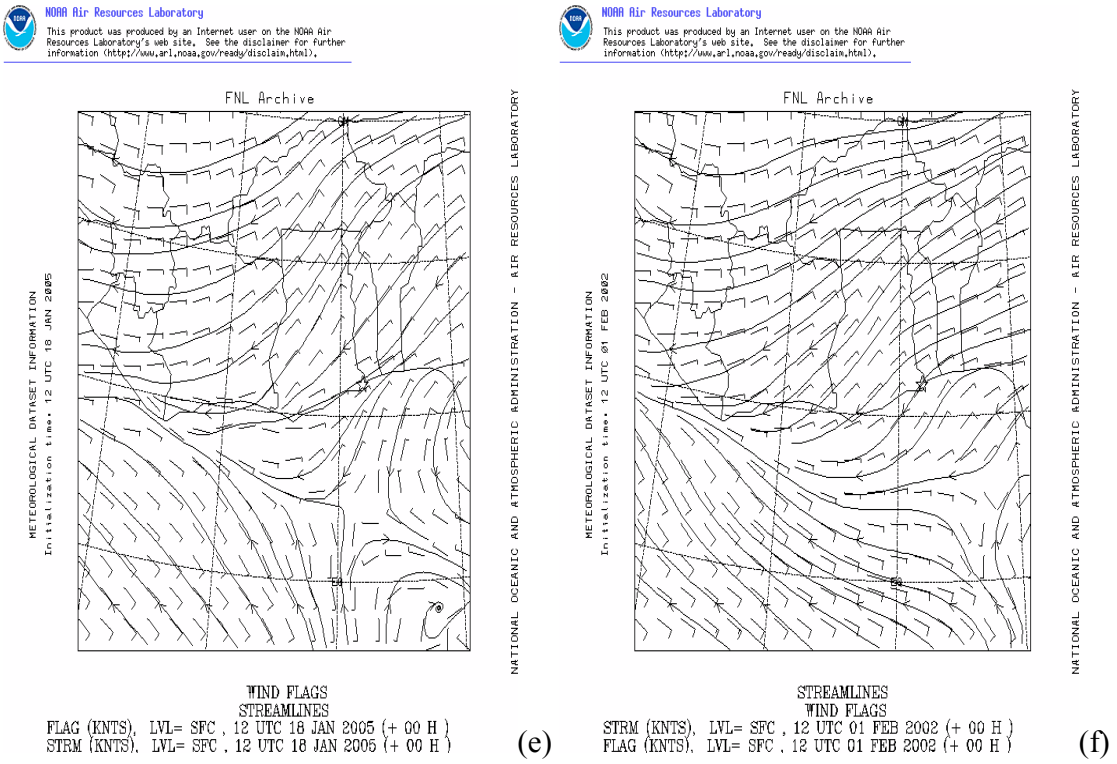

Figure 5.1. (e)-(h) Typical wind streamlines over Ghana during the Harmattan period.

Figure 5.2 shows the scatter plots of all the ITCZ positions, with respect to longitude 0° (Ghana is located between longitudes 1°E and 3°W), during the Harmattan, over the 9-year period, 1997-2005. The locus of the ITCZ positions over Ghana can be described by polynomial functions. These functions show that the average position of the ITCZ moves from high latitudes, around 11°N, at the beginning of the Harmattan, turns round at a lower latitude, of about 6.6°N, around the 13th January (13th Julian day) and then recedes to higher latitudes, beyond 11°N after the Harmattan period. It is worth to note the large intra and inter annual variability of these positions. Nevertheless, a general trend is shown on Figure 5.3, which indicates the average of the ITCZ positions over the period, 1997–2005 fitted with a polynomial function, $y = 0.0007x^2 - 0.017x + 6.72$, where y is the latitudinal position of the ITCZ (with respect to Ghana) as a function of Julian day, x.

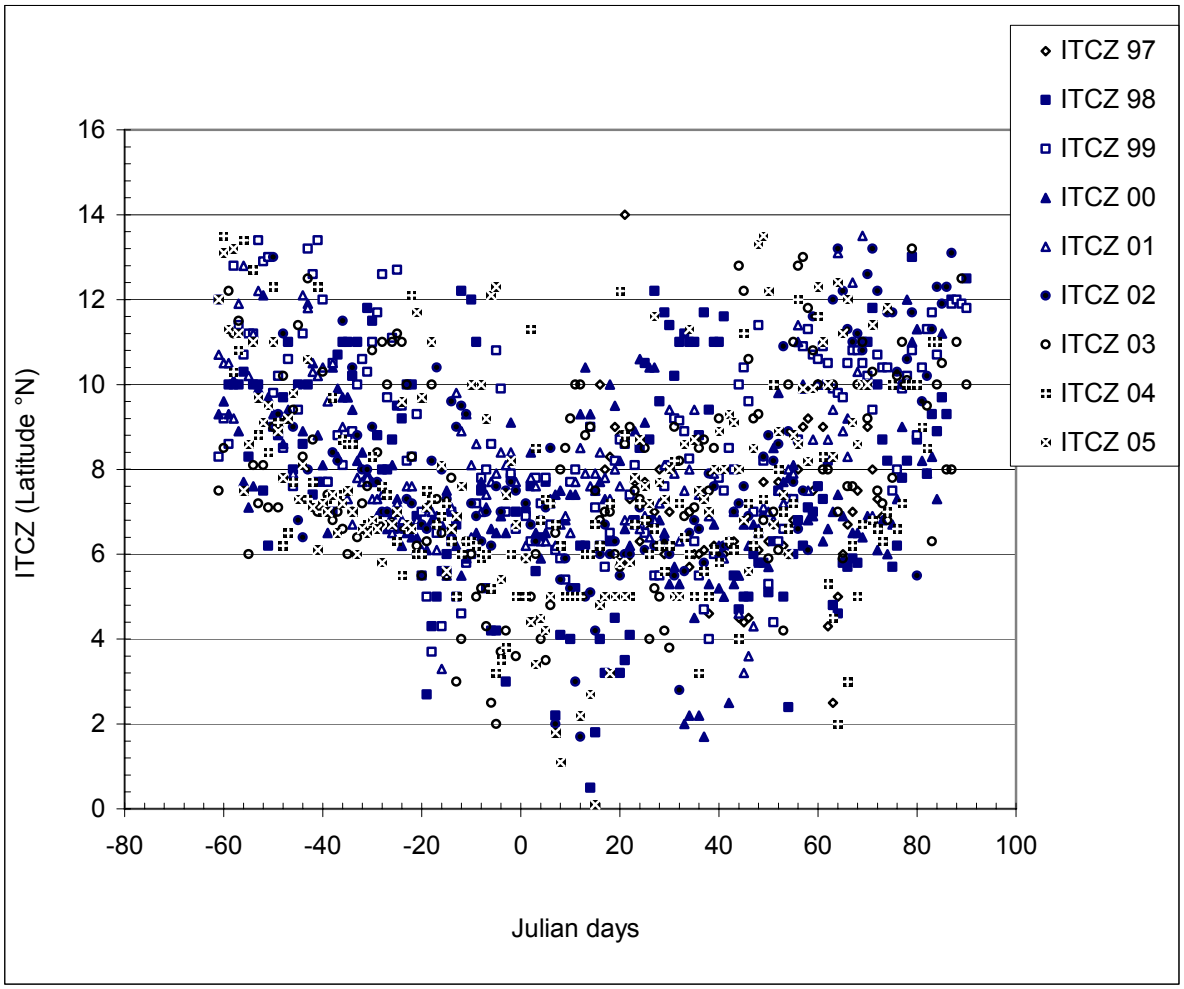

Figure 5.2. ITCZ position with respect to Ghana versus Julian days from November to March: 1997-2005.

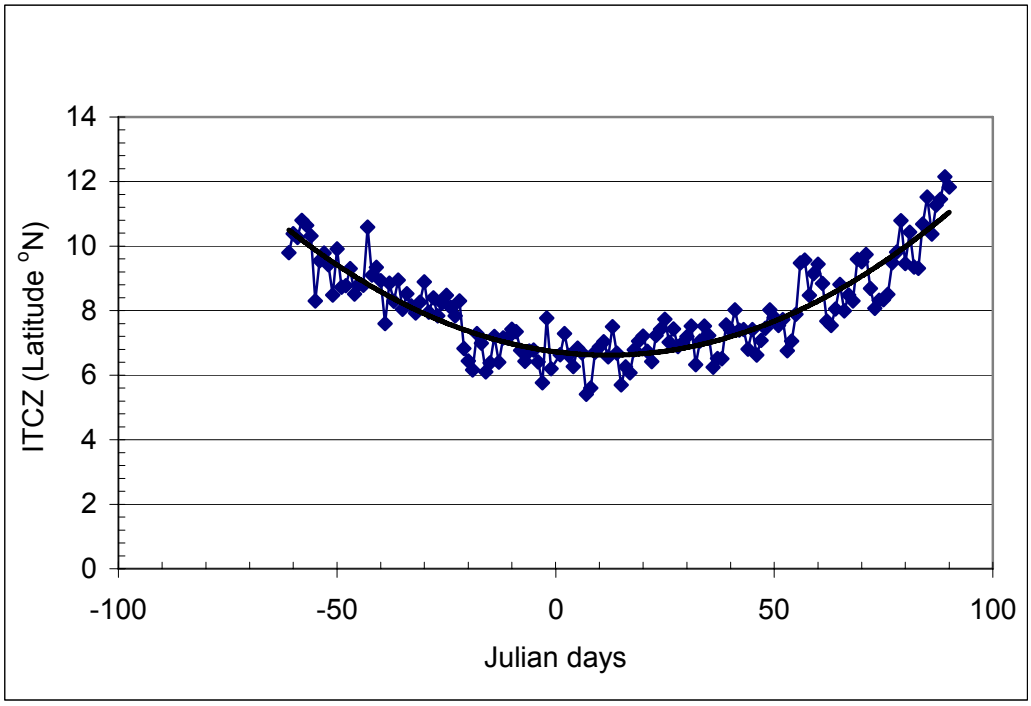

Figure 5.3. Mean position of ITCZ versus Julian days during the Harmattan: 1997-2005.

The mean positions show daily oscillations, which vary from about 1-2^{o} in latitude. Apart from these oscillations, the graph shows a general gradual migration of the ITCZ from high latitudes of about 11^{o}N around Julian day –50 (20th November), at the beginning of the Harmattan season, to a minimum at about latitude 5^{o}N around Julian day 5 (5th January). From the minimum position, the ITCZ then recedes gradually to the higher latitudes (>12°N) while maintaining the daily oscillation movements to the end of the Harmattan period, around Julian day 90 and beyond. Table 5.1 below, based on the polynomial relation, presents values of the position of the ITCZ during the Harmattan period at longitude 0^{o}. These results are in reasonable agreement when compared with the range of 5-10^{o}N for the ITCZ position during the Harmattan at longitude 3^{o}E, reported by Adeyafa et al., (1995) and those reported by Swap et al., (1996) who observed a minimum range of 0-5^{o}N over the Atlantic Ocean in January and the maximum position of 5-10^{o}N in December. The observation of Moulin et al., (1997) who found the minimum position over the North Atlantic Ocean to be at latitude 5^{o}N is also consistent.

Table 5.1. Average ITCZ position during the Harmattan period, 1997-2005.

x (Julian Day)	-40	-20	-10	1	10	20	40	60	80
Y ^{o}N	8.5	7.4	7.0	6.7	6.6	6.7	7.1	8.2	9.8

The lower the ITCZ position from the sampling stations, the stronger and more stable are the northeast trade winds, which transport the Saharan dust over the sampling station. Therefore, the day with lowest ITCZ position signifies the day with most severe Harmattan impact.

5.1.2. The NAO

The NAO is traditionally defined as in section 3.4.2. The sea level pressure measurements are taken at a station, Ponta Delgada (37^o 44' N, 25^o 40' W) on the Azores and another at Reykjavik (64^o 8' N, 21^o 56' W) in Iceland spanning the central latitudes of the North Atlantic. The NAO index defined in section 3.4.2 as a ratio of sea-level pressures over a long period is illustrated in Table 5.2, showing the monthly NAO index from 1995 to 2003. In Figure 5.4, the plot of the monthly NAO index as a function of the months is shown for 1996-2003. The NAO index appears to reach a maximum value in February in most years.

Table 5.2. Monthly NAO index from 1996 to 2003.

Source, Internet: http://www.cru.uea.ac.uk/cru/data/Vinther/nao1821.txt

Month	Month	1995	1996	1997	1998	1999	2000	2001	2002	2003
Jan	1	2.7	-3.27	-1.95	-0.28	0.9	0.35	0.02	2.31	0.15
Feb	2	3.13	-0.12	5.26	2.44	1.8	4.37	0.07	3.01	1.34
Mar	3	1.06	-2.57	2.09	1.24	-0.72	0.54	-0.68	0.09	1.08
Apr	4	-1.81	-0.31	-0.97	-0.39	0.43	-3.34	1.24	0.91	-1.74
May	5	-0.36	-1.5	-1.35	-1.26	1.03	0.31	-0.09	-0.05	1.17
Jun	6	-3.36	1.43	-4.05	-0.85	1.39	0.89	-1.33	0.9	-0.86
Jul	7	-0.96	1.47	1.18	-0.57	-1.85	-2.99	-1.12	-0.71	0.09
Aug	8	-1.33	-0.19	1.78	1.8	-3.67	0.78	1.64	-0.61	-0.99
Sep	9	-1.55	-2.23	-0.67	-3.48	-0.51	-1.1	-3.83	-3.58	0.35
Oct	10	1.22	-0.07	-2.26	1.34	-0.69	2.26	0.88	-1.5	
Nov	11	-2.73	-0.05	-0.99	1.13	0.3	-0.24	0.01	-0.27	
Dec	12	-3.33	-4.7	-0.2	1.95	2.13	-1.41	-2.25	-0.98	

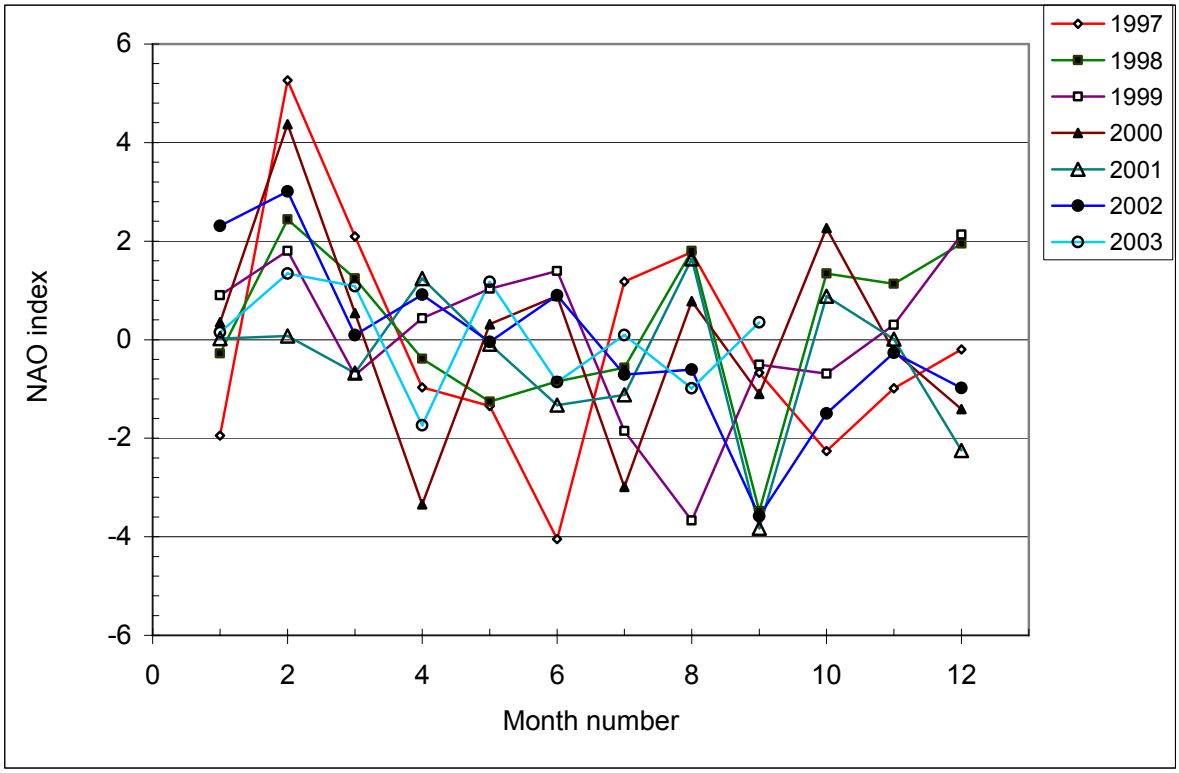

Figure 5.4. Monthly NAO index (1997 - 2003).

5.2. Dust particles in Kumasi

The optical counter reports the results of a sample by the number concentration in each diameter class. The total concentration over the entire size range is also reported. Therefore, the average concentration in each size class and the mean total concentration for a day have been determined. Samples obtained with sampling tube length of 2.5 m at the Kumasi sampling station from 1997 to 2002 were normalized with the samples taken with sampling tube length of 0.15 m. The plots of the mean daily particle concentrations versus Julian days at Kumasi in the various years are presented in Figure 5.5 (a)-(g) for the particle number concentrations and Figure 5.6 (a)-(g) for the mass concentrations. Figure 5.7 and 5.8 show the number and mass concentrations respectively for the set of Harmattan periods from 1997 to 2005.

5.2.1. Number concentration

The dust particle number concentrations at the Kumasi sampling station, measured as a function of Julian days, during the 7-year period, 1997-2005, are shown in separate yearly plots in Figure 5.5 (a)-(g). The particle concentrations range between 100 particles/cm^3 and about 7 particles/cm^3 for the years after 1997 (1998, 1999, 2000, 2001 and 2005) while in 1997 it is between 150 particles/cm^3 and 9 particles/cm^3. The inter-annual variability of the peak concentrations is quite wide while that of the mean nadir is narrow with a mean value of

about 11 particles/cm^3. This lowest point particle number concentration may correspond to the background aerosol during the Harmattan period. Figure 5.7 shows the set of graphs of the number concentrations as a function of Julian days for all the years 1997-2005. The largest number concentrations were observed in 1997, indicating a typically strong Harmattan in that year. On the other hand, the distributions for 1999 and 2001 are significantly weaker. Detailed comparisons of the distributions on a year-to-year basis are reported in Figure 5.5 (a)-(g).

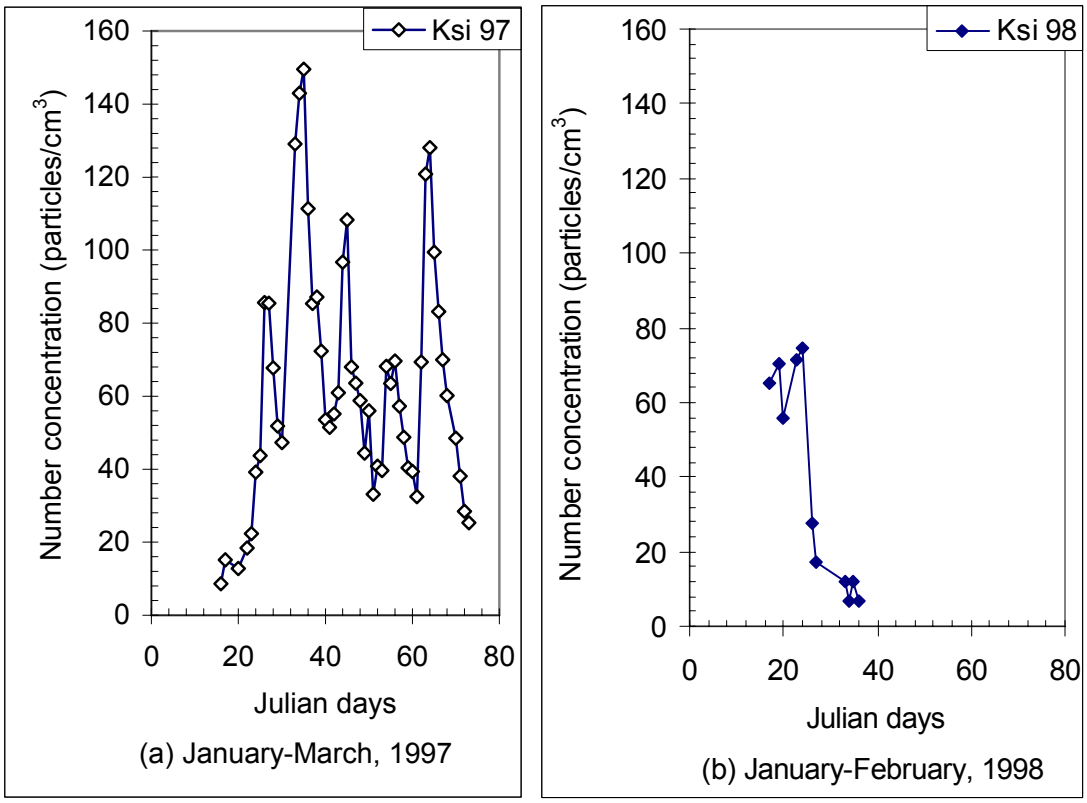

Figure 5.5. (a)–(b) Particle number concentration in Kumasi versus Julian days, 1997 and 1998.

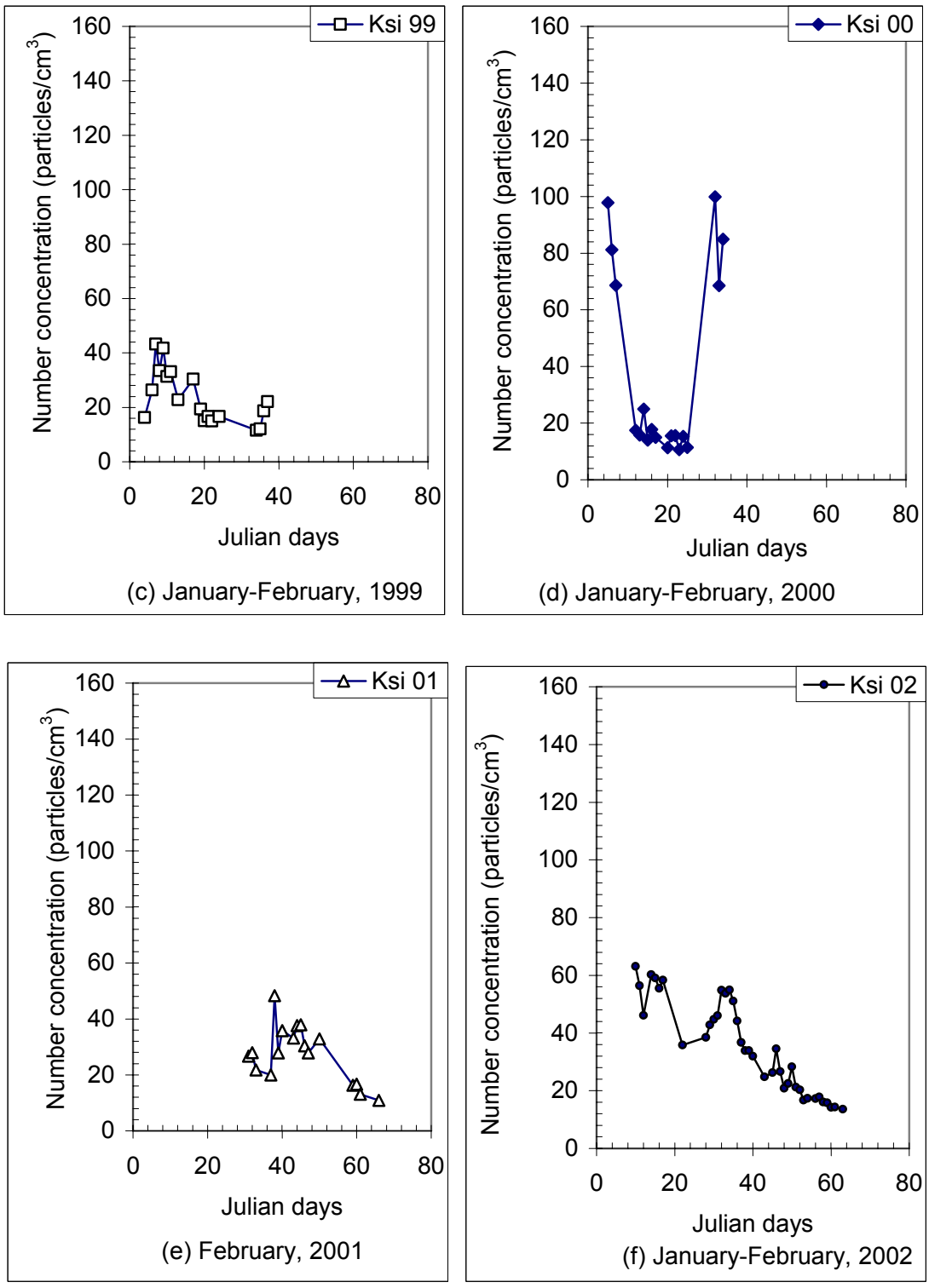

Figure 5.5. (c)–(f) Particle number concentration in Kumasi versus Julian days, 1999-2002.

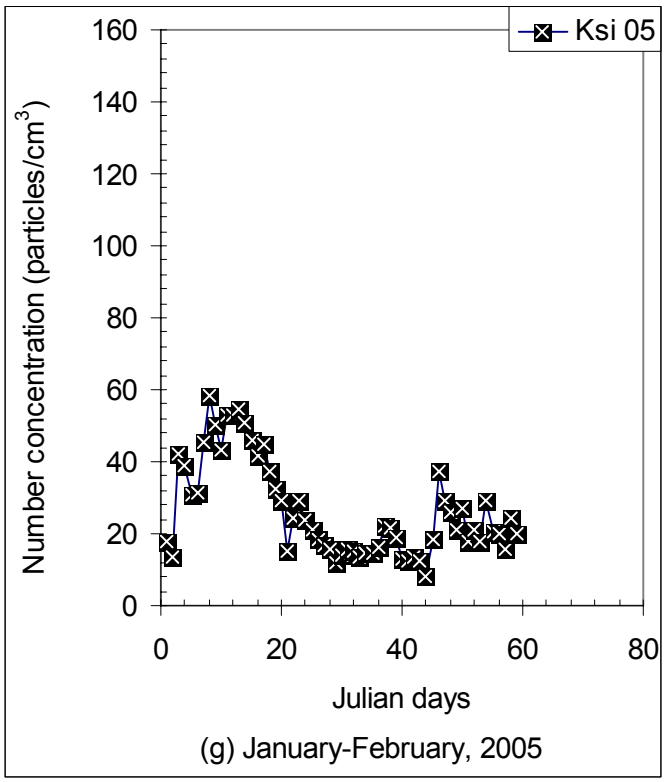

Figure 5.5. (e)–(g) Particle number concentration in Kumasi versus Julian days, 2005.

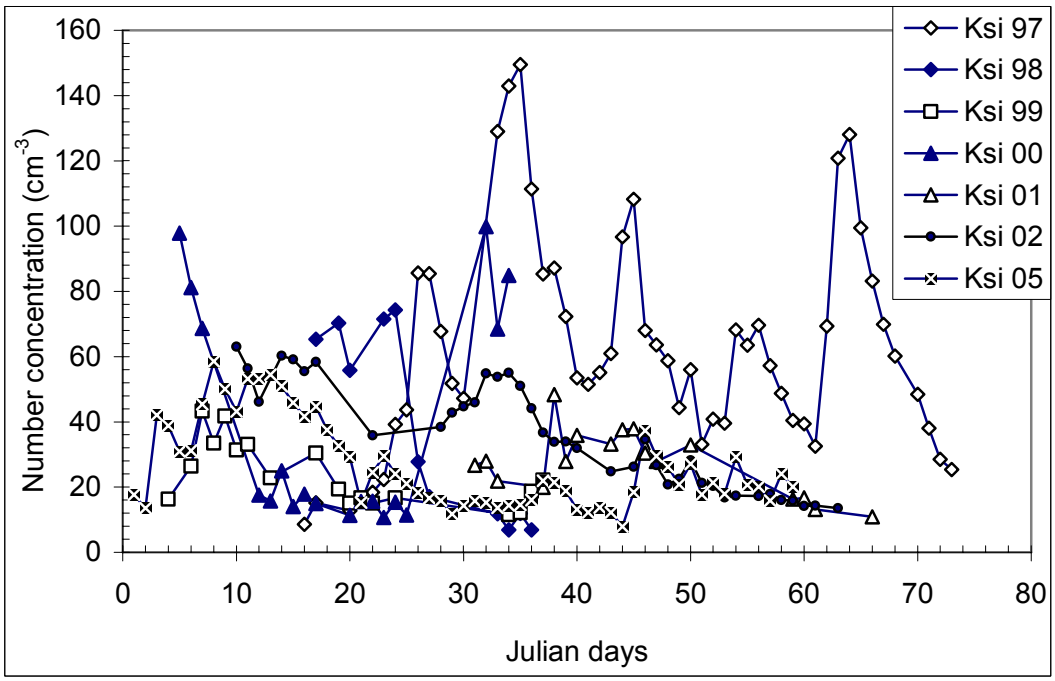

Figure 5.6. Particle number concentration in Kumasi versus Julian days: 1997-2005.

5.2.2. Mass concentration

In order to obtain the mass concentration distributions, the midpoint size of each class was used to calculate the mass of a particle belonging to that size class. This was done by assuming, as a first approximation, a spherical shape for the particles. The mass of a particle with density ρ was obtained as $m = \frac{\pi}{6}\rho D^3$. Given the particle number concentration, N and assuming that the particles were spherical silica particles of density ρ = 2650 kg/m^3, the particle mass concentration is obtained as $ND^3\rho\pi/6$ in μg/m^3. The particle mass concentrations as a function of Julian days at the Kumasi sampling station, in the various years, are shown below in individual yearly plots, Figures 5.6 (a) –(g) and cumulative plots in Figure 5.8.

Comparing the Figures 5.7 and 5.8 (single-chart cumulative number and mass distributions), some interesting observations can be made. For example, comparing the 1997 and 2005 data, it can be seen that the number of particles is much greater in 1997 than in 2005. The reverse is true for the mass distributions, indicating the presence of particles larger in 2005 than in 1997. High particle number concentrations are conspicuous in 1997, 1998 and 2000 while the mass concentrations in 2002 and 2005 are noticeably above the rest in the period. The large difference between the concentrations (number and mass) for the years up to 2000 and years after 2000 is outstanding.

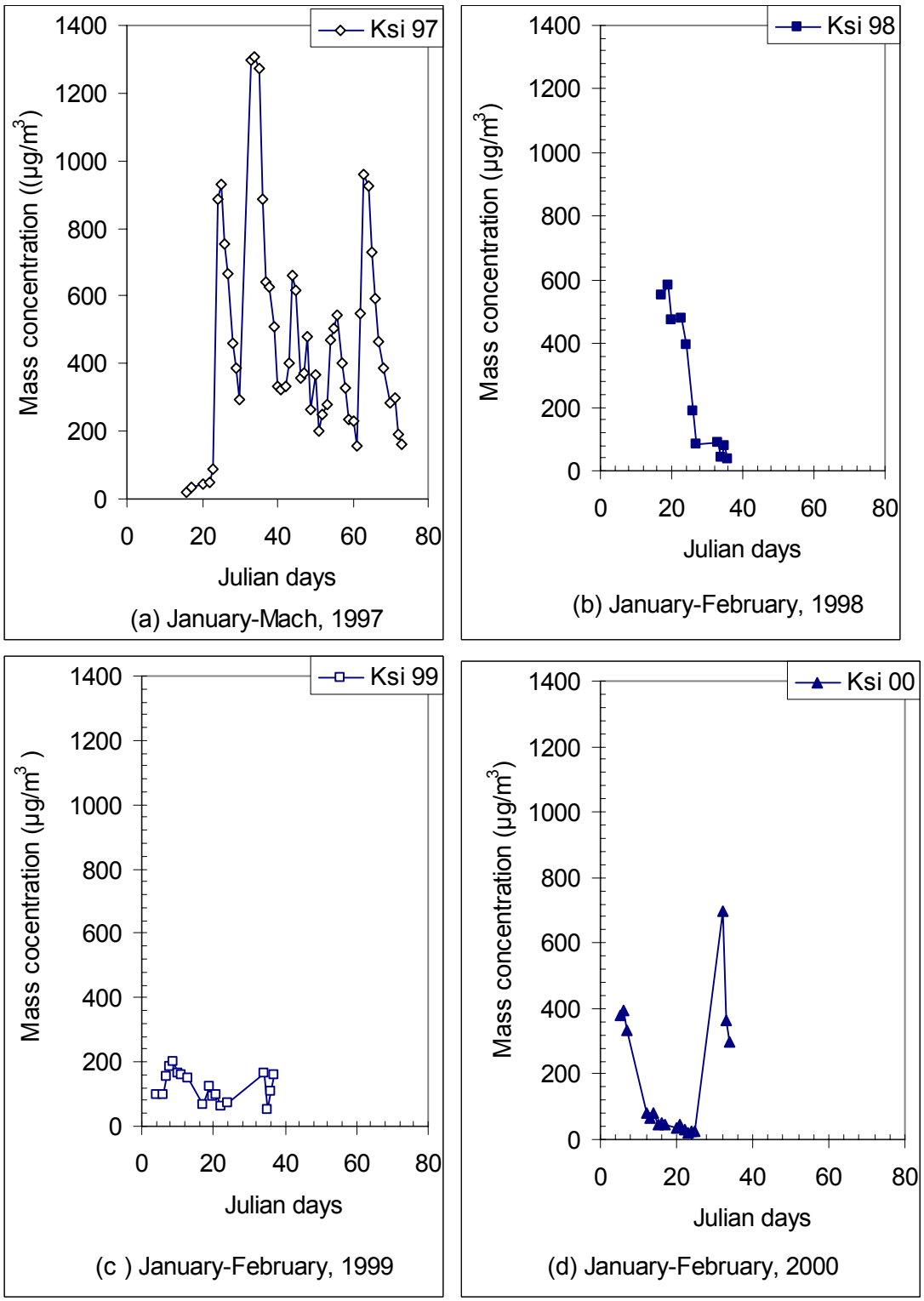

Figure 5.7. (a)–(d) Particle mass concentration in Kumasi versus Julian days, 1997-2000.

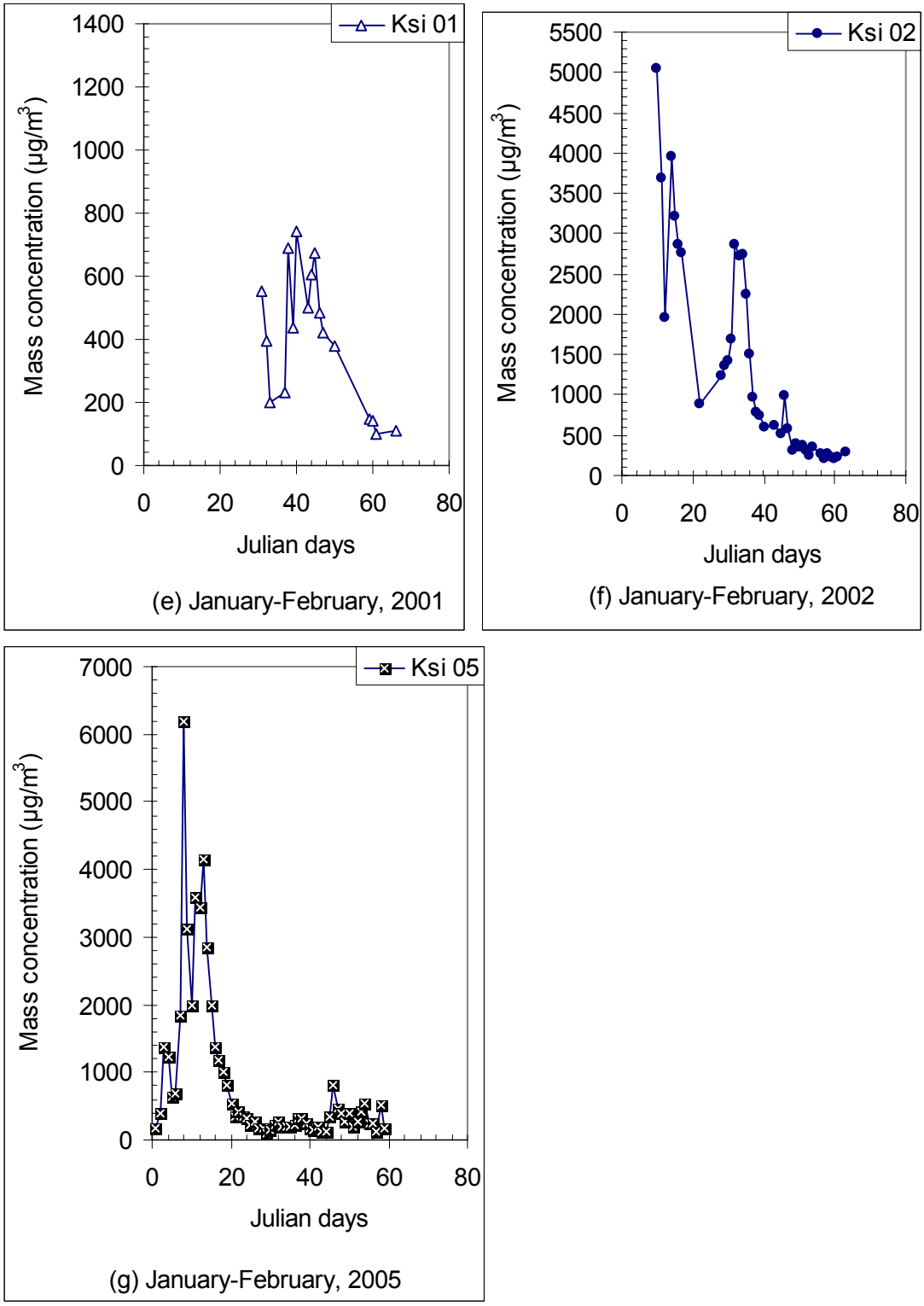

Figure 5.7. (e)–(g) Particle mass concentration in Kumasi versus Julian days, 2001, 2002 and 2005.

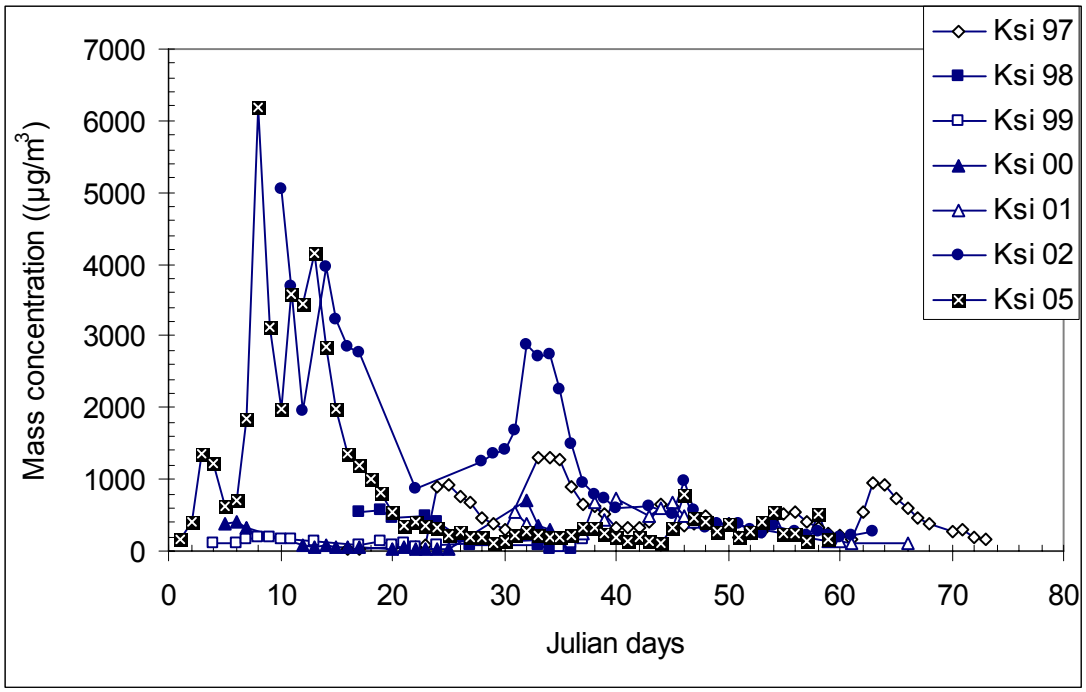

Figure 5.8. Particle mass concentration in Kumasi versus Julian days: 1997-2005.

5.2.3 Number frequency distribution

The particle number concentration is highly variable during the period. Therefore, it was decided to select, for each year, a 6 to 13 days period corresponding to the highest concentrations (number and mass). These selections are shown in Figure 5.9 for the particle number concentrations and Figure 5.10 for the mass concentrations, all plotted as a function of the Julian days in the respective Harmattan periods, 1997-2005. This selection of data points among those available is therefore representative of the maximum strength of the Harmattan for a given year. This is what we would call 'selected period'.

In order to compare the particle concentrations among the various size classes, the concentrations are normalised by dividing the concentration in each size class interval by that class size or the width of that interval. Since the normal distribution is skewed (long tail at large sizes) as for most atmospheric aerosols, the lognormal distribution function is used to analyse the data of size distribution of the particle concentrations. The size distribution curves are obtained by plotting dN/dLogD on the ordinate, where dN is the number of particles/cm^3 over the class interval dLogD. The logarithm of particle diameter D which is taken as the class mid-point size in micrometer (µm), is plotted along the horizontal axis. Both axes are plotted on the natural logarithmic scales. Figure 5.11(a)-(g) shows the number distributions in the various years, 1997-2005 during the Harmattan period. All the number distribution graphs are displayed on a single chart as Figure 5.12. All the graphs exhibit a fairly similar slope. In particular, the graphs have a sharp downward slope from the particle size (diameter) of about D = 3 µm to the larger particles, of size about D = 20 µm. The range of concentrations covers roughly 5 orders of magnitude. The general distributions of

atmospheric particles have been given by Whitby (1978) in Renoux and Boulaud (1998). Comparing Whitby's result to Figure 5.12 of this work, the Saharan dust distributions can be said to fit well into the accumulation mode and the coarse-particle mode, although the accumulation mode is not well developed. Therefore, Figure 5.12 is a summary of the general pattern of the number frequency distributions for the Saharan dust in the study period, 1997-2005. The graphs show that the smallest particles are in the highest numbers, which decrease with particle diameter. By inspection of the graphs, apparent two modes of the distributions can be seen. The peak of the coarse-particle mode can be found around 3.5 μm diameter. No such deduction can be made for the accumulation mode, which is under developed for any statistics estimation. The shape of the curves for the years 1997-2000 is markedly different from the shape of the curves for the years after 2000, particularly 2002 and 2005. This difference can be related to the large difference between the particle number concentrations which are apparently higher for the years before 2000 than the years after 2000.

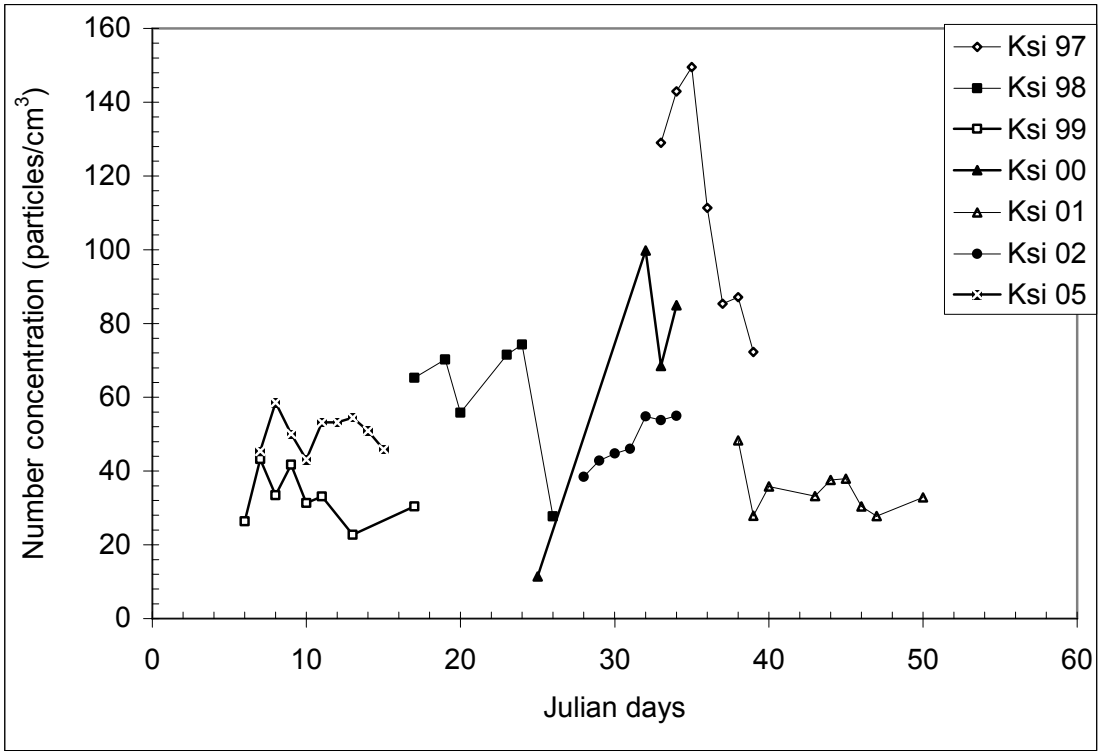

Figure 5.9. Particle number concentration in Kumasi versus selected Julian days:1997-2005.

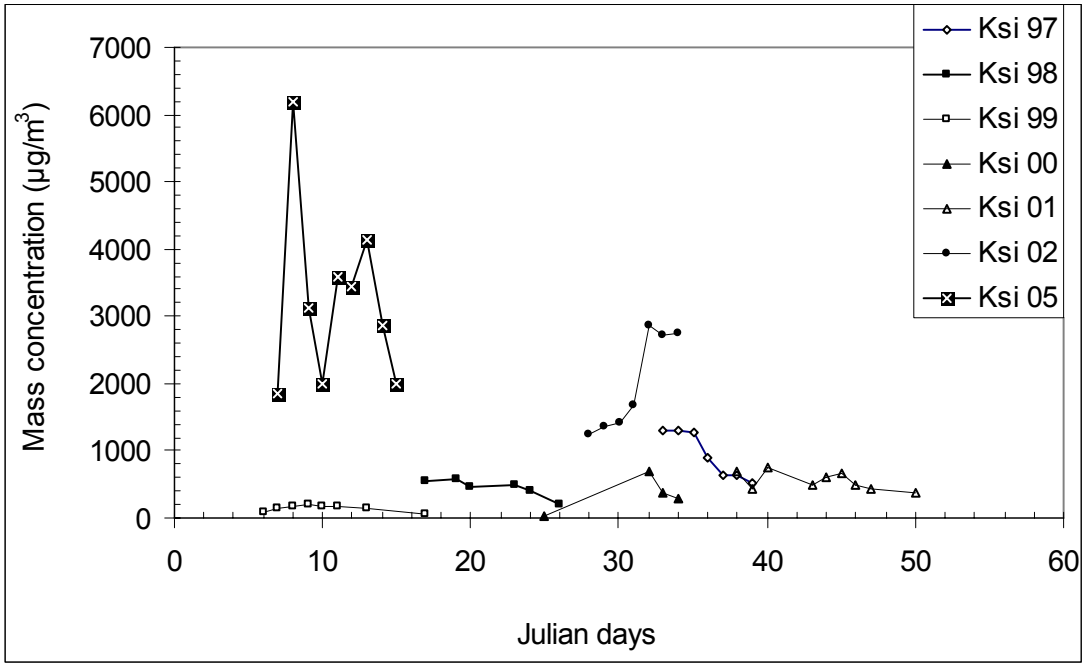

Figure 5.10. Particle mass concentration in Kumasi versus selected Julian days:1997-2005.

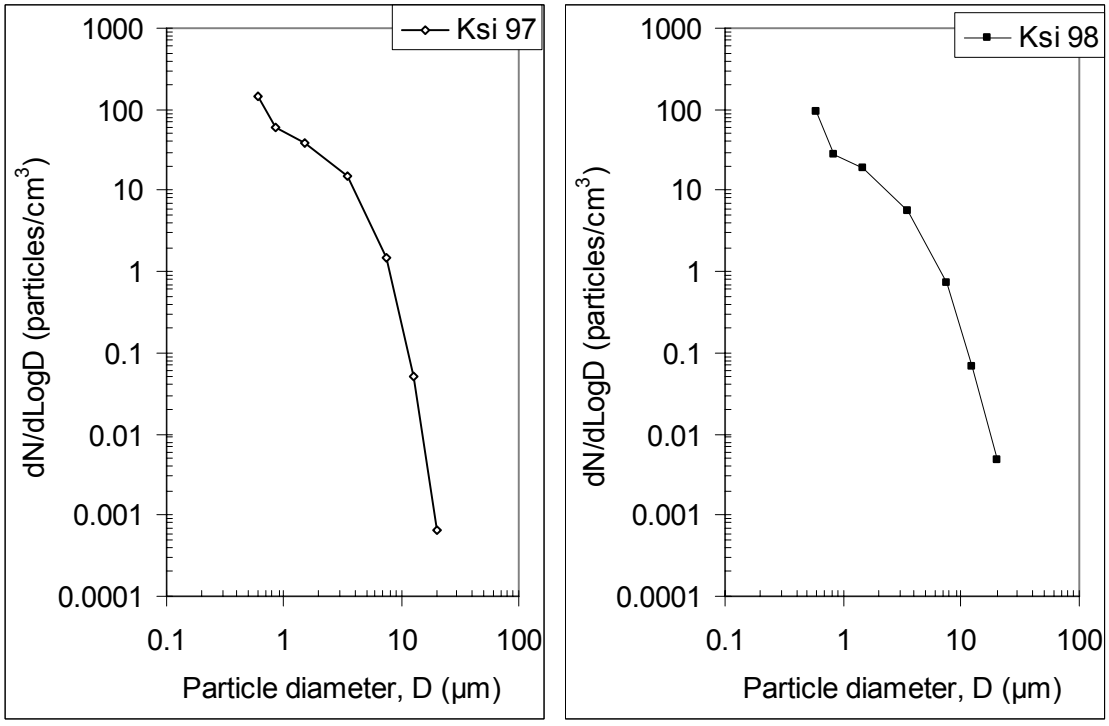

(a) 2-8Feb. 1997 (b) 17-26Jan. 1998

Figure 5.11. (a)-(b) Typical particle number distributions at Kumasi.

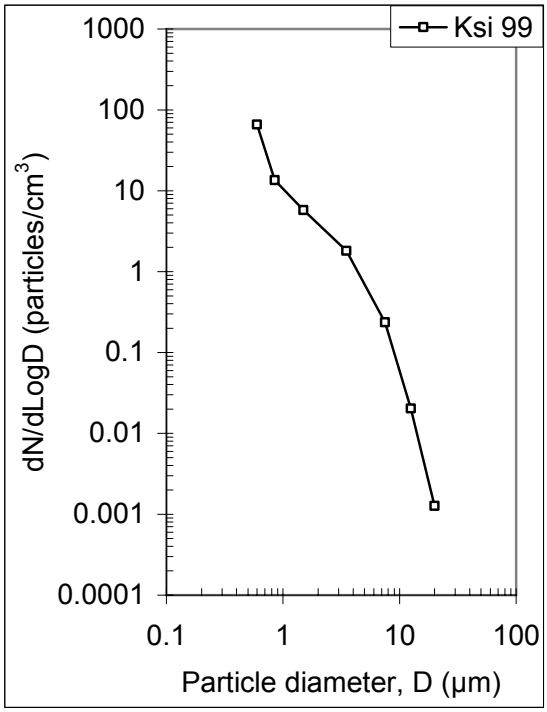

(c) 6-17Jan. 1999

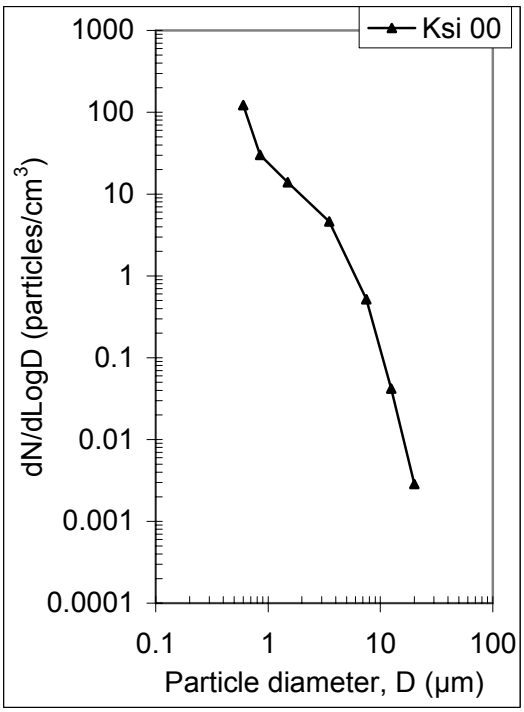

(d) 25Jan.-3Feb. 2000

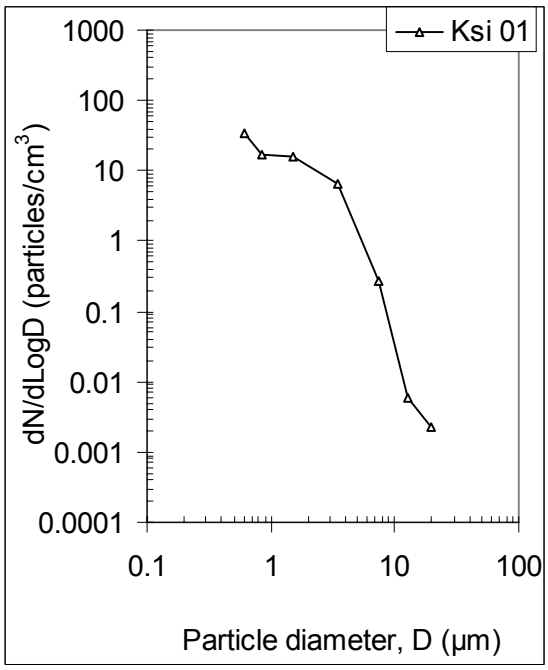

(e) 7-19Feb. 2001

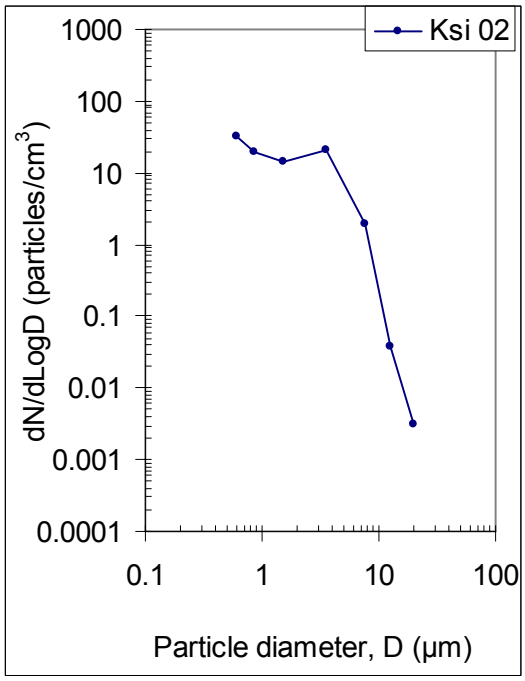

(f) 28Jan.-3Feb. 2002

Figure 5.11. (c)-(f) Typical particle number distributions at Kumasi.

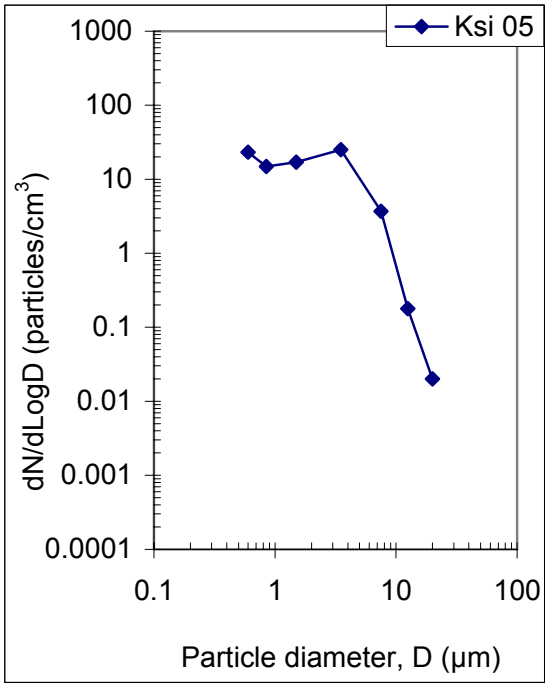

(g) 7-15Jan. 2005

Figure 5.11. (g) Typical particle number distributions at Kumasi.

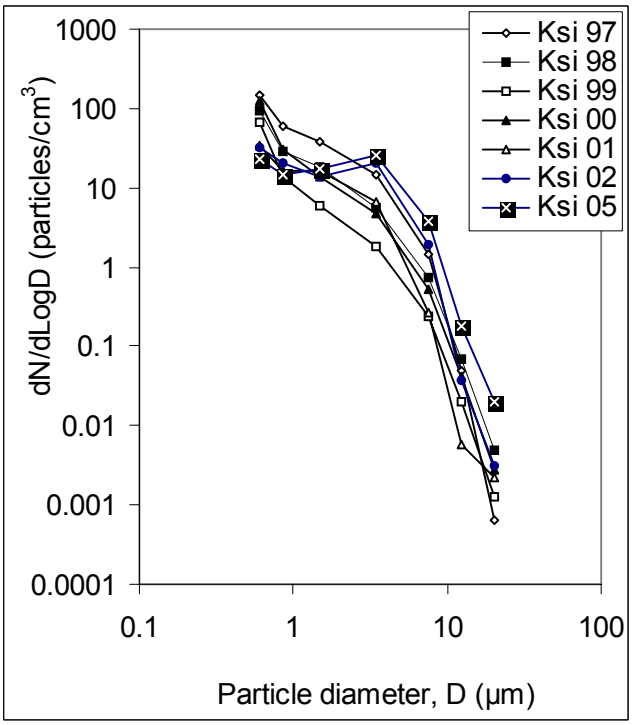

(g) 7-15 Jan. 2005

Figure 5.12. Particle number distribution in Kumasi during the selected Harmattan periods: 1997-2005.

5.2.4. Mass frequency distribution

The mass size distribution curves are obtained by plotting on the ordinate, dM/dLogD, where M is the mass concentration in $\mu g/m^3$ as a function of diameter, D which is the class mid-point size in micrometer (µm), where both are plotted on the natural logarithmic scales. The plots are shown in Figure 5.13(a)-(g). All the mass size distributions during the period are displayed on a chart in Figure 5.14. All the graphs exhibit similar slopes. A steep rise in concentration from the smaller particles of about D = 0.7 µm to a peak concentration at particle size of about D = 3 µm is visible. The peak concentration is clear-cut and is located between particles of size 3 µm and 5 µm diameter, the concentration decreases sharply with diameter between 5 µm and 10 µm.
The mode of the mass distribution corresponds to a particle size of about 3 µm for the 1997-2000 Harmattan period whereas for the 2001-2005 Harmattan period, the mode corresponds to the particle size of about 3.5 µm which falls in the fourth size class, 2-5 µm.

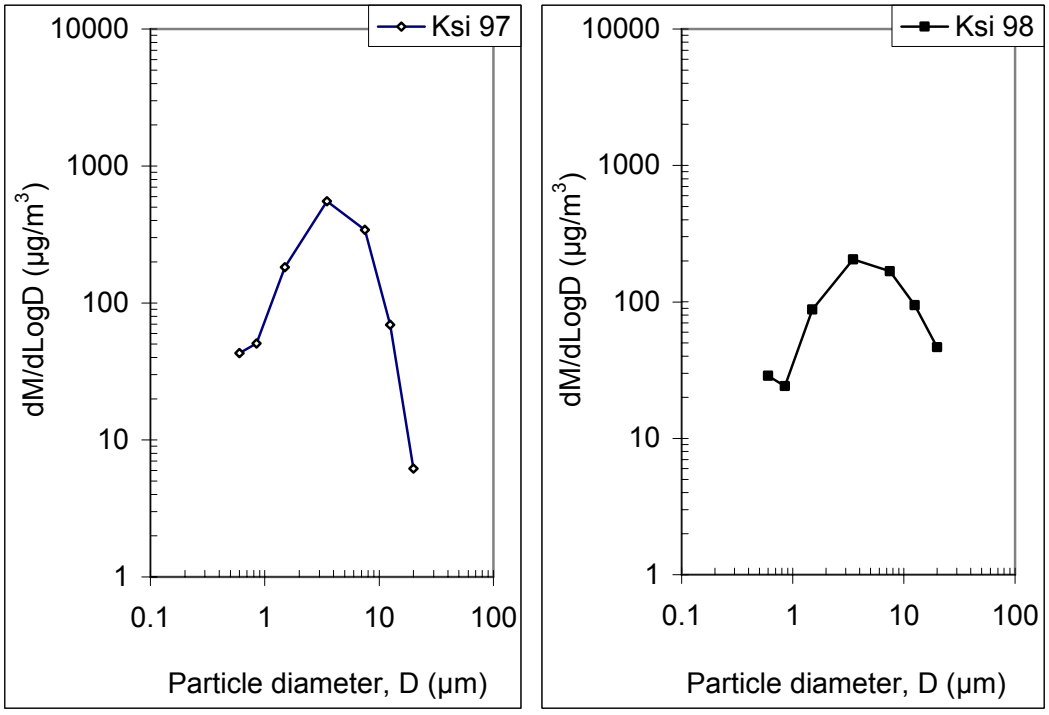

(a) 2-8Feb. 1997 (b) 17-26Jan. 1998

Figure 5.13. (a)-(b) Typical particle mass distributions at Kumasi.

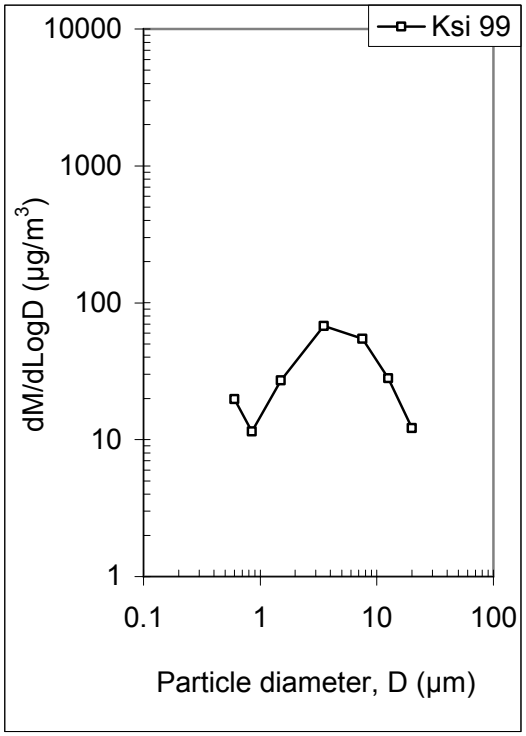

(c) 6-17Jan. 1999

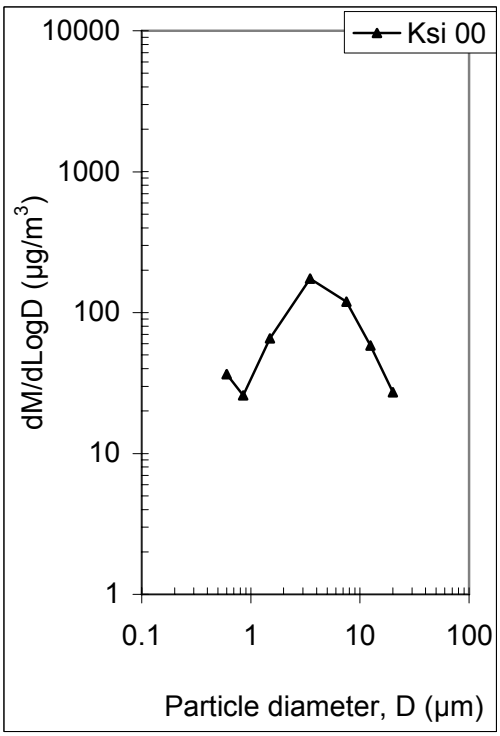

(d) 25Jan.-3Feb. 2000

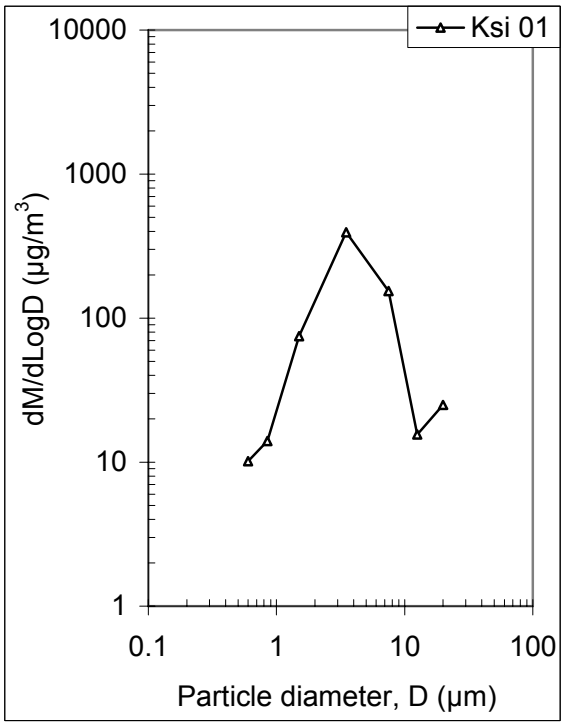

(e) 7-19Feb. 2001

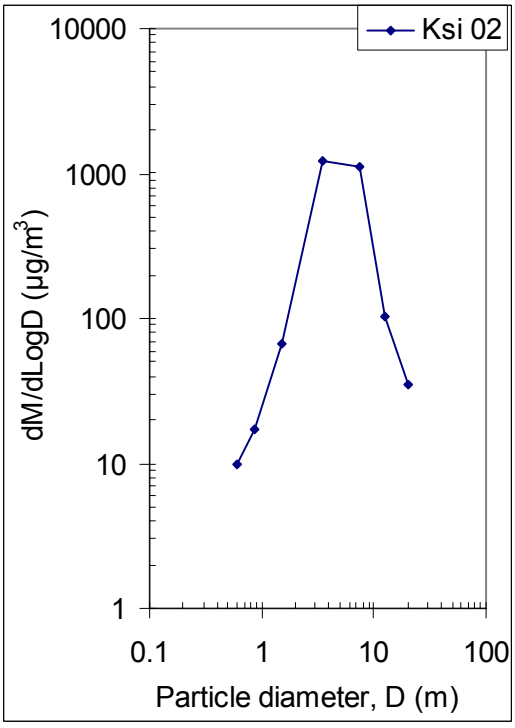

(f) 28Jan.-3Feb. 2002

Figure 5.13. (c)-(f) Typical particle mass distributions at Kumasi

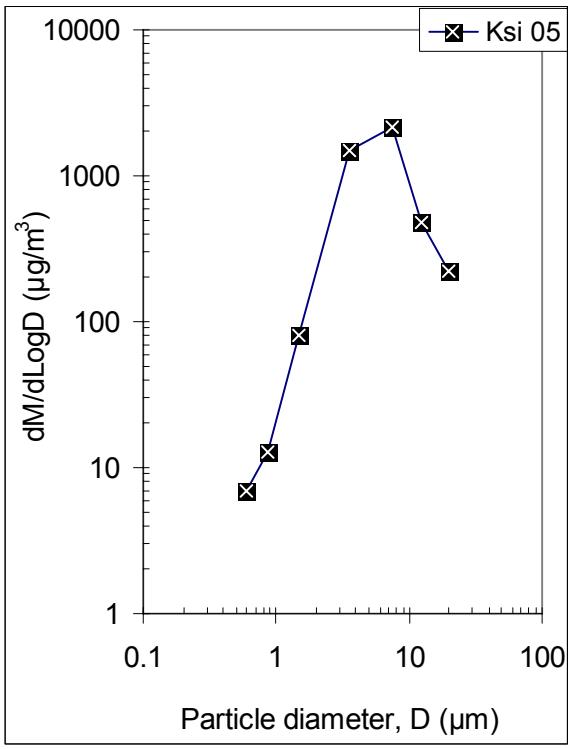

(g) 7-15 Jan. 2005

Figure 5.13. (g) Typical particle mass distributions at Kumasi .

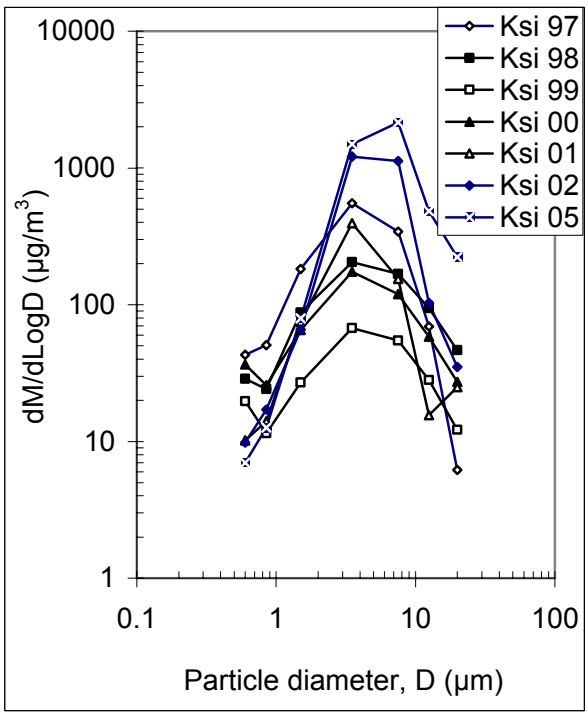

Figure 5.14. Particle mass distribution in Kumasi during the selected Harmattan period: 1997-2005.

5.2.5. Particle concentration and non-Harmattan aerosol distribution

The wet season atmospheric aerosol, referred to as the non-Harmattan (NHA) aerosol, was sampled at Kumasi in May 2001 and September 2004. These particle distributions are shown in Figure 5.15. The graphs show that the non-Harmattan aerosol distributions follow similar patterns. Their number and mass concentrations are identical thus stable for both periods, May and September. The distributions show very low particle number concentrations.

The comparison between the particle concentration of the Harmattan and non-Harmattan aerosol demonstrates the evidence of the dust invasion during the Harmattan period. It reveals to the population the atmospheric aerosol loadings of the two seasons, the dry and the wet seasons. Adaptation to these different aerosol loadings of the atmosphere will include air filter designs that can be done separately for the two seasons. This comparison also reveals the difference in the number and mass concentrations between the two seasons. Although the composition of the atmospheric dust may not be the same for both the Harmattan and non-Harmattan background, it has some similarities (urban aerosol from human activities and traffic are the same. These were prevented in the Harmattan dust particles sampled). Differences may occur from the maritime aerosol transported from the Gulf of Guinea, vegetation emissions and biomass burning which may vary from dry to rainy seasons. The non-Harmattan aerosol may contain a lot of maritime aerosol particles.

In Figure 5.16, the particle concentration taken during the period, 7^{th}-19^{th} February 2001 in the Harmattan period is compared with the non-Harmattan aerosol sampled in April-May 2001. The concentration in 2001 is about ten times the non-Harmattan dust for particle sizes between 0.5 and 10 μm. The concentration becomes about the same as the non-Harmattan aerosol at particle diameter of 15 μm. The distribution patterns are different for the number and mass distributions for the two seasons.

In Figure 5.17 (a) and (b) the particle concentration taken during the period, 7^{th}-15^{th} January 2005 in the Harmattan period is compared with the non-Harmattan dust aerosol sampled in September 2004. These plots show that the number and mass frequency distributions for the 2005 Harmattan are consistently higher than the corresponding non-Harmattan dust for all particle sizes. This confirms the strong Harmattan conditions in 2005, especially for the larger particle sizes.

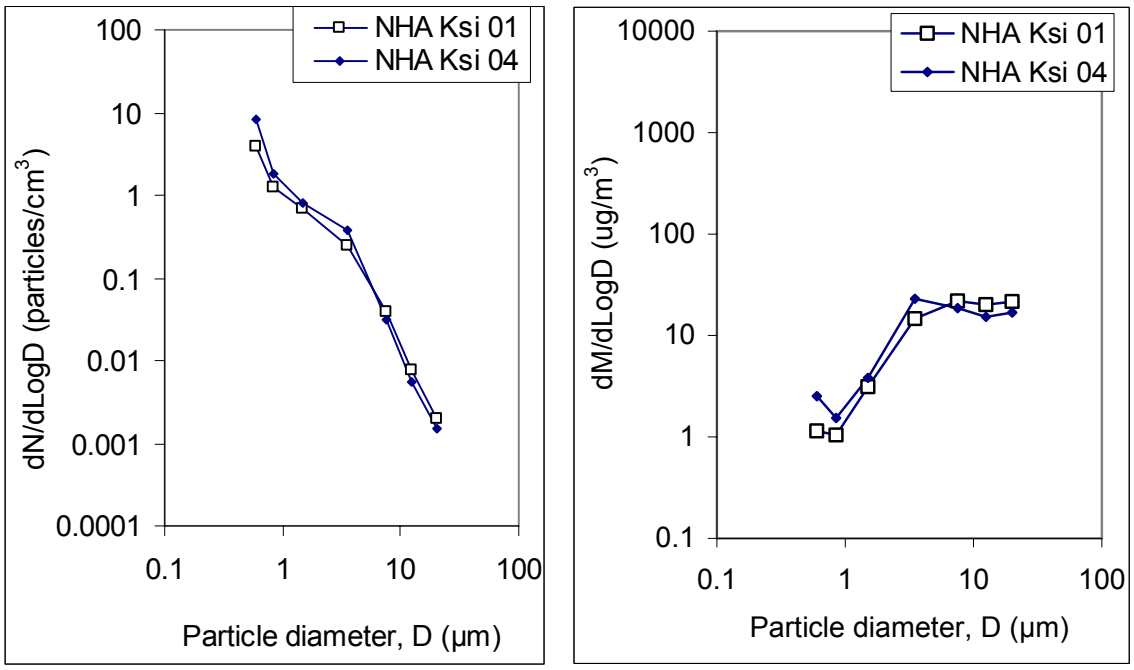

(a) (b)

Figure 5.15. Non-Harmattan aerosol concentration (a) number and (b) mass distributions in Kumasi: May 01 and Sept. 04.

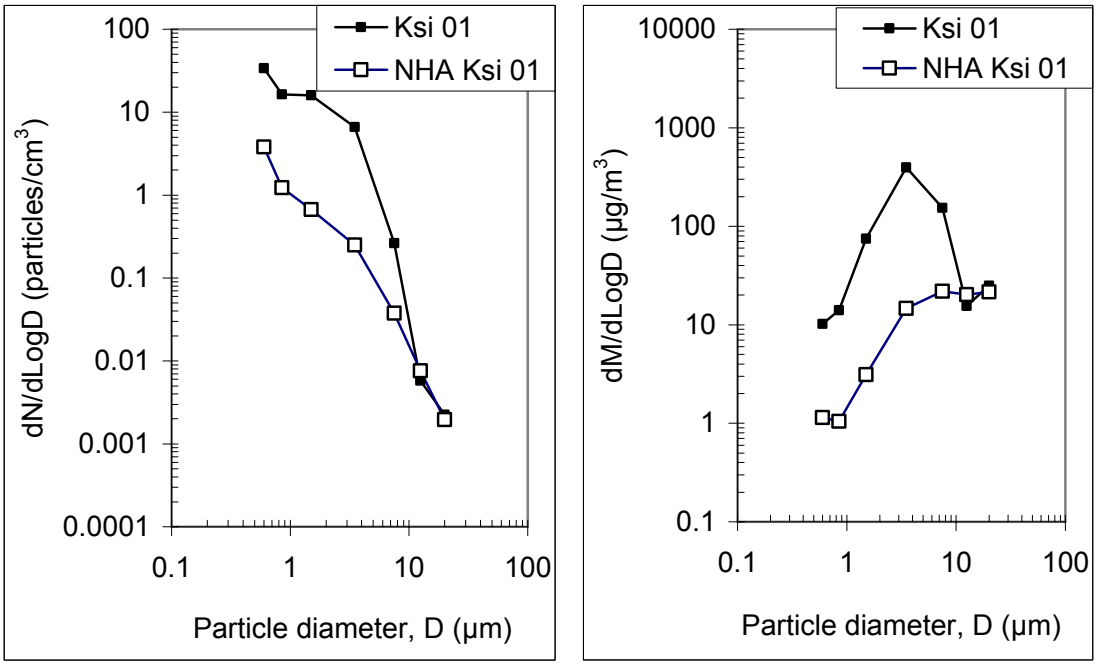

(a) (b)

Figure 5.16. Particle (a) number and (b) mass distributions in Kumasi during Harmattan (7-19 Feb2001) compared to non-Harmattan aerosol (April-May 2001).

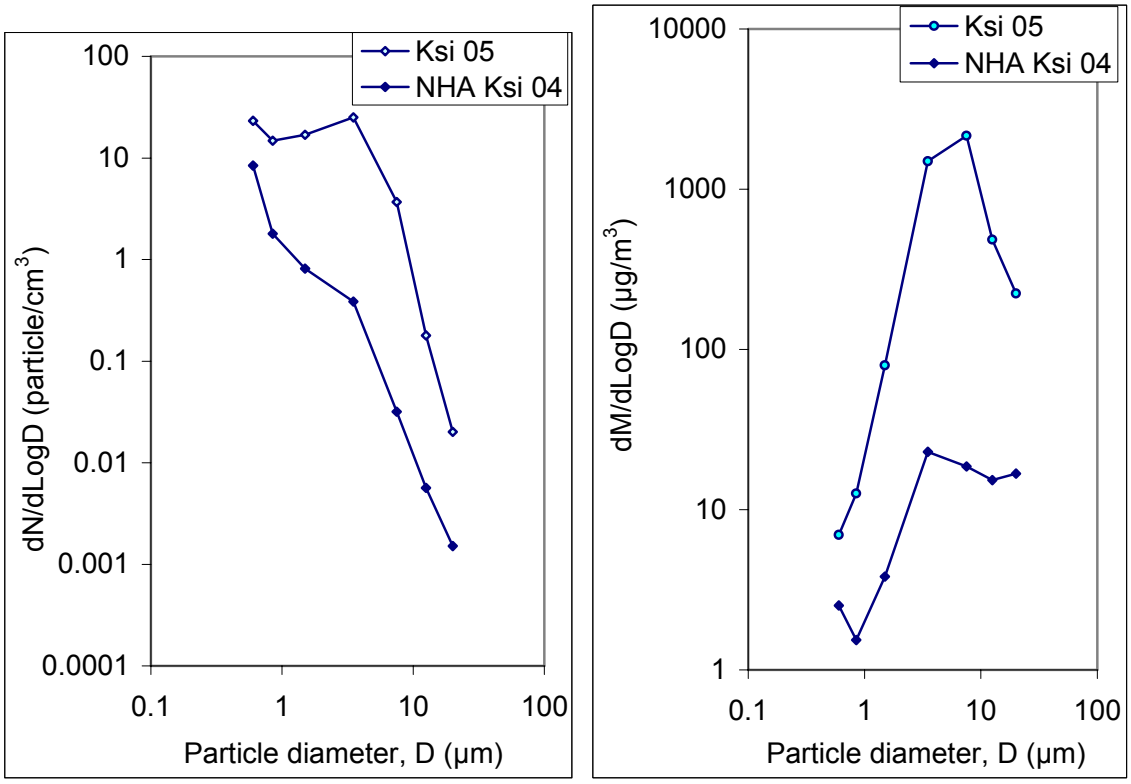

(a) (b)

Figure 5.17. Particle concentration (a) number and (b) mass distribution in Kumasi during Harmattan (7-15 Jan 2005) compared to non-Harmattan aerosol in September 2004.

5.2.6. Mean diameter distribution

The particle size distributions have been analysed statistically. The count mean diameter $\overline{D}$ has been calculated for all the selected Harmattan periods (Figure 5.18) at Kumasi from 1997 to 2005. The count mean diameter is defined as $\overline{D} = \frac{\sum n_i D_i}{\sum n_i}$, where n_i is the number of particles in the size class i having an arithmetic midpoint size D_i and where Σn_i is the total number of particles in all size classes. The seasonal particle mean diameters are: 1.28 µm in 1997, 1.14 µm for 1998, 0.94 µm for 1999, 0.94 µm for 2000, 1.47 µm for 2001, 2.12 µm for 2002 and 2.43 µm in 2005. The mean over the period (1997-2005) is 1.47 µm with a standard deviation of 0.58 µm. This size distribution, according to Bagnold (1971), shows that the mean size falls in the dust particulate range of 1-10 µm particle diameters. The distribution of the mean size is reasonably consistent with the mode diameter, D < 5 µm found by d'Almeida & Schutz (1983). However, according to Eyre (1963), the particle sizes are more of clay particles (D < 2 µm) and little of silt (2 < D < 20 µm) and reasonably little sand sized particles (D > 20 µm). The visibility impact of atmospheric particles is controlled by the concentration of particles in the size range, 0.1 to 2.0 µm. Therefore, the mean size of 1.47 µm makes the Harmattan aerosol effective in extinction of solar radiation and visibility reduction as hinted by Hinds (1999) for atmospheric particulates.

It is also interesting to compare this result with the mean diameters of the Saharan dust measured at two different locations closer to the Sahara Desert: McTainsh et al., (1982) obtained a mean particle size of 8.9 μm at Kano (Nigeria), while Adedokun et al., (1989) reported a mean value of 3.12 μm at Ile Ife, also in Nigeria but at a lower latitude several hundred kilometres south of Kano. In terms of distance from the in the Bodele depression, Kano is closer than Ile Ife and Kumasi is farthest away, towards west direction. Furthermore, Kumasi is located at a lower latitude (6^o 40'N) than either Ile Ife (7^o 30'N) or Kano (12^oN). As is well-known with Harmattan dust propagation, larger (or heavier) aerosol particles sediment out faster than smaller particles as the aerosol travels out to lower latitudes and destinations further away from the source region. The seven-year mean particle diameter of 1.47 μm, which is the characteristic diameter of the Saharan dust in central Ghana, is therefore consistent with the expected systematic decrease of the Harmattan aerosol size parameters with increasing distance from the Sahara Desert.

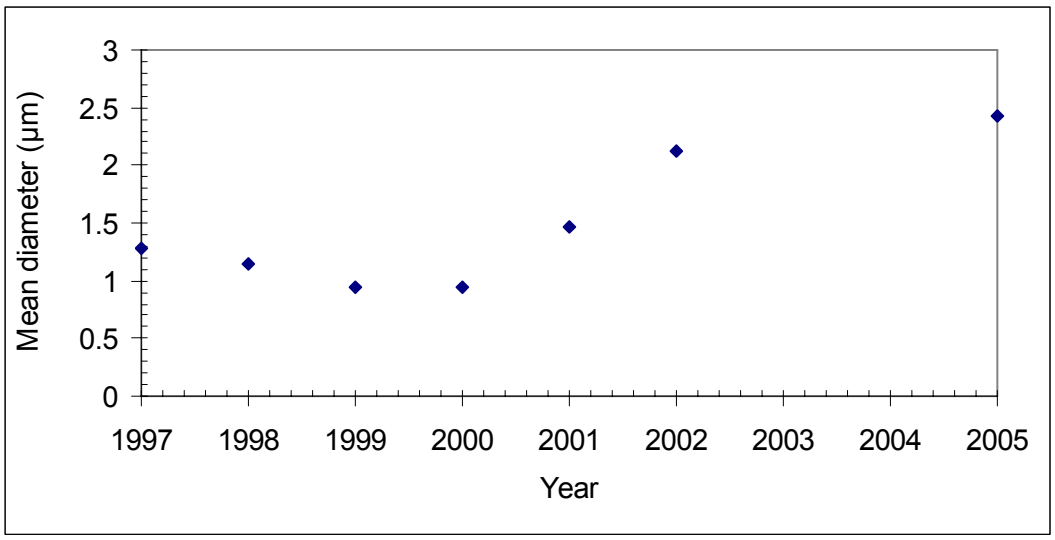

Figure 5.18. Yearly mean particle size in Kumasi during the selected Harmattan period: 1997-2005.

5.3. Dust Particles in Tamale

The measurements in Tamale started in 2000, when the old counter was used to monitor the atmosphere in Tamale from December 2000 to January 2001 before being transferred to Kumasi. From 2001 to 2005 Harmattan periods, the new Hiac/Royco counter of the same make and identical specifications was used to simultaneously sample in Tamale with the old counter sampling in Kumasi. The particle size classes selected, the sample time and delay time were the same as those selected for Kumasi. The two counters were also inter-calibrated before the sampling campaigns.

5.3.1. Number concentration

The plots of the particle number concentrations versus Julian days at the Tamale sampling station for 2001, 2002 and 2005 are shown in Figure 5.19 and grouped together in Figure 5.20. The number concentrations show comparable values.

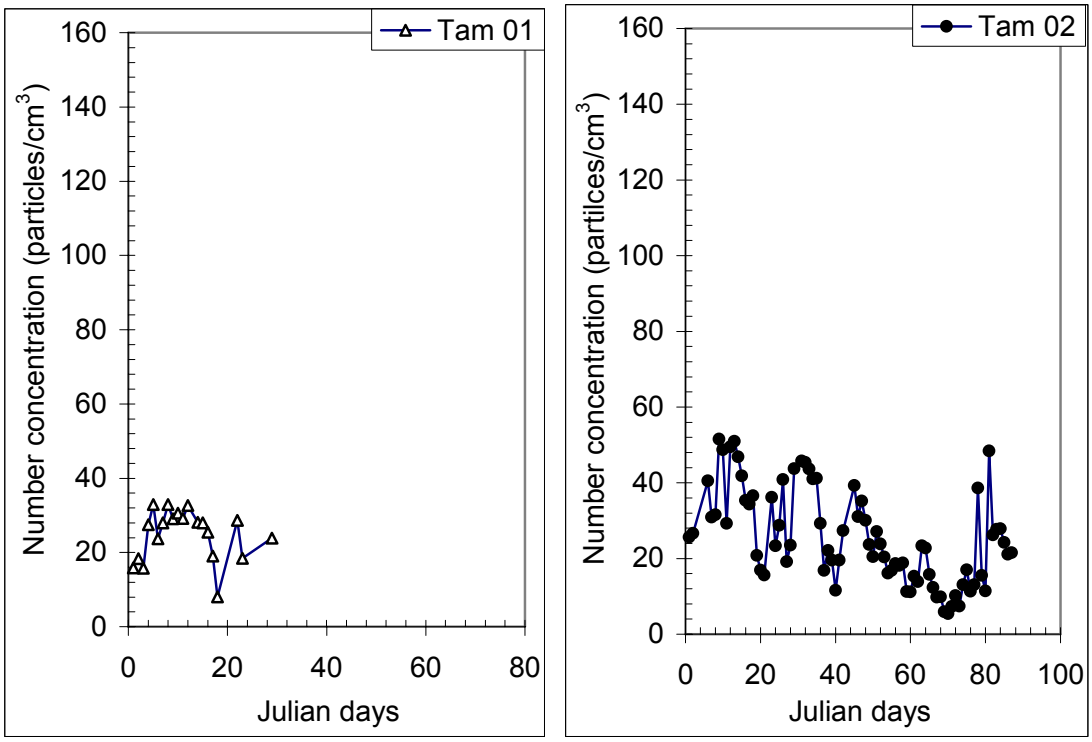

(a) January, 2001 (b) January-March, 2002

Figure 5.19. (a) (b) Particle number concentration in Tamale versus Julian days, 2001 and 2002.

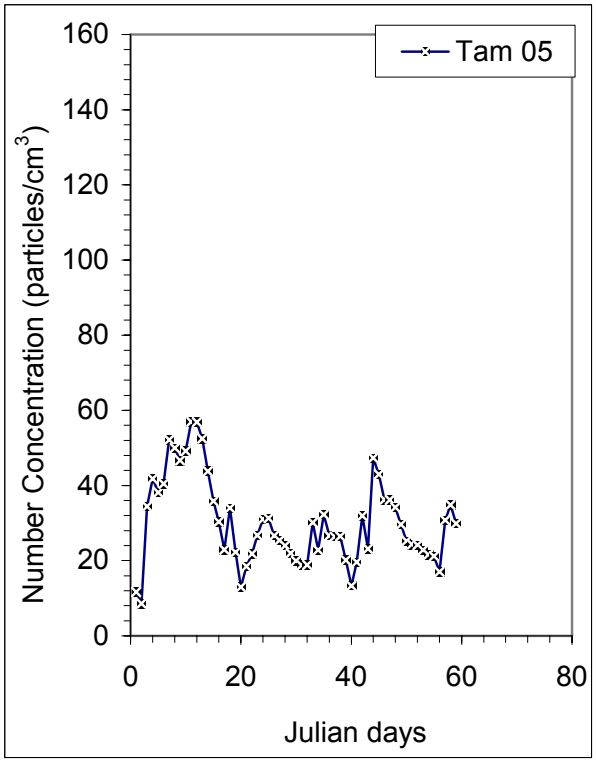

(c) January-February, 2005

Figure 5.19. (c) Particle number concentration in Tamale versus Julian days, 2005.

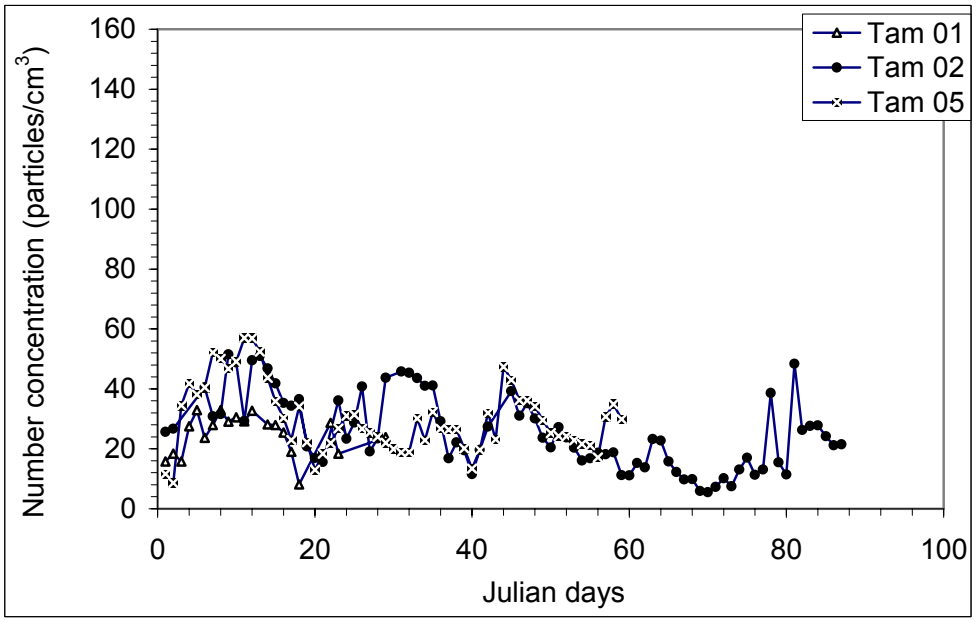

Figure 5.20. Particle number concentration in Tamale versus Julian days: 2001-2005.

5.3.2. Mass concentration

The mass concentrations are shown in Figures 5.21 and grouped together in Figure 5.22. From this last graph (Figure 5.22), one can observe a strong peak in early January for the 2005 Harmattan period, which was not evident with the particle number distribution. This provides evidence of the presence of larger particles in the 2005 sample due to the observed higher wind speeds, 3.48 m/s in 2000 and 4 m/s in 2005.

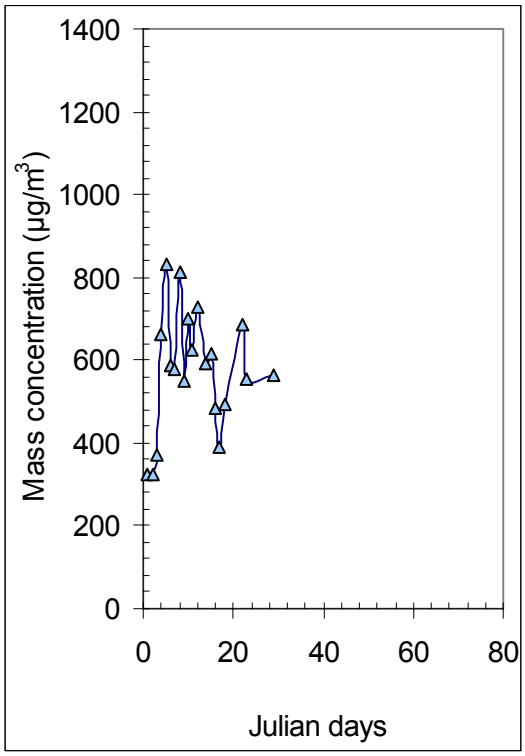

(a) January, 2001

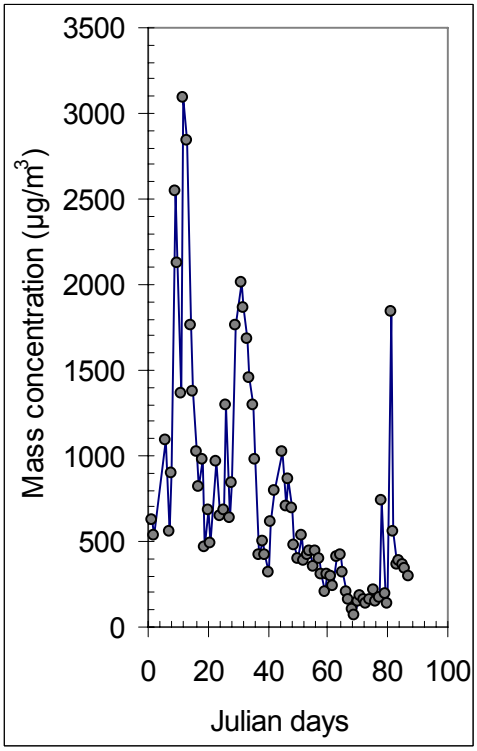

(b) January-March, 2002

Figure 5.21. (a)(b) Particle mass concentration in Tamale versus Julian days in the various years; 2001 and 2002.

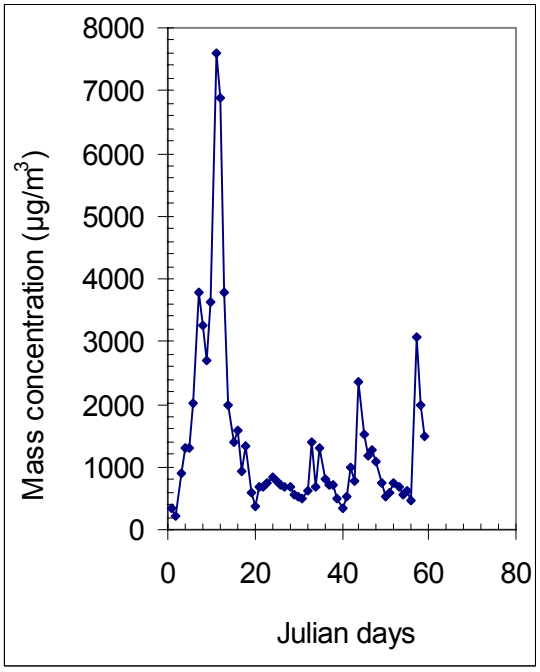

(c) January-February, 2005

Figure 5.21. (c) Particle mass concentration in Tamale versus Julian days in 2005.

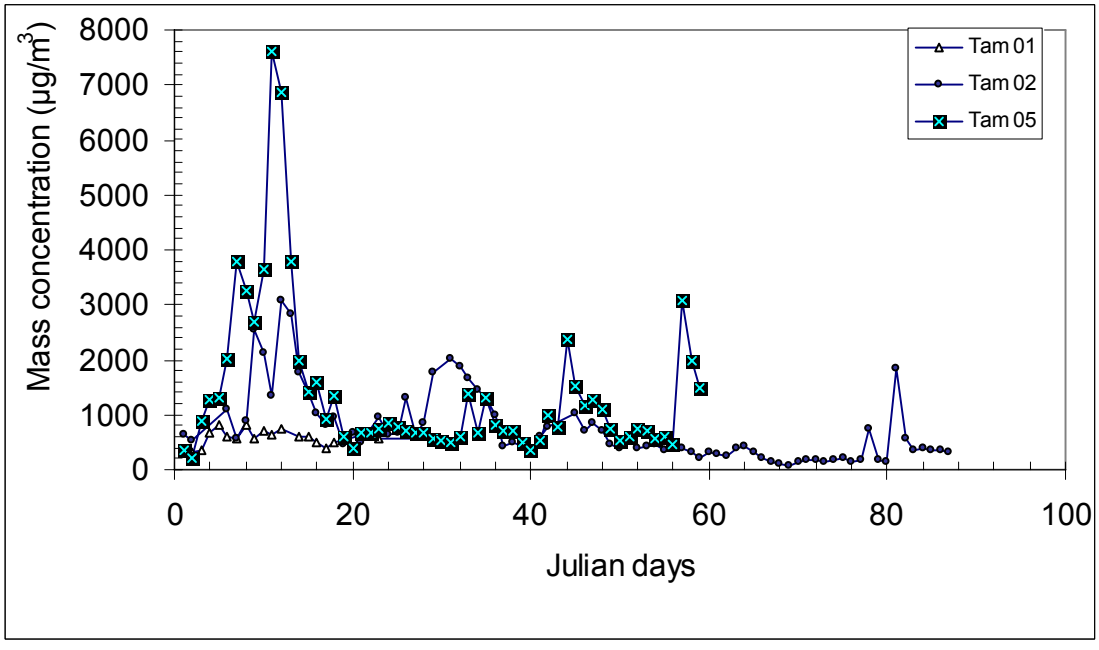

Figure 5.22. Particle mass concentration in Tamale versus Julian days: 2001-2005.

5.3.3. Number frequency distribution

As in the case of the Kumasi data, a selected period was chosen for each Harmattan year. These periods are indicated in Figures 5.23 and 5.24 for the number and mass concentrations respectively.
The number frequency distribution curves are obtained by plotting on the logarithmic scale with the ordinate dN/dLogD, where N is in the units of particles/cm^3 and D is the class mid-point size in micrometer (µm) as done for Kumasi data. The graphs are shown in Figure 5.25 (a) –(c) and grouped together in Figure 5.26.
Figure 5.25a shows the frequency size distribution at Tamale during the 2001 Harmattan period. The size distribution curves are similar to those of the Kumasi data.

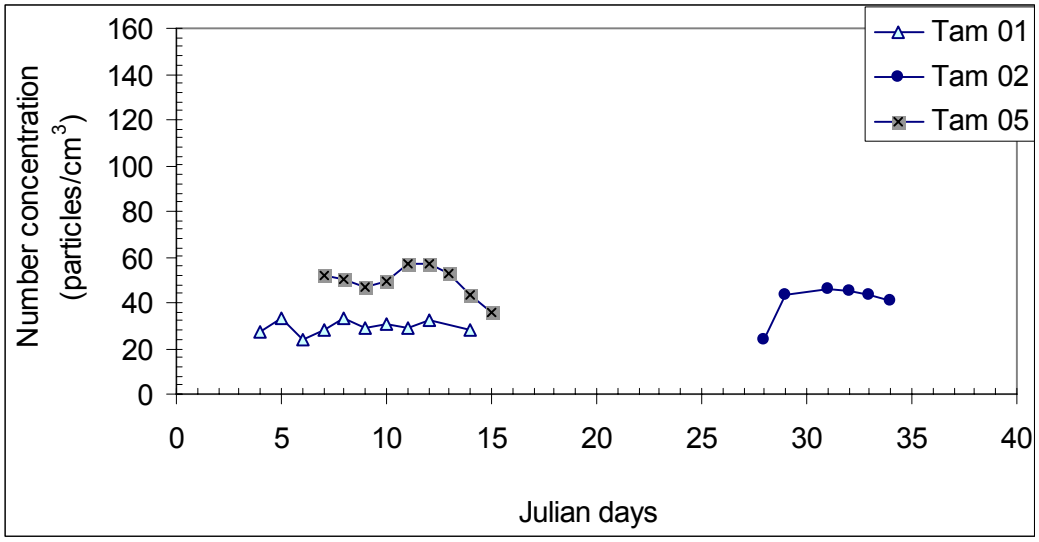

Figure 5.23. Particle number concentration in Tamale versus selected Julian days: 2001-2005.

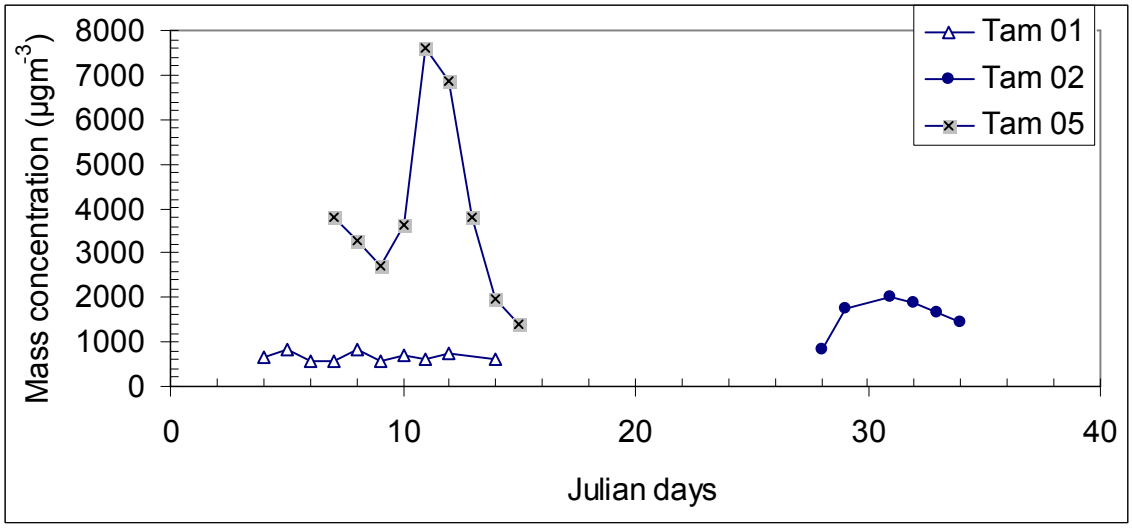

Figure 5.24. Particle mass concentration in Tamale versus Julian days: 2001-2005.

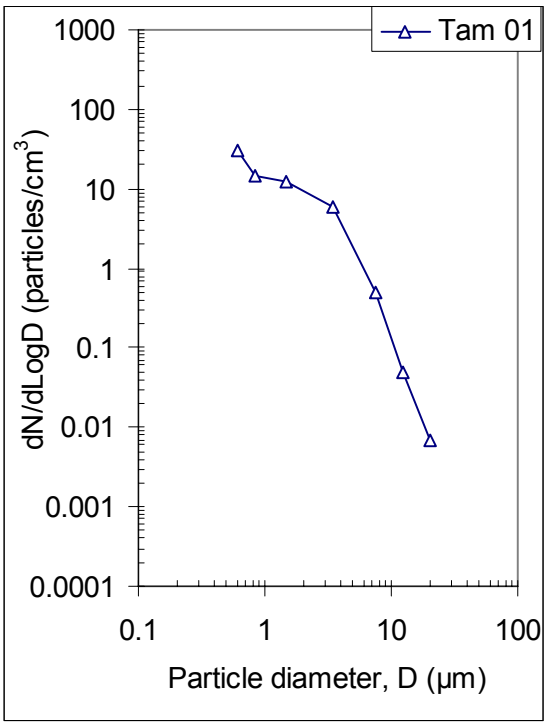

(a) 4-14Jan. 2001

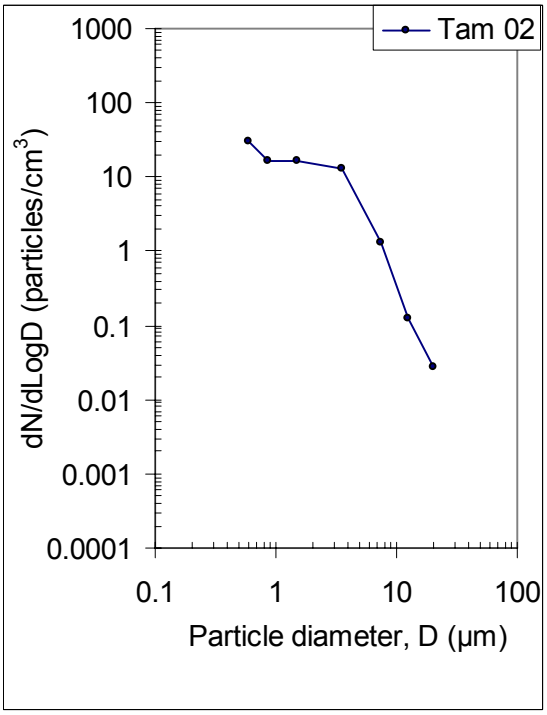

(b) 28Jan.-3Feb. 2002

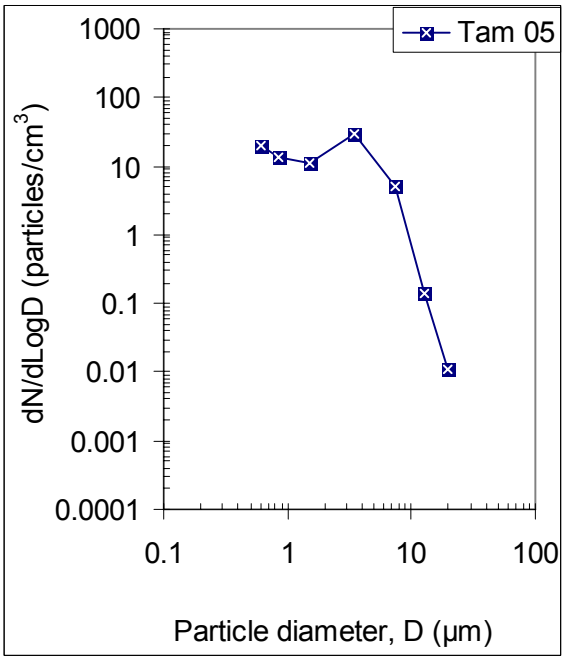

(c) 7-15Jan. 2005

Figure 5.25. (a)-(c) Typical particle number distributions at Tamale, 2001-2005.

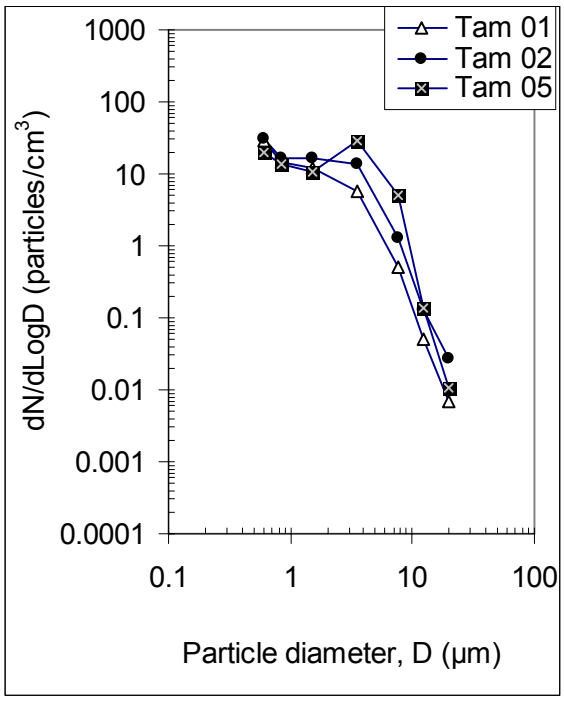

Figure 5.26. Particle number distributions in Tamale during the selected Harmattan periods: 2001-2005.

5.3.4. Mass frequency distribution

Following the same calculation procedure as for Kumasi and assuming the same density for the quartz (>70% of the Saharan dust is composed of quartz mineral particles, Adedokun et al., 1989) dust particles, the mid-point size of each class was used to calculate the mass of a particle belonging to that class size. The plots of the particle mass frequency distributions at Tamale sampling station in the various years are shown in Figure 5.27(a)-(c). Figure 5.28 shows the four mass frequency distribution curves for the 2001, 2002 and 2005 Harmattan period. The curves for 2001, 2002 and 2005 follow a similar pattern.

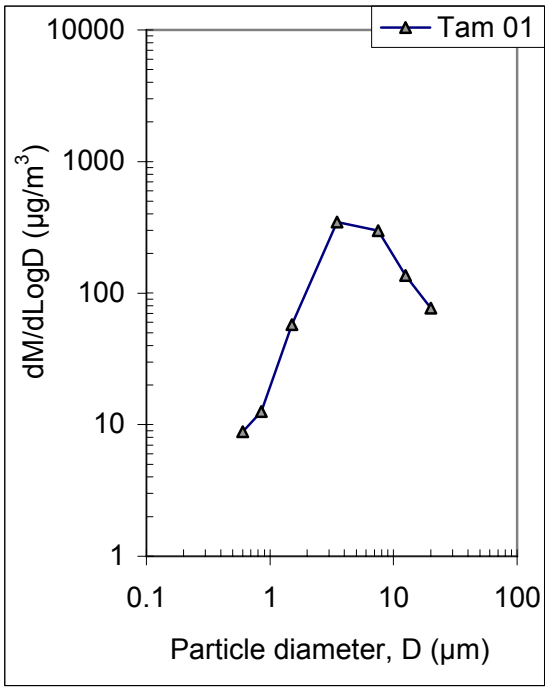

(a) 4-14 Jan. 2001

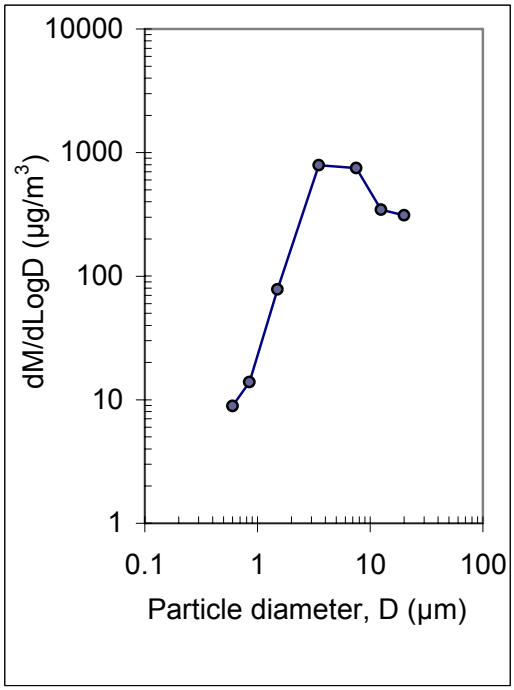

(b) 28 Jan.-3 Feb. 2002

Figure 5.27. (a)(b) Typical particle mass distributions at Tamale in 2001 and 2002.

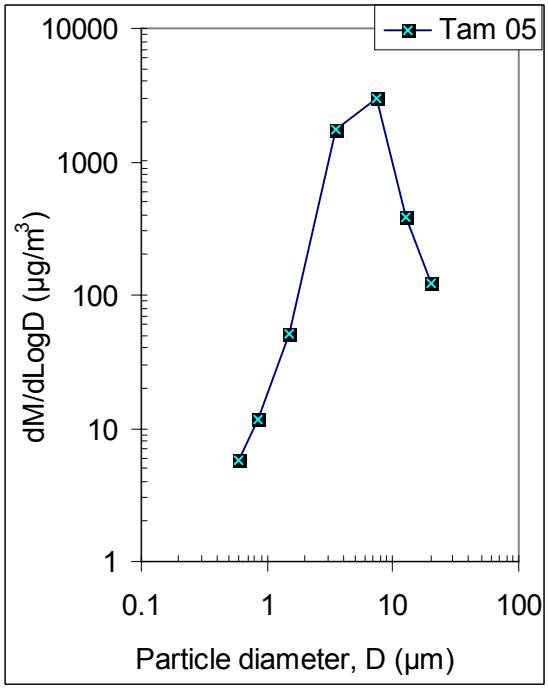

(c) 7-15 Jan. 2005

Figure 5.27. (c) Typical particle mass distributions at Tamale in 2005.

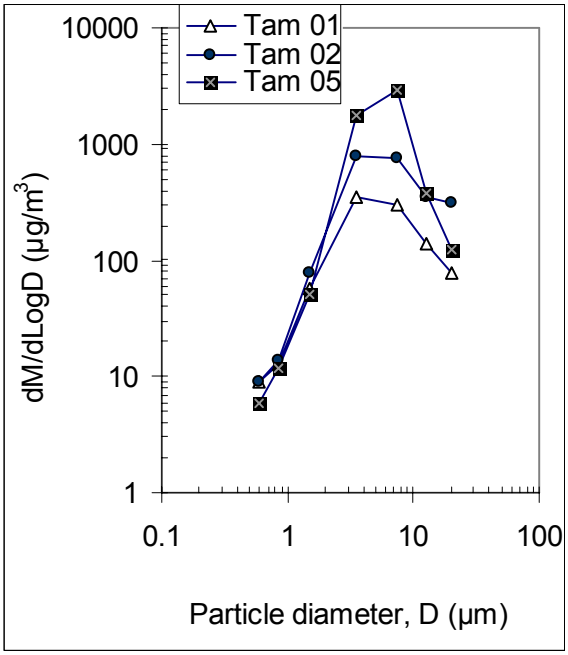

Figure 5.28. Typical particle mass concentration distributions at Tamale during the Harmattan period: 2001-2005.

5.3.5. Particle concentration in the Harmattan and the non-Harmattan periods

In Figure 5.29 (a) & (b), the non-Harmattan period aerosol distributions for Tamale during May 2001 and September 2004 have been compared. The distributions show that aerosol particle concentration (number and mass) during the non Harmattan period in Tamale is higher in September 2001 than in May 2004. The distribution patterns are also different for the two months.

The Saharan dust particle distributions in Tamale during the 2001 are compared with the non-Harmattan period aerosol concentrations in 2001 shown in Figure 5.30 (a) & (b) for the number and mass distributions respectively. Figure 5.31 (a) & (b), shows the Saharan dust particle distributions in Tamale during the 2005 Harmattan period compared with the non-Harmattan period aerosol concentration in 2004. The number distribution is shown in Figure 5.31 (a) and Figure 5.31(b) shows the mass distribution. The graphs for the 2001 Harmattan in Tamale, Figure 5.31 shows that the dust concentration is about ten times higher than the non-Harmattan period aerosol at the smallest particles, between 0.5 and 3 µm diameters.

The 2005 Harmattan in Tamale, Figure 5.31 show that the dust concentration is about the same as the non-Harmattan period aerosol at the smallest particles, but a gap appears of about one order of magnitude between particle size D = 3.5 µm and D = 7.5 µm. The dust concentration decreases to about the same value for the non-Harmattan period aerosol at the largest particle sizes. Both the non-Harmattan period aerosol and the Harmattan dust distributions follow the typical atmospheric dust particle distribution showing part of the accumulation mode and the coarse-particle mode.

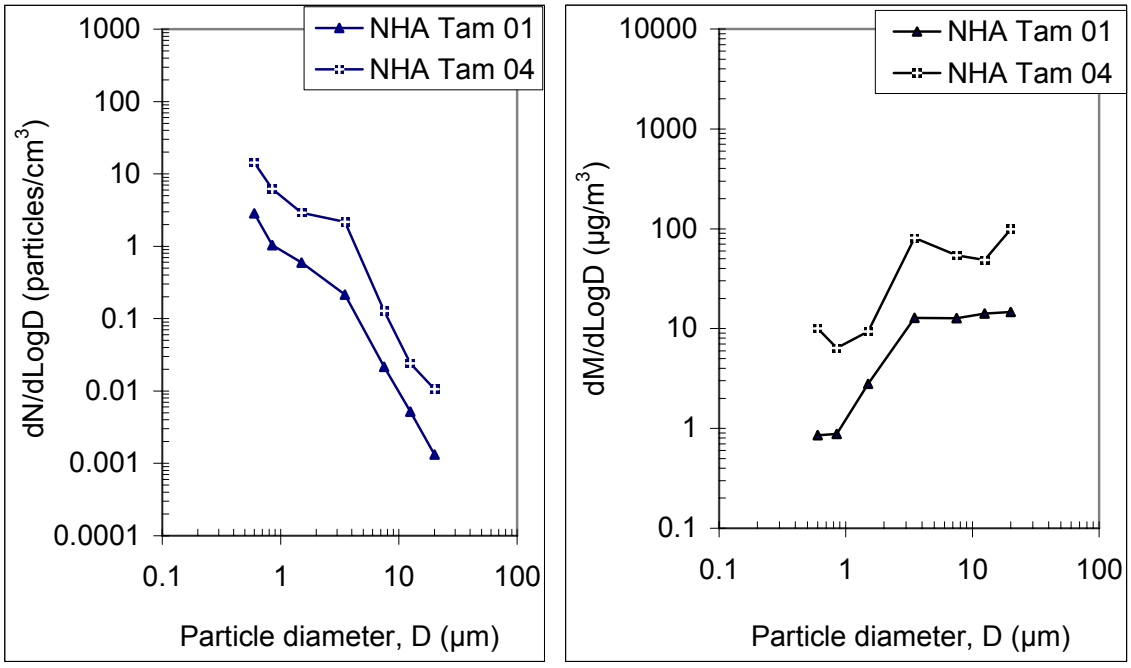

(a) (b)

Figure 5.29. Non-Harmattan aerosol distributions; (a) number and (b) mass concentration in May 2001 and September 2004.

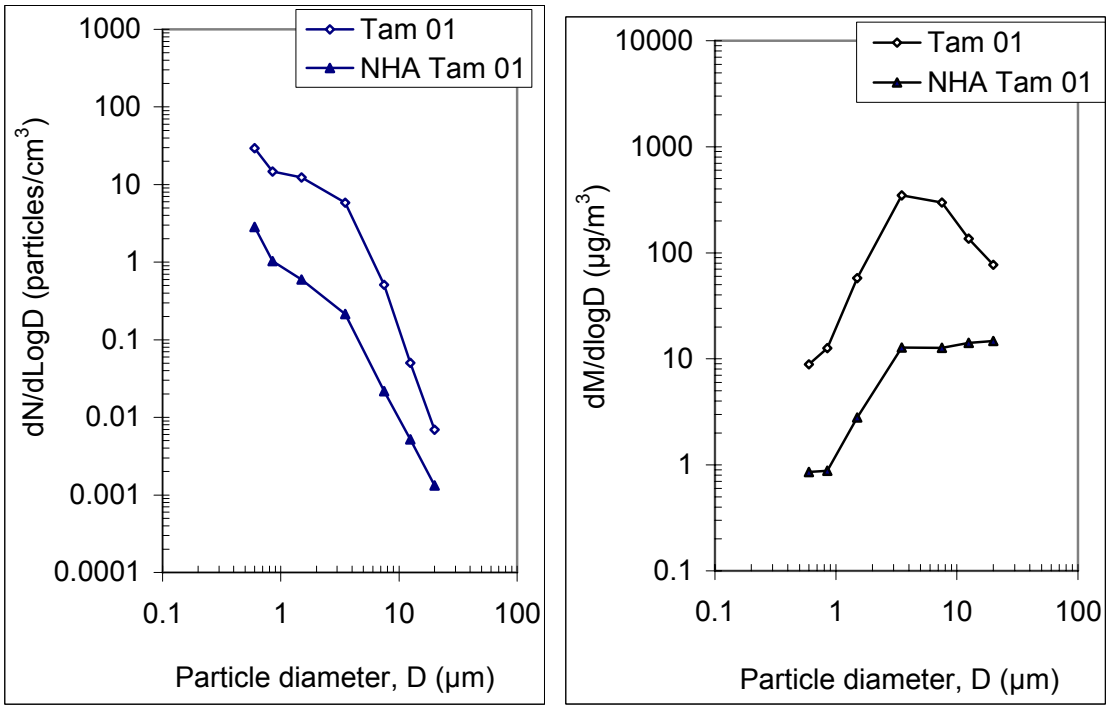

(a) (b)

Figure 5.30. Particle concentrations (a) number and (b) mass distributions in Tamale during the selected period (4-14 Jan. 2001) compared to non-Harmattan aerosol in May 2001.

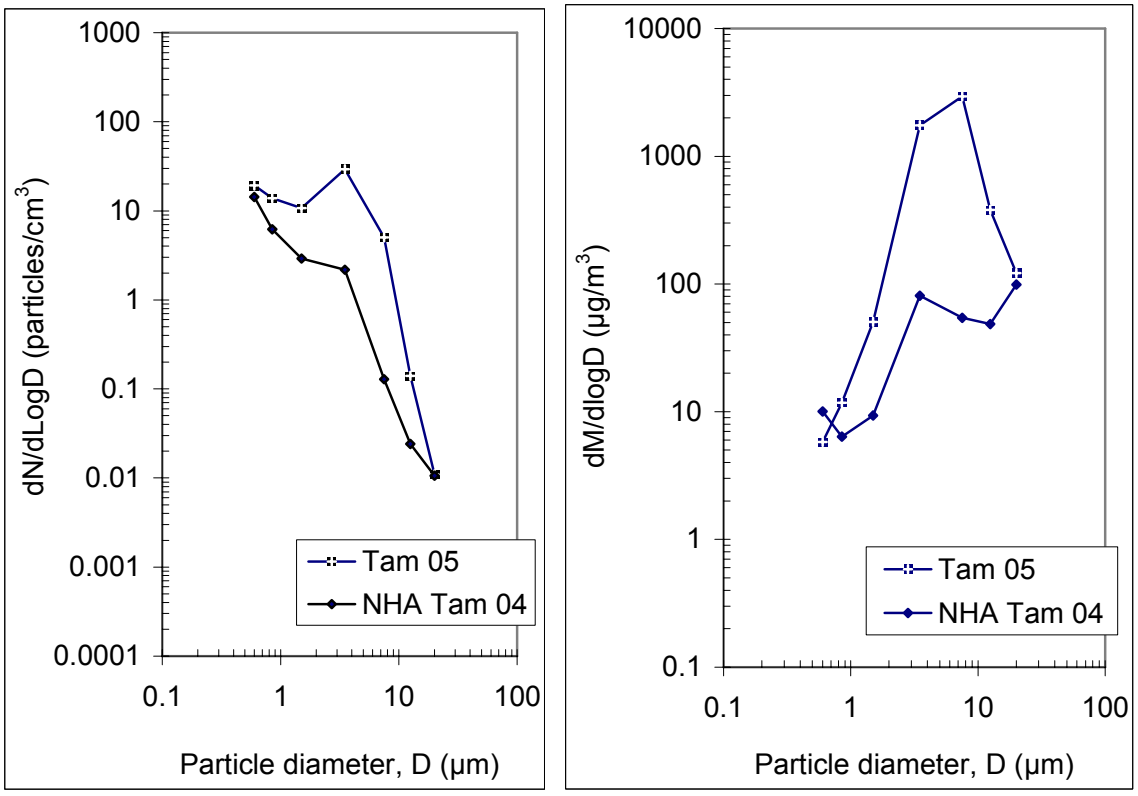

(a) (b)

Figure 5.31. Particle concentrations (a) number and (b) mass distributions in Tamale during the selected period (7-15 Jan. 2005) compared to non-Harmattan aerosol in Sept. 2004.

5.3.6. Mean diameter distribution

The particle size distributions have been analysed statistically. The count mean diameter has been calculated (as done for the Kumasi data) for all the selected Harmattan periods in Tamale from 2001 to 2005. The seasonal mean (which is the same as the yearly mean) particle sizes has also been determined for the three Harmattan periods. The seasonal mean particle diameters are 1.52 µm for 2001, 1.91 µm for 2002 and 2.79 µm for the 2005 Harmattan. The table of the yearly means is shown in Table 5.3. The yearly means range from 1.52 µm in the 2001 Harmattan to 2.79 µm in the 2005 Harmattan season. The arithmetic mean over the three-year (2001-2005) period is 2.07 µm with a standard deviation of 0.6 µm, which is higher than the nine-year mean diameter of 1.47 µm found in Kumasi. This result is expected because Tamale is closer to the dust source than Kumasi.

Table 5.3. Mean particle diameter at Tamale in various years

Year	Particle diameter, D (µm)
2001	1.52
2002	1.91
2005	2.79

5.4. Variation of concentrations in Tamale and Kumasi

The distribution of the Saharan dust is space dependent. Therefore, the particle concentrations and size, at the two sampling locations, are expected to vary according to the distance from the dust source. The distribution of the dust particles in Tamale and Kumasi are compared in the various selected Harmattan periods from 2001 to 2005. First, the non-Harmattan aerosols at the two locations are shown in Figure 5.32, for the number and mass distributions. The non-Harmattan dust in 2001 and 2004, at the two locations, Figure 5.32 (a) and (b), show comparable number and mass distributions while the non-Harmattan dust at the Tamale station in 2004 shows higher particle number and mass concentrations.

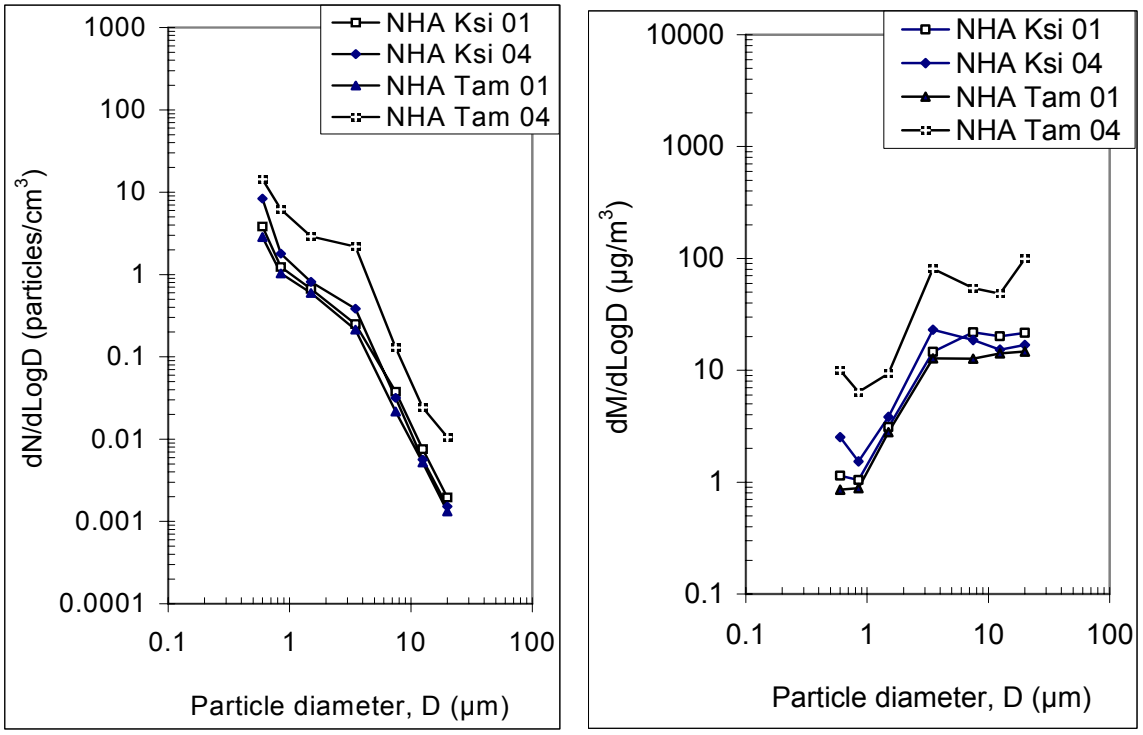

(a) (b)

Figure 5.32. Non-Harmattan aerosol distribution at Tamale in May 01 and Sept. 04, and at Kumasi in May 01 and Sept. 04; (a) number and (b) mass concentrations.

5.4.1. Number frequency distribution

The variations in number concentrations are shown in Figure 5.33 (a), (b) and (c) during the 2001, 2002 and 2005 Harmattan periods. The number concentrations in Tamale are higher than in Kumasi for particles in the size range, greater than D = 10 µm for the 2002 Harmattan period while for the 2005 Harmattan, the mid-size range particles between D = 3.5 µm and D = 7.5 µm are higher. The 2002 and 2005 Saharan dust particles were sampled simultaneously at the two locations. The average concentration determined as the arithmetic mean of the yearly averages of 2001, 2002 and 2005 (2001-2005) is also shown in Figure 5.34.

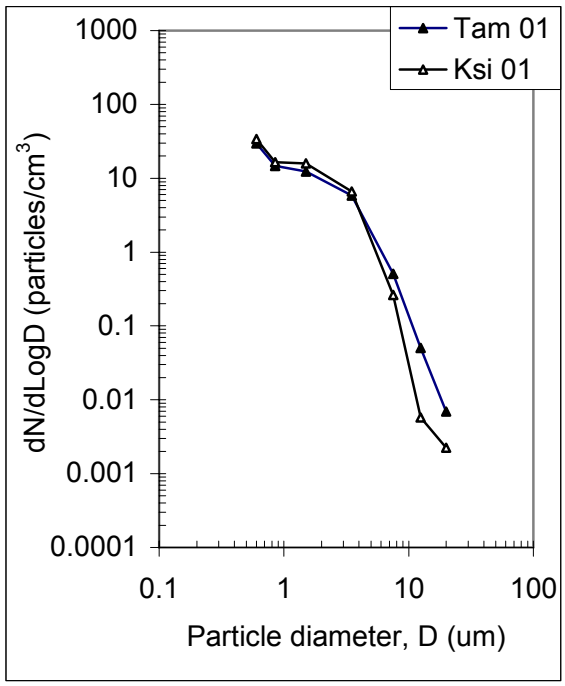

(a) 2001

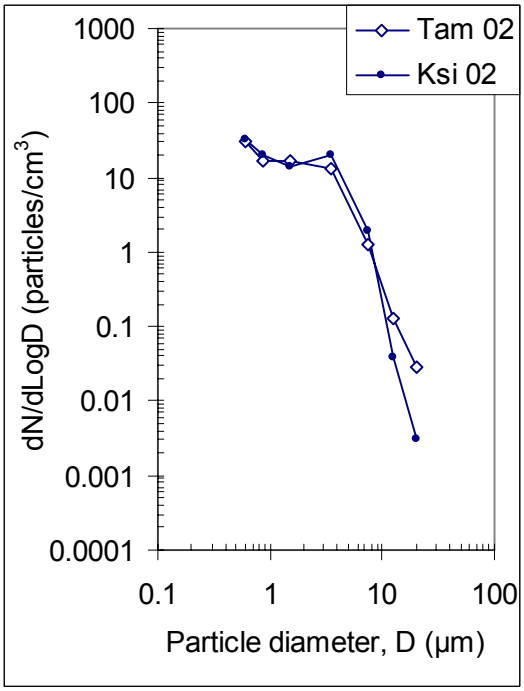

(b) 2002

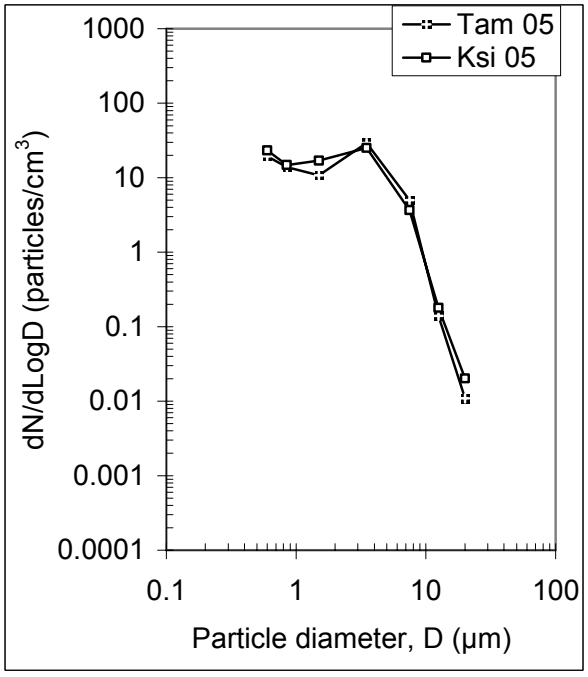

(c) 2005

Figure 5.33. (a), (b) and (c) Comparison of particle number concentration in Tamale and Kumasi during the Harmattan periods (2001- 2005).

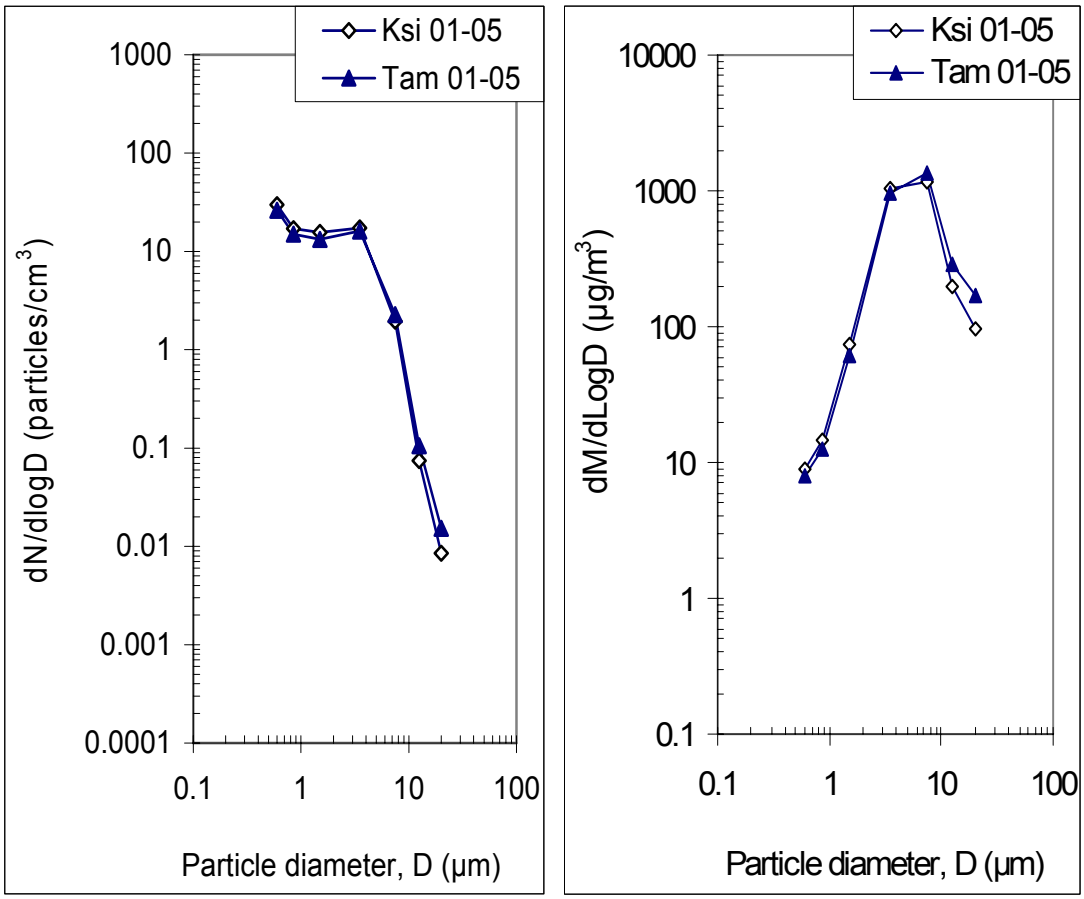

(a) (b)

Figure 5.34. Comparison of particle distribution in Tamale and Kumasi during the Harmattan 2001-2005: (a) number and (b) mass concentrations.

5.4.2. Mass frequency distribution

The particle mass concentration variations are shown in Figure 5.35 (a), (b) and (c) for the 2001, 2002 and 2005 Harmattan periods, respectively. The superior mass concentrations in Tamale than in Kumasi during the 2002 Harmattan are promoted by particles in the large size range greater than D = 10 µm. For the 2005 Harmattan period, the higher mass concentration at Tamale over Kumasi are promoted by the mid-size range particles between D = 3.5 µm and D = 7.5 µm.

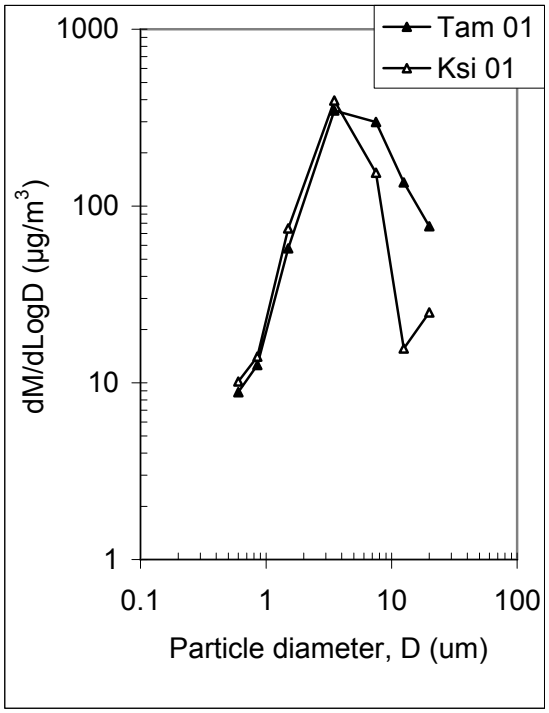

(a) 2001

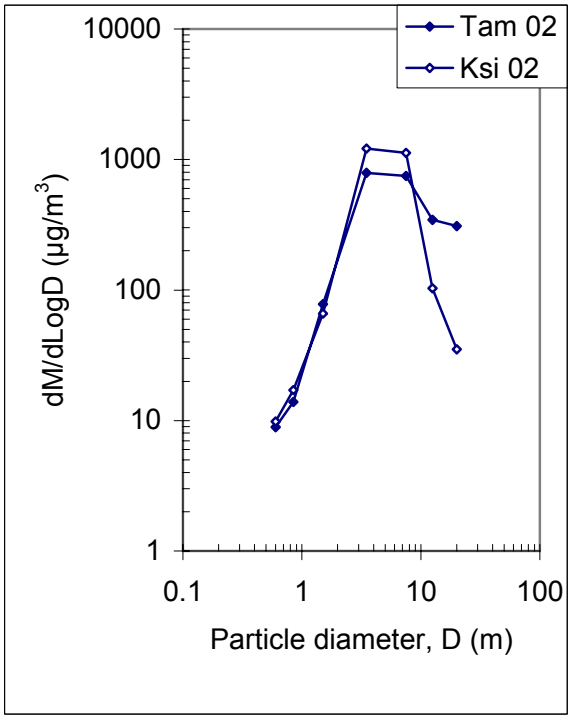

(b) 2002

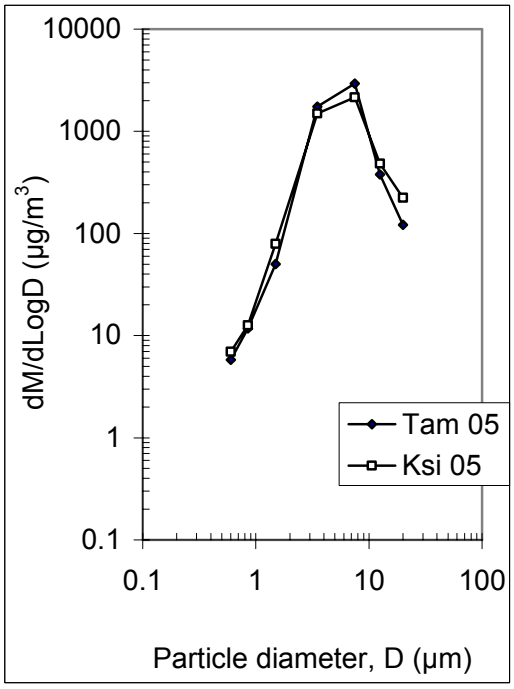

(c) 2005

Figure 5.35. (a), (b) and (c) Comparison of particle mass distribution in Tamale and Kumasi during (a) 2001, (b) 2002 and (c) 2005 Harmattan periods.

5.4.3. Mean diameter

The particle mean diameters during the selected periods from 2001 to 2005 are shown in Table 5.4 with Tamale recording a mean value of 2.8 μm in 2005 as against 2.4 μm in Kumasi. In 2002 Kumasi recorded 2.1 μm while Tamale recorded 1.9 μm.

Table 5.4. Mean particle diameter in Tamale and Kumasi in 2001, 2002 and 2005.

Year	Mean particle diameter (μm)	
	Tamale	Kumasi
2001	1.52	1.47
2002	1.91	2.12
2005	2.79	2.43

5.5. Dust transport characteristics

In this section, the dust transport characteristics are calculated based on the dust deposition data obtained at Tamale and Kumasi sampling stations during the 2002 and 2005 Harmattan periods.

5.5.1. Transit time

Can the transit time for a dust particle to travel from Tamale to Kumasi be estimated from the data obtained? In order to answer this question we can consider the particle number and mass distributions obtained at the two measurement sites (Figures 5.36 - 5.39) during the 2002 and 2005 Harmattan seasons. From these diagrams, several peaks associated with significant dust spells can be observed.
These observations confirm that successive peaks correspond to the following Julian days for both the Tamale and Kumasi data. In 2002, the peak occurring on Julian day 31 (31st January) corresponds to that detected on Julian day 32 (1st February) at Kumasi. Similarly, the peak of Julian day 45 (14th February) at Tamale corresponds to the peak recorded on Julian day 46 (15th February) at Kumasi.
In 2005, the peak observed on Julian day 7 (7th January) at Tamale was detected a day later on Julian day 8 (8th January) at Kumasi. The other pairings are Julian days 11 and 44 at Tamale for Julian day 13 and 46 at Kumasi respectively. It can be estimated, therefore, that dust particles take between one and two days to travel from Tamale to Kumasi.
In order to verify this experimental observation, a rough calculation of the dust transit time, T (in seconds) between Tamale and Kumasi, separated in a straight north-south (slightly East-West) direction by a distance, L= 320 km approximately, is done using the relation, $T=\frac{L}{U}$, where U is the mainstream wind velocity and is estimated from the expression $U = V_{15}/0.8$, where V_{15} is the measured velocity at a height of 15 m above ground level. Using the mainstream wind speed of U = 3.48 m/s (2002), we have in a first approximation:

Transit time, T = L/U = 320000/3.48 = 91 954 s (25 hours) or T ≈ 1 day (1 day =86 400 s), which is in accordance with the experimental observations. Similarly, using a mainstream wind speed of U = 4 m/s (2005), we have T = L/U = 320 000/4 =80 000 s (22 hours) or T ≈ 1 day.

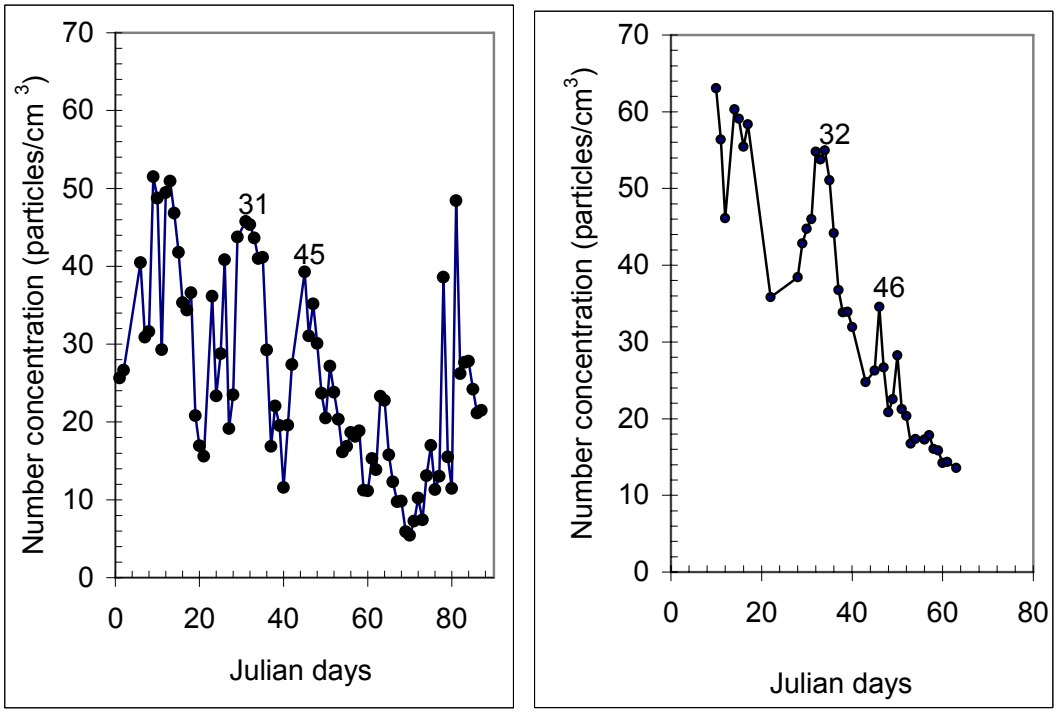

Figure 5.36. Particle number concentration in (a) Tamale and (b) Kumasi versus Julian days: January-March, 2002.

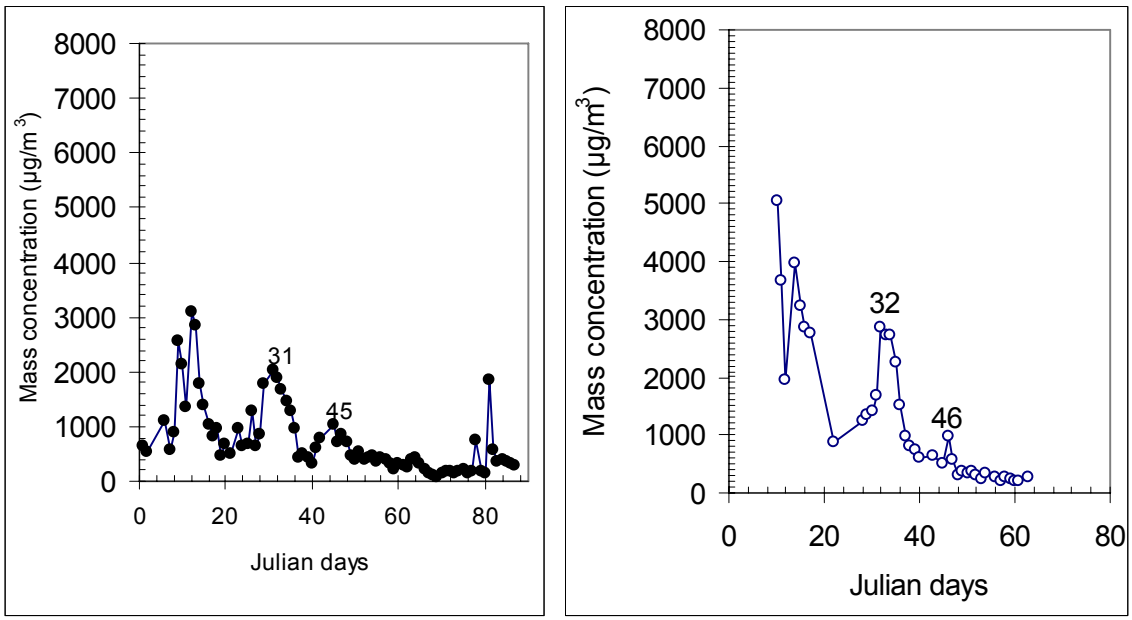

(a) (b)

Figure 5.37. Particle mass concentration in (a) Tamale and (b) Kumasi versus Julian days: January-March, 2002.

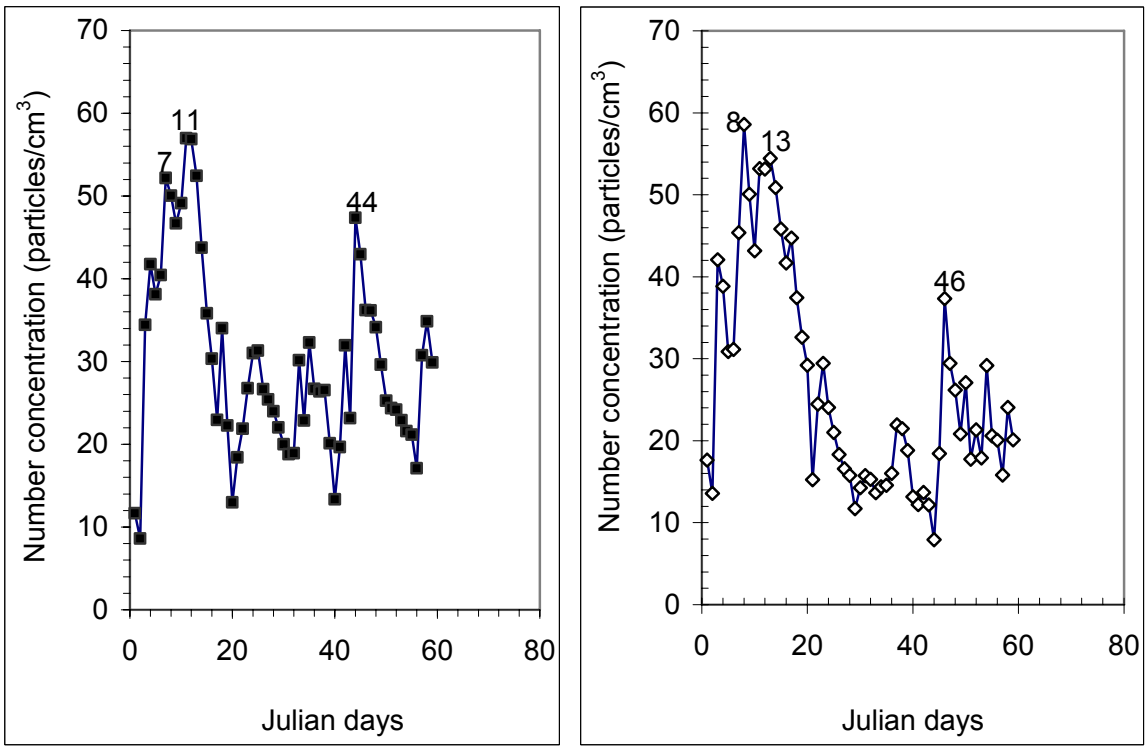

(a) (b)

Figure 5.38. Particle number concentration in (a) Tamale and (b) Kumasi versus Julian days: January-February 2005.

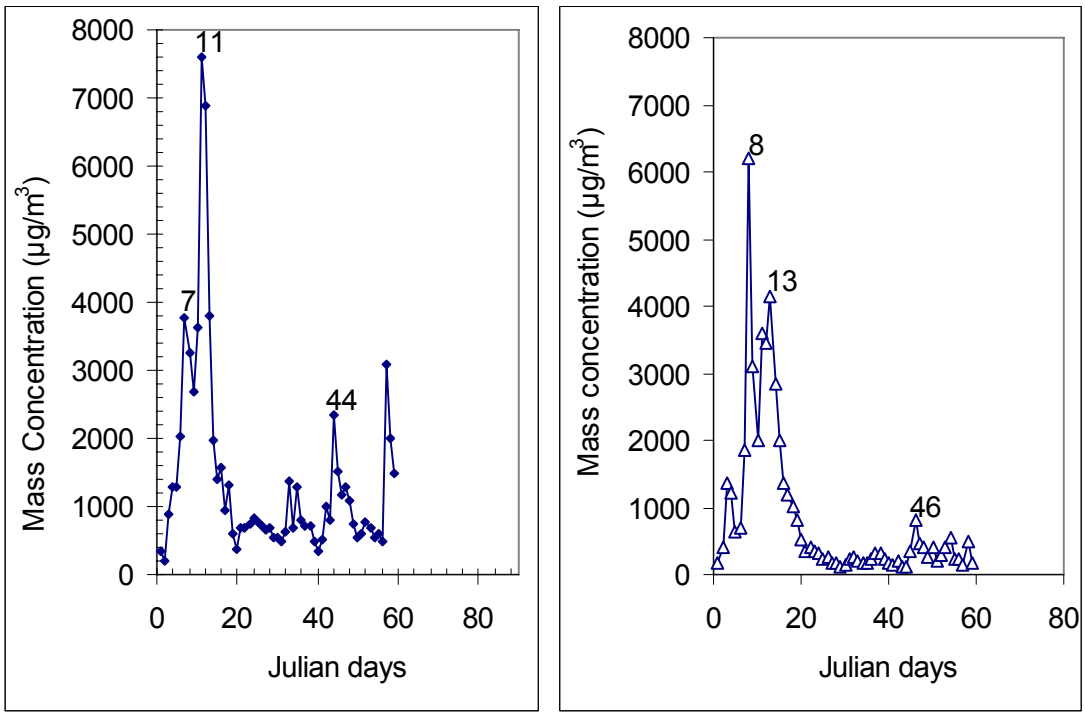

(a) (b)

Figure 5.39. Particle mass concentration in (a) Tamale and (b) Kumasi versus Julian days: January-February 2005.

5.5.2. Dust flux and deposition rate

The theoretical expression for the dust deposition flux per square meter, F_d has already been given in chapter 3 by equation (3.20):

$F_d = V_d M_1$

where the deposition velocity V_d is obtained from

$$V_d = \frac{h}{T} Ln \frac{M_1}{M_2}$$

where h is the height of the atmospheric boundary layer (taken here as h = 1000 m), M_1 and M_2 are the respective particle mass concentrations at the two measurement locations (Tamale and Kumasi) and T is the transit time between the locations and given by:

$T = L/U$.

Using the data obtained simultaneously at Tamale and Kumasi during the same selected period, and represented in Figures 5.35b and 5.35c, it is possible to calculate the total flux deposited between Tamale and Kumasi using equation 3.20. The values indicated in the following tables (Table 5.5 and 5.6) are easily calculated for both the 2002 and 2005 Harmattan seasons. In 2002, the selected period was between 28th January and 3rd February for which the average measured wind speed V_{15} was 2.78 m/s, leading to a U value of 3.48 m/s and a transit time T of 91954 seconds. In 2005, the selected period was 7th to 15th January, the average wind speed V_{15} was 3.2 m/s, corresponding to a U of 4 m/s and a transit time T of 80000 seconds. Computations of the dust flux is given in the tables 5.5 and 5.6.

Table 5.5. Determination of dust flux in 2002.

D	M_1	M_2		V_d	F_d
(μm)	Tam 02	Ksi 02	$Ln(M_1/M_2)$	$1000/T.Ln(M_1/M_2)$	$V_d x M_1$
	($\mu g/m^3$)	($\mu g/m^3$)		(m/s)	($\mu g/m^2/s$)
0.6	8.92	9.84	-0.10	-0.0010	-0.0096
0.85	13.92	17.10	-0.21	-0.0022	-0.0312
1.5	78.00	65.89	0.17	0.0018	0.1431
3.5	790.74	1210.52	-0.43	-0.0046	-3.6619
7.5	748.39	1123.50	-0.41	-0.0044	-3.3066
12.5	345.20	103.22	1.21	0.0131	4.5320
20	309.71	35.11	2.18	0.0237	7.3326
					$\sum F_d = 4.9984$

Table 5.6. Determination of dust flux in 2005.

D	M_1	M_2		V_d	F_d
(μm)	Tam 05	Ksi 05	$Ln(M_1/M_2)$	$1000/T.Ln(M_1/M_2)$	$V_d x M_1$
	($\mu g/m^3$)	($\mu g/m^3$)		(m/s)	($\mu g/m^2/s$)
0.6	5.79	6.97	-0.18	-0.00231	-0.01338
0.85	11.77	12.63	-0.07	-0.00088	-0.01036
1.5	50.37	79.45	-0.46	-0.00570	-0.28696
3.5	1747.41	1495.91	0.16	0.00194	3.39428
7.5	2938.45	2159.95	0.31	0.00385	11.30566
12.5	379.35	483.89	-0.24	-0.00304	-1.15417
20	121.50	223.49	-0.61	-0.00762	-0.92558
					$\sum F_d = 12.30949$

From Table 5.5, the deposition flux, F_r for the selected period in 2002 is
$F_r = \sum F_d = 5.00 \times 10^{-6}$ t/km^2/s.
In order to estimate the annual deposition rate for 2002, F_t, we assume (based on our observations and in a first approximation), a Harmattan duration of two months in the year, starting 1st January and ending 28th February, making a total of 59 days or 5,097,600 seconds, with the peak production occurring during the selected period. Assuming that there is no dust production before the 1st of January and after the 28th of February, the integral value over the active period will be half the peak production value. The total flux deposited in 2002 is therefore given by
$F_t = ½ F_r (59.24.60.60) = 1/2 . 5.00 . 10^{-6} . 59 . 86{,}400 = 12.74$ t / km^2/yr
Thus the total flux deposited is about 13 t/km^2/yr in 2002 and 31 t/km^2/yr in 2005. Assuming the particles were mainly silt or quartz particles with a density of 2650 kg/m^3, the corresponding thickness of the dust layer deposited e can be estimated from the expression
$m = \rho A e$
where m is the mass deposited and A is the surface area covered by the dust particles. This corresponds to a surface layer dust thickness of 4.8 μm per unit area in 2002 and 11.8 μm per unit area in 2005.

Although the deposition rates obtained seem globally reasonable, it can be seen from Figures 5.35b and 5.35c that different particle sizes contribute differently to the deposited flux. In 2002, only particles larger than 10 μm contribute to the deposition flux, while in 2005 only particles between 2 μm and 10 μm contribute to the flux deposited. It is even possible, in some cases, that slight production of particles from non-Harmattan sources may have occurred between Tamale and Kumasi. It is clear, however, that within the range of particle sizes considered (0.5 μm – 25 μm in diameter), the total flux is indeed a deposition flux, even if for certain class sizes the situation is less obvious. In any case, it is the total mass flux that really accounts for the quantity of dust particles that finally was deposited on the ground and other surfaces. The deposition flux, F_d is the mass flux per unit meter per second over the various class sizes. The total deposition flux concerns the mass flux over all size classes and takes into consideration the variation of the particle concentration from the start to the end of the Harmattan episode as well as the duration of the Harmattan phenomenon in the year. The thickness of the dust layer on a surface depends on this duration and hence the total deposition flux is used to estimate the dust layer thickness, e. The relationship between these values is shown in Table 5.7.
These deposition rates may be compared with the values in the range of 137 to 181 t/km^2/yr obtained by McTainsh and Walker (1982) in Kano (Nigeria) which is much closer to the main source of the Saharan dust.

Table 5.7. Deposition flux and thickness of dust layer.

Year	Deposition flux, F_d ($\mu g\ m^{-2}\ s^{-1}$)	Total flux deposited ($t\ km^{-2}\ yr^{-1}$)	Thickness of dust layer, e (μm)
2002	4.99	12.74	4.8
2005	12.30	31.4	11.8

5.6. Influence of the ITCZ and NAO

As noted before, the ITCZ and NAO are the two large-scale phenomena that affect weather in the northern Hemisphere. Their variability, which has significant influence on the Saharan dust haze episode in West Africa, is discussed here below.

5.6.1 Influence of the Inter-Tropical Convergence Zone (ITCZ)

Figure 5.40 shows the variation of the particle number concentration in the Kumasi sampling station and the ITCZ position during the Harmattan periods of 1997-2005. It shows the scatter plots of the observed daily mean particle concentration with the ITCZ position of the day. The scatter plot is fitted with a natural logarithmic relation as $y = -1.7434\ln(x) + 12.988$, where y is the ITCZ position in degrees latitude, which lies between 0^o and 15^o (with respect to Ghana), during the Harmattan period and x is the concentration in particles/cm^3. Generally, there is a build-up of particles as the ITCZ position decreases from the latitude 10^oN towards latitude 6^oN, while below latitude 6^oN, particle concentrations can reach high values above 100 particles/cm^3. This confirms the influence of the ITCZ on the Harmattan events in Ghana. Based on this natural logarithmic relation, the concentrations at Kumasi for various ITCZ positions are shown in Table 5.8.

Table 5.8. Latitudinal (Y^oN) position and particle concentration (x particles/cm^3).

x(particles/cm^3)	30	50	70	90	100	120	150	160	170
Y(^{o}N)	7.1	6.2	5.6	5.1	5.0	4.6	4.3	4.1	4.0

As the ITCZ migrates to higher latitudes, the concentrations logically decrease.
Figure 5.41 shows the variation of the particle number concentration in the Tamale sampling station (9.5^{o}N) and the ITCZ position during the Harmattan periods of 2001-2005. The figure shows the scatter plot of the observed daily mean particle concentration as function of the daily mean ITCZ position. The plot is fitted with a natural logarithmic relation, y = -1.8189Ln(x) + 13.221, where y is the ITCZ position in degrees latitude, which lies between 0^o and 15^{o}N, during the Harmattan period and x is the concentration in particles/cm^3. As the ITCZ position moves down south of the sampling station, the particle number concentration increases. The particle concentration increased markedly when the ITCZ position moves down to latitude 7^{o}N, about 2.5^o down south of the sampling station. And the particle concentration shows highest concentration around 53 particles/cm^3 when the ITCZ moves further down south to about 6.1^{o}N. Clearly, the concentration in Tamale increases when the ITCZ migrates to lower latitudes. The graph shows a gradual decrease of the ITCZ position with increasing particle number concentration.

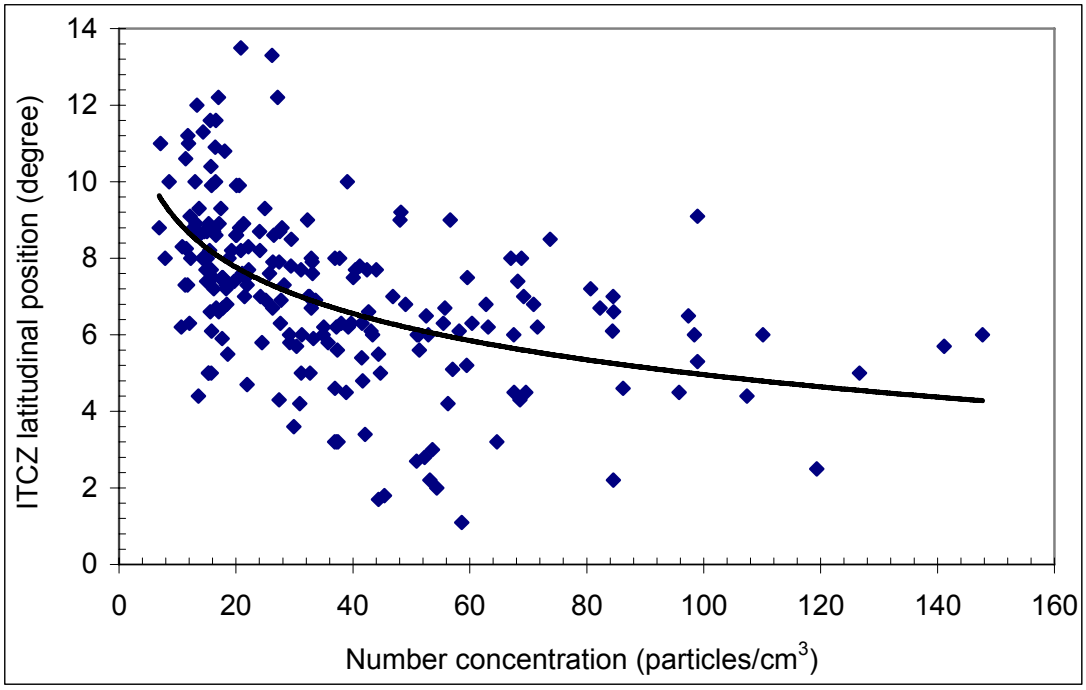

Figure 5.40. Variation of particle concentration in Kumasi and shift in ITCZ latitudinal position during the Harmattan: 1997-2005.

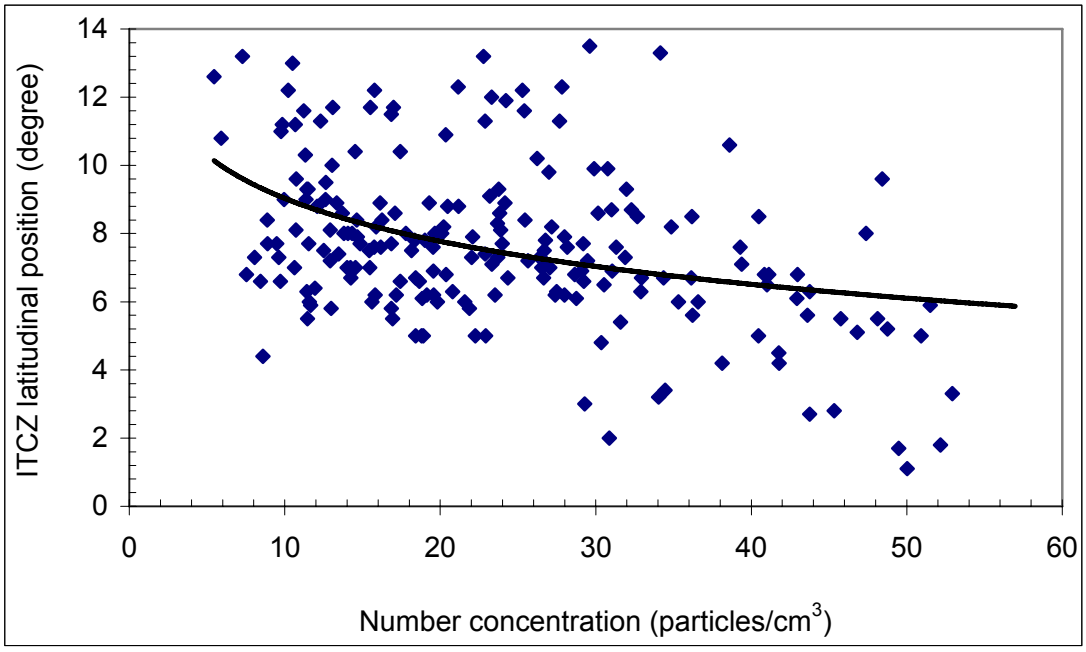

Figure 5.41. Variation of particle concentration in Tamale and shift in ITCZ latitudinal position during the Harmattan: 2001-2005.

5.6.2. Influence of the North Atlantic Oscillation (NAO)

Table 5.8 shows the periodic (also taken as the yearly) mean dust particle concentration in Kumasi and the values of the NAO index in February of the same year. In Figure 5.42, the NAO index is plotted in comparison with the mean dust concentration at Kumasi in February from 1997 to 2002. A linear equation is fitted to the relationship between the NAO index and the dust particle concentration of Figure 5.43 as $y = 0.0441x + 1.0397$, where x is the concentration in particles/cm^3. The graph shows how the NAO index is related to the Saharan dust haze phenomenon over Ghana.

Table 5.9. NAO index in February and mean particle concentration in Kumasi.

Year	1997	1998	1999	2000	2001	2002
NAO indices	5.26	2.44	1.8	4.37	0.07	3.01
Number conc. (particles/cm^3)	63	38	24	38	27	35
Mass conc. (µg/m^3)	477	273	122	168	401	1331

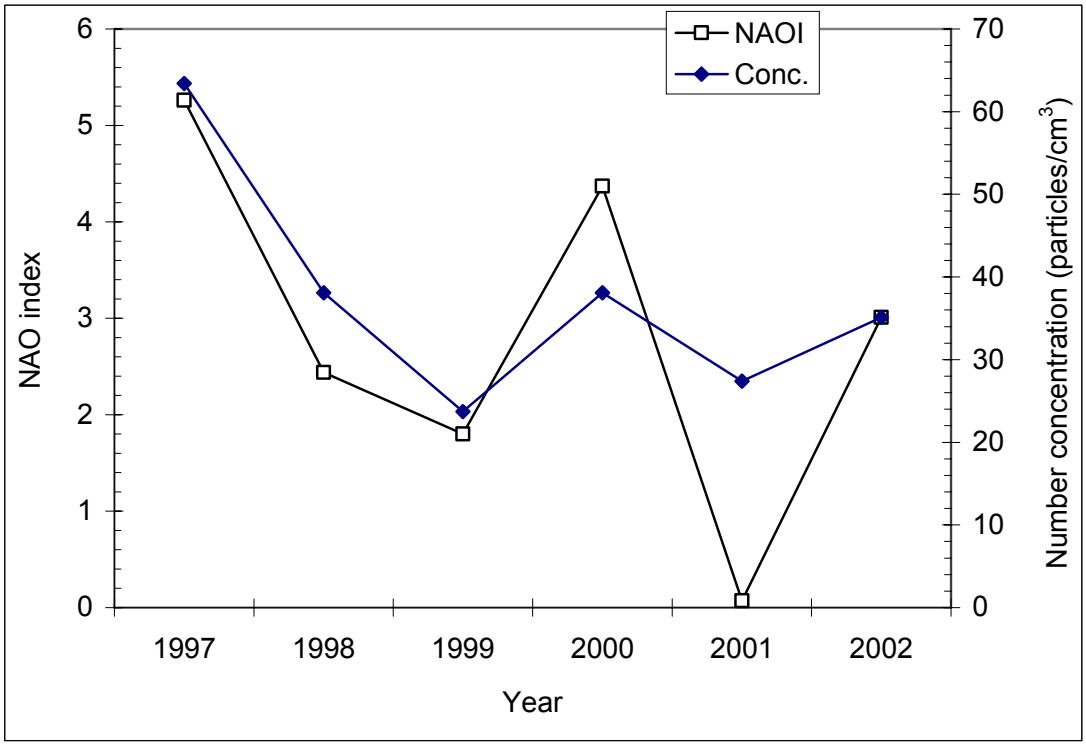

Figure 5.42. Comparison of NAO index in February and mean particle concentration at Kumasi in February: 1997-2002.

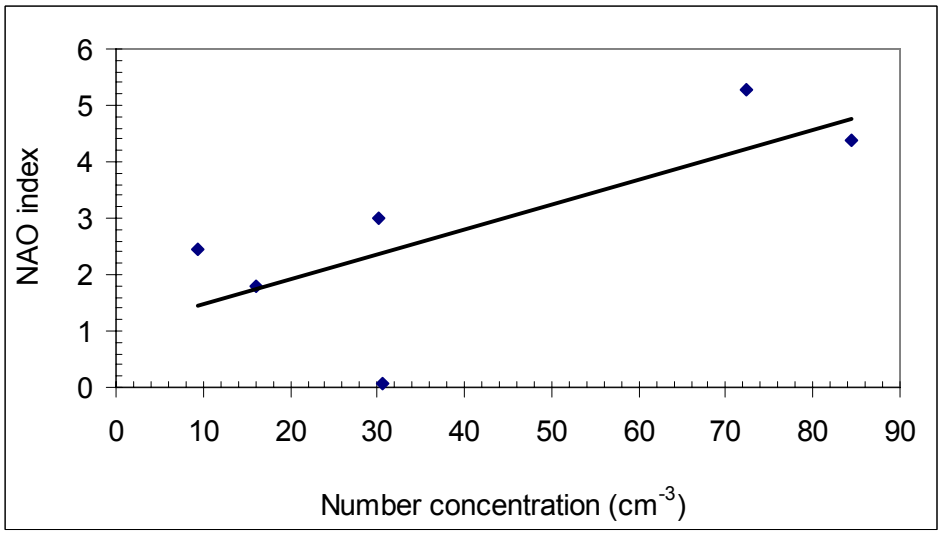

Figure 5.43. Variation of mean particle concentration at Kumasi in February with NAO index in February: 1997-2002.

6. CONCLUSION

The results reported in this study give the main physical characteristics of the Saharan dust in Ghana (4° N to 12° N and 1°E to 3°W), near the Gulf of Guinea, during the Harmattan period, for seven years within the period, 1997-2005. The Saharan dust particle size and concentrations were measured in Kumasi (6°40'N, 0° 34'W) from 1997-2005 and in Tamale (9°34'N, 0°52' W) from 2000-2005. The location of the sampling stations, 15 m above ground level and beyond the reach of local fugitive dust, and the extent to which observations were made may be regarded as free from accidental local dust and atmospheric influences; hence these results are typical of the locations. The study has embraced a comprehensive definition of the Harmattan, its importance and the current state of knowledge before this work. This work has focused on the measurement of the size, number and mass distributions of the Saharan dust particles in Ghana. Measurements were conducted during the northern winter months of December to the following March. The non-Harmattan dust aerosol was also measured outside the Harmattan season. The Saharan dust particles in the range between 0.5 μm and 25 μm were measured using a high-tech automatic optical particle counting equipment. The size range was divided into eight classes and the particle concentration in each class was monitored. Atmospheric circulations, which have influence on the Sahara dust transport, were also studied. The results cover the relationship between the dust produced during the Harmattan period and the ITCZ and NAO, the dust concentration at the sampling stations (Kumasi and Tamale) and the deposition rate between the two sampling.

This study has confirmed that the presence of the Harmattan is strongly dependent on the ITCZ position with respect to the two sampling locations. The locus of the average ITCZ positions over Ghana could be described by a polynomial function. This function shows that the average position of the ITCZ moves from high latitudes, around latitude 11^{o}N, at the beginning of the Harmattan, hovers around latitude 6.6^{o}N, in mid January, and then recedes to high latitudes, beyond 11^{o}N, after the Harmattan period. The average ITCZ positions over the period, 1997–2005 are described by a polynomial function of the Julian day. The mean positions showed a daily oscillation, with a standard deviation of about one to two latitudinal degrees.

The dust particle number concentration measured at Kumasi during the 7-year period (1997-2005) showed the largest number concentration in 1997 which was a typically strong Harmattan. Typical weak Harmattan periods were obtained in 1999 & 2001. The corresponding particle mass concentration measured at Kumasi during the same period revealed that the 2005 Harmattan was the most severe. Compared with the highest number concentration in 1997, the number concentrations showed that the phenomenon exhibited the largest particle sizes and mass concentrations in 2005.

Comparing the general number distributions of atmospheric particles given by Whitby (1978), to the Saharan dust number distributions, it was clear that the Saharan dust distributions fitted well into the coarse mode and partially into the accumulation mode. The fully developed coarse mode was at a diameter, D = 3.5 μm; the accumulation mode was, however, only faintly developed. The Saharan dust number distribution showed that large particle sizes were in low numbers and smaller sizes were in high numbers.

The comparison of the particle concentration with the non-Harmattan aerosol demonstrated evidence of the dust invasion during the Harmattan period. The non-Harmattan aerosol concentrations in Kumasi were found to be constant for the months of May and September, during which the non-Harmattan aerosol was sampled.

Statistical analysis of the mean diameters obtained for all the selected Harmattan periods at the Kumasi station, from 1997 to 2005, showed that the arithmetic count mean diameters were as follows: 1.28 μm in 1997, 1.14 μm in 1998, 0.94 μm in 1999, 0.94 μm for 2000, 1.47 μm for 2001, 2.12 μm for 2002 and 2.43 μm in 2005. The mean over the period (1997-2005) is 1.47 μm with a standard deviation of 0.58. This result compares well with published observations of 8.9 μm at Kano (latitude 12^{o}N) and 3.12 μm at Ile Ife (latitude 7^{o} 30'N), all in Nigeria. These results confirmed the expectation that the mean diameter of the particles reaching Ghana would be smaller than those found closer to the Saharan dust source in Nigeria. As is well-known with the Saharan dust propagation, larger (or heavier) aerosol particles sediment out progressively faster than smaller particles as the aerosol travels out to lower latitudes and destinations further away from the source region. The seven-year mean particle diameter of 1.47 μm, which is the characteristic diameter of the Saharan dust at the Kumasi station in central Ghana, is therefore consistent with the expected size distribution of the Harmattan aerosol.

The particle frequency distributions of the non-Harmattan aerosol in Tamale showed that the non-Harmattan aerosol sampled in September 2004 was higher than the non-Harmattan aerosol in May, 2001. The dust concentration distributions showed a maximum of about one and half orders higher than the non-Harmattan aerosol while both the non-Harmattan aerosol and the Saharan dust haze distributions follow the typical atmospheric dust particle distribution showing part of the accumulation mode and showing the coarse mode fully.

The Saharan dust particle count mean diameters for the Tamale sampling station were: 1.52 μm for the 2001 Harmattan period, 1.91 μm for 2002 and 2.79 μm in the 2005 Harmattan seasons, respectively. The arithmetic count mean diameter over the three-year period (2001-2005) is 2.07 μm with a standard deviation of 0.6 μm. The mean size in Tamale is higher than that in Kumasi which was 1.47 μm.

It was estimated that the dust particles take between one and two days to travel from Tamale to Kumasi. In 2002, the deposition flux, 5.00 x 10^{-6} t/km^2/s, was corresponding to a yearly deposition rate of 12.74 t/km^2/yr and a dust layer of 4.8 μm. The corresponding values for 2005 were 31.4 t/km^2/yr and 11.8 μm. These deposition rates may be compared with the values in the range of 137 to 181 t/km^2/yr obtained by McTainsh and Walker (1982) in Kano (Nigeria) which is much closer to the main source of the Saharan dust.

The variation of the particle number concentration at the Kumasi sampling station and the ITCZ position during the Harmattan periods of 1997-2005 follow a relationship that is described by a natural logarithmic function. The particle concentration in Kumasi, which is at latitude 6.6^{o}N, increased as the ITCZ position moved south of this latitude.

The variation of the particle number concentration at the Tamale sampling station (9.5^{o}N) and the ITCZ position during the Harmattan periods of 2001-2005 was related by a natural logarithmic function.

The North Atlantic Oscillation is often characterised by the NAO index. Graphs of the relationships and correlations between the Saharan dust transport and the NAO revealed that the NAO index reached a maximum value in February in all the years considered except 2001, where the NAO index appeared as a minor peak. A peak NAO index often

corresponded to a peak maximum dust concentration. A linear relationship describes the relationship between the NAO index and the dust particle concentration in Kumasi.
These results were the quantitative analyses of the Saharan dust haze reaching Ghana and the Gulf of Guinea during the dry season or northern winter for the past seven years (1997-2005). The experiments were carefully conducted with a sophisticated particle analyzer, making these results reliable and characteristic of the West African sub-region. In the introduction and also partly in the chapter on the literature review, we particularly insisted on the importance of this study and the implications that it could have in several domains (including climate, meteorology, agriculture, etc.) in multiple technical applications (such as deposition, visibility, engineering, energy, etc.) or in health (for example food conservation, respiratory problems, epidemic outbreaks, etc.) We think the results that we have obtained over a 7-year period are representative enough of the yearly Harmattan phenomenon for them to be used in practical applications in the countries along the Gulf of Guinea. On our part, we hope to specifically exploit these results in the area of engineering science. We also hope, however, that others will find the results useful in other domains like meteorology, agricultural food production, and in the prevention of health risks. In this way, we would have attained, at least partially, the main objective of this study, which is to obtain a set of reliable basic data on the physical characteristics of the Saharan dust haze aerosol that can be directly exploited by scientists, engineers and technologists.

BIBLIOGRAPHY/ REFERENCES

1. Adedokun J. A., Emofurieta W. O. and Adedeji O. A. (1989). Physical, mineralogical and chemical properties of Harmattan dust at Ile-Ife, Nigeria. Theor. & Appl. Climatology, Vol. 40, 161-169.
2. Adeyefa Z. D., Holmgren B. and Adedokun J. A. (1995). Spectral solar irradiance under Harmattan conditions. Renewable Energy, Vol. 6, No. 8, pp. 989-996, Elsevier Science Ltd.
3. Afeti G. M., Resch F. J. and Sunnu A. K. (1998). Size and number distribution of the Harmattan dust aerosol in central Ghana. J. Aerosol Sci., Vol. 29, Suppl. 1, pp. s173-s174.
4. Allen M. D. and Raabe O. G. (1985). Slip correction measurements of spherical solid aerosol in an improved Millikan apparatus. Aerosol Sci., Tech. 4, 269-286.
5. Allen T. (1981). Particle size measurement. 3rd ed. Chapman & Hall.
6. Anderson K. (1994). Analysis of Harmattan dust over Accra, Ghana. M.Phil. Thesis. University of Ghana, Legon.
7. Arimoto R., Duce R. A., Ray B. J., Ellis Jr. W. G., Cullen J. D. and Merrill J. T. (1995). Trace elements in the atmosphere over North Atlantic. J. Geophys. Res., 100, 1199-1214.
8. Arimoto R., Duce R. A., Savoie D. L. and Prospero J. M. (1992). Trace elements in aerosol particles from Bermuda and Barbados: Concentrations, sources and relationships to aerosol sulphate. J. Atmos. Chem. 14, 439-457.
9. Babiker A. G. A. G., Eltayeb I. A. and Hassan M. A. H. (1987). A statistical model for horizontal mass flux of erodible soil. J. Geophys. Res., Vol. 92, (No. D12) 845-849.
10. Bagnold R. A. (1971). The physics of blown sand and desert dunes. London, Chapman & Hall, pp. 265.
11. Bagnold R. A. (1941). The Physics of blown sand and dunes. Methuen, London.
12. Balogun E. E. (1974). The phenomenology of the atmosphere over West Africa. Proceedings of Ghana Scope's conference on environment and development in West Africa. Ghana Acad. of arts and Sciences, 19-31.
13. Barry R. G. and Chorley R. J. (1992). Atmosphere, weather and climate. Routledge 6th ed.
14. Bergametti G., Gomes L., Remoudaki F., Desbois M., Martin D. and Bush-Menard P. (1989). Present transport and deposition of dust to the north-western Mediterranean, in paleoclimatology and paleometrology: Modern and past patterns of global atmospheric transport, edited by M. Leinen and M Sarnthein, pp. 227-252. Kluwer Acad. Boston. Mass.,
15. Bertrand J. J., Baudet J. and Drochon A. (1974). Importance des aérosols naturels en Afrique de I'ouest. J. Rech. Atmos., Vol. 8, 846-860.
16. Bird B. R., Stewart W.E. and Lightfoot E. N. (1960). Transport phenomena. Wiley, New York.
17. Borma S. and Jaenicke R. (1987). Wind tunnel experiments on the resuspension of sub-micrometer particles from a sand surface. Atmos. Environ., 21, 1891-1898.
18. Brimblecombe P. (1986). Air composition and chemistry. Univ. of Cambridge Press, Cambridge, pp. 52-73.

19. Brooks N. and Legrand M. (2000). Dust variability over northern Africa and rainfall in the Sahel. In Linking climate change to land surface change. Editted by S. J. Mclaren and D. R. Kniveton. Kluwer academic publishers, Netherlands, pp. 1-25.
20. Carlson T. N. and Prospero J. M. (1972). The scale movement of Sahara air outbreaks over the equatorial north Atlantic. J. Appl. Meteor., 16, 1368-1371.
21. Carruthers D. J. and Choularton T. C. (1986). The microstructure of hill cap clouds. Quarterly Journal of Royal Meteor. Soc. 112, pp. 113-129.
22. Cautenet, G., F. Guillard, B. Marticorena, G. Bergametti, F. Dulac, and J. Edy (2000), Modelling a saharan dust event, Meteorologische Zeitschrift, 9 , 221-230.
23. Chepil W. S. (1945). Dynamics of wind erosion. Soil Sci., 60, pp. 305-320.
24. Chester R. and Johnson L. R. (1971). Atmospheric dust collected off the West Africa coast. Nature, Vol. 229.
25. Chiapello I., Bergametti G., Gomes L. and Chatenet B. (1995). J. Geophys. Res. Lett. Vol. 22, No. 23, pp. 3191-3194.
26. Chiapello I. and Moulin C. (2002). TOMS and METEOSAT Satellite records of the variability of Saharan dust transport over the Atlantic during the last two decades. Geophys. Res. Lett., Vol. 29, No. 8, pp. 17.1-17.4.
27. Chiapello I., Moulin C. and Prospero J. M. (2005). Understanding the long-term variability of African dust transport across the Atlantic as recorded in both Barbados surface concentrations and large-scale Total Ozone Mapping Spectrometer (TOMS) optical thickness. J. Geophys. Res. Vol. 110.
28. Cloudsey-Thompson J. L. (1964). Man and the Biology of arid zones. Edward Arnold, London.
29. Cox E., Mazurek M. A. and Simoneit B. R. T. (1982). Lipids in Harmattan aerosols of Nigeria. Nature, Vol. 296.
30. D'Almeida G. A. (1985). Recommendation on sun photometer measurements in the BAPMON as based on the experiment of a dust transport study in Africa. WMO /TD- 67, pp. 30.
31. D'Almeida G. A. and Schutz L. (1983). Number, mass and volume distributions of mineral aerosol and soils of the Sahara. J. Climate & Appl. Meteor. Vol. 22, 233-243.
32. D'Almeida G. A. (1986). A model for Sahara dust transport. Climate & Appl. Meteor. Vol. 25, 903-916.
33. Delaney A. C., Parkin D. W., Griffin J. J., Goldberg E. D. and Reiman B.E.F. (1967). Airborne dust over Barbados. Geochim. Cosmochim. Acta 31: 885-909.
34. Dubief J. (1979). Review of the North Africa Climate with particular emphasis on the production of Aeolian dust in the Sahel zone and in the Sahara. Sahara Dust: Mobilization, Transport, Deposition, C. Morales, Ed., Wiley & Sons, 27-48.
35. Eyo O. E., Menkiti A. I. and Udo S.O. (2003). Microwave signal attenuation in Harmattan weather along Calabar-Akampkpa line-of-site link. Turk J. Phys. 27 153-160 TÜBITAK.
36. Eyre S. R. (1963). Soils and vegetation. Edward Arnold, London, pp. 25-44.
37. Fairall C. W. and Davidson K. L. (1986). Dynamics and modelling of aerosols in the marine atmospheric boundary layer, in oceanic whitecaps. Edited by Monahan E.C. and Niocaill G. Reidel, Hingham, Mass., pp. 195-208.
38. Fairchild C. I. and Tillery M. I. (1982). Wind tunnel measurements of resuspension of ideal particles. Atmos. Environ., 16, 229-238.

39. Garvey D. M. and Pinnick R. G. (1983). Response characteristics of the particle measuring systems active aerosol spectrometer probe (ASASP-X). Aerosol Technol. 2:477-88.
40. Ganor E. (1991). The composition of clay minerals transported to Israel as indicators of Sahara dust emission. Atmos. Environ. 25A: 2657-2684.
41. Gatz D. F. and Prospero J. M. (1996). A large silicon –aluminium aerosol plume in central Illinois: North African desert dust? Atmos. Environ., 30, 3789-3799.
42. Gibbins C. J. (1980). The effects of the atmosphere on radio wave propagation in the 50-70 GHz frequency band. J. IERE, Vol. 58, No. 6, pp. 229-240.
43. Gillette D. A. (1980). Major contributions of natural primary continental aerosols: source mechanisms. Ann. N. Y. Acad. Sci. Vol. 338, 348-358.
44. Gillette D. A. Blifford D. A. and Fryer D. W. (1974). The influence of wind velocity on size distributions of soil wind aerosols. J. Geophys. Res. Vol. 79, 4068-4075.
45. Gillette D. A. (1974). On the production of soil wind erosion aerosols having the potential for long range transport. J. Rech. Atmos., 8, 735-744.
46. Gillette D. A. (1981). Production of dust that may be carried great distances. Desert dust: Origin, characteristics, and effect on Man. Spec. Pap. Geol. Soc. Am., 186, 11-26.
47. Gillette D. and Goodwin P. A. (1974). Microscale transport of sand-sized soil aggregates eroded by wind. J. Geophys. Res. Vol. 79, No. 27.
48. Gillette D. and Passi R. (1988). Modelling dust emission caused by wind erosion. J. Geophys. Res., Vol. 93, No. D11, pp. 233-242.
49. Gillette D. (1986). Wind erosion in soil conservation: Assessing the National Resources Inventory. Vol. 2, pp. 129-158. National Academy Press, Washington D.C.
50. Ginoux P., Prospero J. M., Torres O. and Chin M. (2005). Long-term simulation of global dust distribution with GOCART model: Correlation with North Atlantic Oscillation. Elsevier environmental modelling and software. Vol. 19 issue 2, 2004, pp. 113-128.
51. Glaccum R. A. and Prospero J. M. (1980). Saharan aerosols over the tropical North Atlantic- Mineralogy. Mar. Geol., 37, 295-321.
52. Glaccum R. A. (1978). The mineralogy and elemental composition of mineral aerosols over the tropical North Atlantic: The influence of Sahara dust. 161 pp, M.S. Thesis, Univ. of Miami, Flo.
53. Griffiths J. F. and Soliman K. H. (1972). Climates of Africa. In World survey of climatology. H. E. Landsberg, Ed. 10: 75-131. Elsevier Publishing Company. Amsterdam, the Netherlands.
54. Hamonou E., Chazette P., Balis D., Dulac F., Schneider X., Galani E., Ancellet G. and Papayannis A. (1999). Characterization of the vertical structure of Saharan dust export to the Mediterranean basin. J. Geophy. Res., Vol. 104, No. D18, pp. 22 257-22 270.
55. Hameed S. W., Shi J., Boyle J. and Santer B. (1995). Investigation of the centres of action in the northern Atlantic and north pacific in the ECHAM AMIP Simulation, proceedings of the first International AMIP Scientific Conference. WCRP-92, WMP/TD. No.732, 221-226.
56. Hamilton R. A. and Archbold J. W. (1945). Metrology of Nigeria and adjacent territory. – Q. J. R. Meteorol. Soc., 71: 231-265.
57. Hasager C. B. and Jensen N. O. (1999). Surface-flux aggregation in heterogeneous terrain. Quarterly Journal of Royal Meteor. Soc. 125, pp. 2075-2102

58. Hassan M. H. A. and Eltayeb I. A. (1991). Suspended transport of wind-eroded sand particles. Geophys J. Int 104, 147-152.
59. Hayward D. F. and Oguntoyinbo J. S. (1987). Climatology of West Africa. Hutchinson Education, New Jersey.
60. Herman J. R., Bhartia P. K., Torres O., Hsu C., Seftor C. and Celarier E. (1997). Global distribution of UV-absorbing aerosol from Nimbus 7/TOMS data. J. Geophys. Res., 102, 16911-16922.
61. Herwitz S. R., Muhs D. R., Prospero J. M., Mahan S. and Vaughan B. (1996). Origin of Bermuda's clay-rich Quartenary paleosols and paleoclimatic significance. J. Geophys. Res. 102, 16911-16922.
62. Hinds C.W. (1999). Aerosol technology: Properties, behavior, and measurement of airborne particles. John Wiley & Sons Inc. New York.
63. Holben B.N., Eck T. F., Slutsker I., Tanre D., Buis J. P., Setzer A., Vermote E., Reagan J. A., Kaufman Y., Nakajima T., Lavenu F., Jankowiak I., and Smirnov A. (1998). AERONET - A federated instrument network and data archive for aerosol characterization, Rem. Sens. Environ., 66, 1-16
64. Hurrel J. W. Decadal trends in the Northern Atlantic Oscillation: Regional temperatures and precipitation. (1995). Science 269, 676-679.
65. Husar B., Prospero J. M., and Stowe L. L. (1997). Characterisation of tropospheric aerosols over the ocean with NOAA advanced very high-resolution radiometer optical thickness operational product, J. Geophys. Res., 102, 16889-16909.
66. Jaenicke, R. Kandler K. Kulzer S., Schutz L., Diouri M. and Elhitmy M. Saharan dust transport over Morocco to mid-Europe. Internet, http//www.uni-mainz.de/FB/Physik/IPA/
67. Junge C. E. (1963). Air chemistry and radioactivity. Academy Press, pp. 382.
68. Kalu A. E. (1977). The Africa dust plume: Its characteristic and propagation across West Africa in winter. In: Sahara Dust (Morales, ed.) New York, Wiley & Sons, pp. 95-118.
69. Karyanpudi V. M., Palm S. P., Reagan J. A., Fang H., Grant W. B., Hoff R. M., Moulin C., Pierce H. F., Torres O., Browell E. V. and Melfi S. H. (1999). Bulletin of the American Meteorological Society, Vol. 80, No. 6, 1045-1075.
70. Kaufman Y. J., Koren J., Remer L. A., Tanré D., Ginoux P. and Fan S (2005). Dust transport and deposition observed from the Terra-Moderate Resolution Imaging Spectroradiometer (MODIS) spacecraft over the Atlantic ocean. J. Geophys. Res. Vol. 110, DS10s12, doi: 10.1029/2003JD004436, 2005.
71. Lepple F. K. (1975). Aeolian dust over the North Atlantic Ocean. Ph. D. Thesis. University of Delaware. Newark Del.
72. Legrand M., Cautenet G. and Burier J. C. (1992). Thermal impact of Saharan dust over land, II, Application to satellite IR remote sensing. J. Appl. Meteorol., 31. 181-193, 1992.
73. Legrand M., N'Doume C. and Jankowiak I. (1994). Satellite-derived climatology of the Sahara aerosol. In Passive infrared remote sensing of clouds and the atmosphere II. Editted by Lynch D. K. Proc. SPIE 2309, 127-135.
74. Marticorena B. and Bergametti G. (1995). Modelling the atmospheric dust cycle: I Design of soil-derived dust emission scheme. J. Geophys. Res. 100, pp. 16415-16430.
75. Marticorena B., Bergametti G., Aumont B., Callot Y., N'doume C. and Legrand M. (1997). J. Geophys. Res., Vol. 102, No. D4, pp. 4387-4404.
76. Massey B. S. (1994). Mechanics of fluids. Chapman & Hall UK.

77. May D. A., Stowe L. L., Hawkins J. D. and McClain E. P. (1992). A correction for Sahara dust effect on satellite sea surface temperature measurement, J. Geophys. Res., Vol. 97. No. C3, pp. 3611-3619.
78. McTainsh G. H. (1991). Dust transport and deposition. In Aeolian Environment, Sedimentation and landforms. Editted by A. S. Goudie, I Livingston and S. Stokes. John Wiley & Sons, LTD., pp. 205.
79. McTainsh G. (1980). Harmattan dust deposition in northern Nigeria. J. Nature, Vol. 80.
80. McTainsh G. H. and Walker P. H. (1982). Nature and distribution of Harmattan dust. Zeitschrift fur Geomorphologie, 26, 417-435.
81. Morales C. (1981). A case study of a dust storm weather situation, in the Sudan in April 1973. Appl. Geophys. Vol. 19, 658-676.
82. Morales C. (1979). The use of meteorological observations for studies of Saharan soil dust. Saharan dust mobilization. C. Morales (Ed) John Wiley Chichester, pp. 119-131.
83. Moulin C., Lambert C. E., Dulac F. and Dayan U. (1997). Control of atmospheric export of dust from north Africa by the north Atlantic oscillation. Letters to nature, Vol. 387, pp. 691-694, June 1997.
84. Newell R. E. and Kidson J. W. (1979). The tropospheric circulation over Africa. Saharan dust, Scope Rep. 14, C Morales, Ed., Wiley & Sons, 133-170.
85. Oduro-Afriyie K. and Anderson K. (1996). Analysis of dust over Accra, Ghana. Quarterly J. Hungar. Meteor. Serv., Vol. 100, No. 4.
86. Pasquill F. (1962). Atmospheric diffusion. D. Van Nostrand, Princeton N. J., U.S.A., p. 112.
87. Perry K. D., Cahill T. A., Eldred R. A., Dutcher D. D. and Gill T. E. (1997). Long-range transport of North Africa dust to the east United States. J. Geophys. Res., 102, 11225-11238.
88. Peterson S. T. and Junge C. E. (1971). Sources of particulate matter in the atmosphere. Man's impact on the climate. W.W. Kellog and G. D. Robinson, Eds., MIT Press, 310-320.
89. Piazzola J. (1996). Etude de la repartition verticale des particules d'aerosols au voisinage de l'interface Mer-Air en zone côtière méditerranéenne. Ph.D. Thesis. Univ. de Toulon, France.
90. Propero J. M. and Carlson T. N. (1977). Sahara air outbreaks: Meteorology, aerosols and radiation. In Proceedings of the Garp Atlantic Tropical Experimental Workshop, Boulder, Colo., U.S.A.
91. Prospero J. M. and Carlson T. N. (1972). Vertical and areal distribution of Sahara dust over the western equatorial North Atlantic Ocean. J. Geophys. Res., 77, 5255-5265.
92. Prospero J. M., Ginoux P., Torres O., Nicholson S. E. and Gill T. E. (2002). Environmental characterization of global sources of atmospheric soil dust identified with the NIMBUS 7 Total Ozone Mapping Spectrometer (IOMS) absorbing aerosol product. Res. Geophys. 40 (1).
93. Prospero J. M. (1979). Mineral and sea salt aerosol concentration in various ocean regions. J. Geophys. Res., Vol. 84, No. C2, 725-731.
94. Prospero J. M. (1999). Long-term measurements of the transport of Africa mineral dust to the southern United States: Implications for regional air quality. J. geophys. Res., Vol. 104 No. D13, pp. 15917-15927.

95. Prospero J. M. and Nees R. T. (1977). Dust concentration in the atmosphere of equatorial North Atlantic; Possible relationship to the Sahelian drought. Science 196: 1196.
96. Pye K, (1987). Aeolian dust and dust transport. Academic Press London.
97. Renoux A. and Boulaud D. (1998). Les aérosols physique et métrologie. Technique et documentation. Lavoisier, Paris.
98. Resch F., Afeti G. and Sunnu A. (2002). Influence of large scale atmospheric systems on the Harmattan dust aerosol. J. Abstracts of the sixth international aerosol conference. September 9-13, 2002 Taipei, Taiwan.
99. Romero O. E., Lange C. B., Swap R. and Wefer G. (1999). Eolian-transport freshwater diatoms and phytoliths across the equatorial Atlantic record: Temporal changes in the Saharan dust transport patterns. J. Geophys. Res., Vol. 104, No. C2, pp. 3211-3222.
100. Rognon P., Coude-Gaussen G., Bergametti G. and Gomes L. (1989). Relationship between the characteristics of soils, the wind energy and dust near the ground, in the Western Sandsea (N.W. Sahara). In Paleoclimatology and paleometeorology: Modern and past patterns of global atmospheric transport. (Edited by Leinen M and Sarnthein M) Kluwer academic Publishers Dordrecht., pp. 167-187.
101. Samways J. (1975). A synoptic account of an occurrence of dense Harmattan dust at Kano in Feb. (1974). Savanna. Vol. 4,187-190.
102. Schutz L. and Jaenicke R. (1974). Particle number and mass distribution above 10^{-4} cm radius in sand and aerosol of the Sahara desert, J. Appl. Meteor., 13, 863-870.
103. Schutz L. (1977). Die Saharastaub-Komponente uber demsubtropischen Nord- Atlantik, Ph.D. Thesis, University of Mainz, Federal Republic of Germany.
104. Schutz L. (1980). Long range transport of desert dust with special emphasis on the Sahara. Ann. N. Y. Acad. Sci., Vol. 338, 515-532.
105. Schutz L. and Sebert M. (1987). Mineral aerosols and source identification. J Aerosol Sci. 18, 1-10
106. Schwikowski M., Seibert P., Baltensperger U. and Gäggeler H. W. (1995). A study of an outstanding Saharan dust at the High-Alpine site Jungfraujoch, Switzerland, J. Atmos. Environ., Vol. 29, No. 15, pp. 1829-1842.
107. Seinfeld J. H. and Pandis S. N. (1998). Atmospheric Chemistry and Physics: From Air Pollution to Climate Change. John Wiley & Sons Inc.
108. Shi W. (1999). On the relationship between the interannual variability of the northern Hemisphere subtropical high and the eastern-west divergent circulation during summer. Ph.D. Thesis. State University of New York at Stony Brook, USA.
109. Skidmore E. L. (1986). Soil erosion by wind: An overview. In Physics of desertification. (EI-Baz F. and Hassan M.H.A., eds. Martinus Nijhoff Publishers, Dordrecht, pp. 261-273.
110. Slinn W. G. N. (1983). Air to sea transfer of particles. In Air-sea exchange of gases and particles. (Liss P. S. and Slinn W. G. eds.) D. Reidel, Dordrecht, pp. 299-407.
111. Stern C. A., Boubel R. W., Turner D. B. and Donald L. F. (1984). Fundamentals of air pollution 2nd ed., AP., pp. 227-256, for the genesis of aeolian sediments. Geagr. Annlr. Vol. 37, 94-III.
112. Sunnu A. K. (1997). Characterization of the Harmattan dust aerosol in central Ghana, M.Phil. Thesis, UST, Kumasi.

113. Swap R., Ulanski S., Cobbet M., and Garstang M. (1996). Temporal and spatial characteristics of Saharan dust outbreaks. J. Geophys. Res., Vol. 101, No. D2, pp. 4205-4220.
114. Swap R., Garstang M., Greco S, Talbot R, and Kallberg P. (1992). Sahara dust in Amazon Basin, Tellus 44(B), 133-149.
115. Tiessen H., Hauffe H. K. and Mermut A. R. (1991). Deposition of Harmattan dust and its influence on base saturation of soils in Ghana, Geoderma, Vol. 49, 285-299.
116. Touchebeuf de Lussigny. (1969). Monographie hydrologique de lac. Rapport Orstom.
117. Tsoar H. and Pye K. (1987). Dust transport and the question of desert loess formation, Sedimentology, Vol. 34, 139-153.
118. Walker G. T. and Bliss E. W. (1932). World weather. V. Mem. Roy. Meteor. Soc. 4, No. 36, 53-84.
119. Willeke K. and Baron P. A. (1993). Aerosol measurement- principles, techniques and applications. John Wiley & Sons Inc. New York.
120. Whitby K. J. (1978). The physical characteristics of sulfur aerosol. International symposium of Sulfur in the atmosphere. Dubrovnick, Yugoslavia and Atmos. Env., 12, 135-1
121. Wilson R. and Spengler J. (1996). Particles in our air-concentrations and health effects, Harvard University Press
122. Yaalon D.H. (1997). Comments on the source, transport and deposition scenario of Saharan dust to southern Europe. J. Arid environments, 36, 193-196.